Review

What is ultrasound?

Timothy G. Leighton*

Institute of Sound and Vibration Research, Southampton University, Highfield, Southampton, SO17 1BJ, UK

Available online 15 August 2006

Abstract

This paper is based on material presented at the start of a Health Protection Agency meeting on ultrasound and infrasound. In answering the question 'what is ultrasound?', it shows that the simple description of a wave which transports mechanical energy through the local vibration of particles at frequencies of 20 kHz or more, with no net transport of the particles themselves, can in every respect be misleading or even incorrect. To explain the complexities responsible for this, the description of ultrasound is first built up from the fundamental properties of these local particle vibrations. This progresses through an exposition of the characteristics of linear waves, in order to explain the propensity for, and properties of, the nonlinear propagation which occurs in many practical ultrasonic fields. Given the Health Protection environment which framed the original presentation, explanation and examples are given of how these complexities affect issues of practical importance. These issues include the measurement and description of fields and exposures, and the ability of ultrasound to affect tissue (through microstreaming, streaming, cavitation, heating, etc.). It is noted that there are two very distinct regimes, in terms of wave characteristics and potential for bioeffect. The first concerns the use of ultrasound in liquids/solids, for measurement or material processing. For biomedical applications (where these two processes are termed diagnosis and therapy, respectively), the issue of hazard has been studied in depth, although this has not been done to such a degree for industrial uses of ultrasound in liquids/solids (sonar, non-destructive testing, ultrasonic processing etc.). However, in the second regime, that of the use of ultrasound in air, although the waves in question tend to be of much lower intensities than those used in liquids/solids, there is a greater mismatch between the extent to which hazard has been studied, and the growth in commercial applications for airborne ultrasound.
© 2006 Elsevier Ltd. All rights reserved.

Keywords: Ultrasound; Infrasound; Effects

Contents

*Tel.: +44 23 8059 2291; fax: +44 23 8059 3190.

E-mail address: tgl@soton.ac.uk.

1. Introduction

The question 'what is ultrasound?' illustrates perhaps the major difficulty with the subject: the answers seem simple and obvious. This is borne out by the fact that acoustics is a discipline with such an established history that many imprudent physicists consider it to be 'solved': the important equations were written, they believe, a century ago, leaving today's acousticians simply with the task of translating that established physics into useful technology. Such an approach can lead scientists to underestimate complexity, engineers to rely on received wisdom, and industry to complacency when manufacturing or using ultrasonic systems. It is therefore not surprising that ultrasound as a technology for material processing has a reputation for unpredictability, difficulty in scale-up, and a reputation as a 'black art' (Mason et al., 1992). Since the assessment of ultrasound safety (a specific topic of this volume) must quite rightly include the involvement of specialists in fields other than ultrasound physics, it is important to raise awareness of the complexities peculiar to ultrasound, in order that the field can be dealt with as a predictable and understandable science, and not an unpredictable 'black art'.

Another reason for this complacency with respect to the basic science is the ubiquitous and historic nature of our interaction with acoustic waves. With no other radiation do we interact to such a degree, both as a source and a receiver, and this can lead to an unwarranted complacency in the 'physical feel' we have for the radiation. We feel familiar with both positive and negative aspects of acoustics. Its ability to annoy might make the news through noise problems associated with roads, aircraft and neighbours, and yet, through speech, acoustics has dominated our communications for millennia. Acoustical engineering underpins not only recorded music, but also effective 'live' transmissions, from entertainment in theatres and concert venues, to well-designed public address systems. Many other of our acoustical interactions go unrecognised as such by the public. Often this is because although our experience for millennia has been dominated by audiofrequency sound in air, today we use ultrasound for both detection and material processing (the equivalent terms 'diagnosis' and 'therapy' being used if the application is biomedical). In terms of diagnosis, in the developed world, ultrasonic scanning of the foetus or other organs is commonplace (Duck et al., 1998; Szabo, 2004). The most familiar ultrasonic diagnostic application is external foetal scanning using 3–10 MHz ultrasound.

The question of the safety of diagnostic ultrasound is regularly and professionally reviewed (Barnett et al., 2000), although every few years or so the issue appears in the popular press. A notable exchange occurred in 1984, by which time it was estimated that probably well over a quarter of a million foetuses were being exposed to ultrasound each year in Britain alone (Chalmers, 1984). Public concern prompted Mr John Patten,

Junior Health Minister in the United Kingdom, to warn against the routine use of ultrasound in pregnancy in a letter to the Association for Improvements in Maternity Services. Quoted in the *Daily Mail* (22 October 1984) and 5 days later in *Lancet*, he said, "Given the publicity there has recently been about the possible risk of ultrasound scanning we would not expect any health authority to be advocating screening for all mothers as a routine procedure". However in the same year Davies (1984) stated in the British Medical Journal that "the accumulated clinical experience of the past quarter century should be reassuring enough". In response to Davies (1984), Chalmers (1984) however warned against complacency in the light of a lack of evidence to the contrary. He cited the two interesting historical cases. X-rays were first used in obstetrics in 1899, and by 1935 clinicians were recommending their routine use. Then in 1956 it was suggested that such a practice might predispose to the development of leukaemia in children (Stewart et al., 1956). Subsequent research supported this hypothesis (Bithell and Stewart, 1975). It may be noted that both X-rays and ultrasound have at times in the past been perceived to be non-invasive. Citing in addition the history of the use of the drug diethylstilboestrol, which was first used in obstetrics in the early 1940s (Smith et al., 1946), and in 1969 was proposed to predispose young women to vaginal adenocarcinoma (Herbst and Scully, 1970), Chalmers (1984) noted that none of the adverse effects in either case were "clinically obvious" to radiologists and obstetricians, and in fact were identified through the research of non-clinicians. Ziskin (1987) commented that "There is nothing that I'm aware of that has a safer record than that of diagnostic ultrasound". Foetal ultrasonic scanning is now so established in industrialised nations that it would now be difficult to find a control group for epidemiological studies.

Nowadays many more anatomical sites are benefiting from ultrasonic scanning. Innovations include the development of probes for use whilst inserted into body cavities, and the exploitation of frequencies in excess of 30 MHz for use on shallow sites in dermatological and ophthalmic work (where enhanced spatial resolution is required, but the increased absorption which occurs at these frequencies is not debilitating). Non-imaging diagnostic methods have also developed, for example in the use of ultrasound to investigate bone health and osteoporosis through measurement of sound speed and attenuation (Langton et al., 1984; Hosokawa and Otani, 1997; Strelitzki et al., 1998; Hughes et al., 1999, 2001, 2003; Njeh et al., 1999; Wear and Armstrong, 2001; Lin et al., 2001; Lee et al., 2003; Wear, 2005). The role of ultrasound in non-destructive testing has a long history e.g. for crack detection, but in addition industry has found applications ranging from nuclear power (Watkins et al., 1988) to potteries (Leighton, 2004). The diagnostic requirements of military sonar have driven many of the oceanic developments in acoustic monitoring and measurement. From the Second World War to the present conflicts, sonar has had an unrivalled role in the underwater battlespace (Urick, 1983). The end of the Cold War prompted a move away from the study of low frequency acoustics (a few kHz and below) in deep waters that had been used, for example, to detect nuclear submarines beneath the polar icecaps (Leighton and Heald, 2005). In the last decade military engagements have tended to occur in shallower coastal waters, and research interests have reflected this, leading to the development of the new discipline of *acoustical oceanography* (Leighton, 1997; Medwin and Clay, 1998; Leighton et al., 2001; Medwin, 2005). As an oceanic sensor, acoustic systems map petrochemical reserves and archaeological sites, and monitor a huge variety of parameters of commercial and environmental importance, from fish stocks to the effect of global warming on the oceans (Medwin and Clay, 1998; Leighton et al., 2001, Leighton, 2004; Medwin, 2005).

Exploration of higher acoustic frequencies in these shallow waters promises many oceanographic spin-offs (Leighton and Heald, 2005). These include monitoring of zooplankton (Holliday, 2001), the seabed and suspended sediment (Thorne and Haynes, 2002; Richards et al., 2003), and archaeological investigations (Dix et al., 2001).

In terms of processing and therapy, the use of ultrasonic cleaning (for jewellery, computer chips, tool sterilization, etc.) is commonplace (Zeqiri et al., 1997; Leighton et al., 2005a). Industry has for example used ultrasound in the preparation of foodstuffs, pharmaceuticals and other domestic products (Leighton, 2004). Biomedical applications range from lithotripsy (the ultrasonic destruction of kidney stones) (Sass et al. 1991; Chaussy et al., 2002; Fedele et al., 2004) to surgery (Bailey et al., 2003), to physiotherapy. Ter Haar et al. (1987) published the results of a survey on the practices of physiotherapists in England and Wales in 1985. They concluded that the number of treatments was very considerable (about a million per year in the English and Welsh National Health Service Departments, and 150,000 in the private practices, that replied to the questionnaire).

Sonochemistry (the enhancement of chemical reactions using ultrasound, almost always in liquids) typifies many of the issues facing the use of ultrasound. It is by necessity a multidisciplinary activity, since effective exploitation of the technology requires knowledge of the chemistry, fluid dynamics, acoustics and transducer technology. The field is therefore a fruitful one for discoveries, but in turn a difficult one for understanding, scale-up and exploitation (see Section 5.2). To the author's knowledge, there has not been a period within the last forty years when the field was not said by many to be on the verge of realising its commercial potential, but this expectation has, for the most part, not yet materialised. This is probably because of the requirement fully to solve, in a given project, the issues raised by the chemistry, engineering, physics and acoustics of the problem in equal measure.

Almost all of the above applications refer to the use of ultrasound in liquids or tissue, with a few (such as ultrasonic non-destructive testing, NDT) relating to the use of ultrasound in solids (Krautkramer and Krautkramer, 1977). Historically there have been fewer applications of ultrasound in air. Whilst some diagnostic applications have appeared over the decades (such as in range finding or intruder detection), there have often been competing technologies which have not suffered the high signal attenuation experienced by ultrasound in air (see Section 2.2 and Table 2). Whilst diagnostic applications in air are rare, those relating to processing are more scarce yet. Some, whilst they may appear at first sight to be processing applications of ultrasound in air (such as the ultrasonic knife, or the dental drills, filing apparatus and scalers—also known as descalers), they in fact rely on the vibration of the working solid tool, and are neither acoustic nor ultrasonic (in that their successful operation does not require the *propagation* of ultrasound in air, although this may be unwanted side-effect). Some proposed applications would use ultrasonic radiation forces (see Section 3.5) to agglomerate, filter or fractionate objects, such as particles suspended in air (de Sarabia et al., 2000; Kogan et al., 2004; Goddard and Kaduchak, 2005; Riera et al., 2006). These are techniques which, in liquids at least, might become more common as engineers attempt to fabricate microscopic scale fluid handling and analysis systems (Hawkes and Coakley, 2001; Harris et al., 2003; Hill, 2003; Townsend et al., 2004; Kuznetsova and Coakley, 2004; Wiklund et al., 2004; Pangu and Feke, 2004; Martin et al., 2005; Petersson et al., 2005a, b; Lilliehorn et al., 2005; Haake et al., 2005; Kumar et al., 2005).

The limiting feature for the use of ultrasound in air is the severe absorption which rapidly reduces the amplitude of the field, as it propagates away from the source, to levels which are too low for most processing activities, or even to provide sufficient signal-to-noise ratios (SNRs) for many diagnostic applications. There is however one exception, the manifestation of which illustrates a key point which must be appreciated in the assessment of the safety of ultrasound in air.

The human ear is an extremely sensitive sensor for acoustic waves. Intensities which are low by the standards used for ultrasonic diagnostic technology, and certainly for ultrasonic processing, are generally very much higher than the maximum intensities which the human ear can sustain at audio frequencies without damage. Therefore when ultrasound is used to generate signals to which the ear can responds (which may not necessarily be restricted to audiofrequencies—see Section 6), whilst the resulting intensities may be thought of as 'low' from the perspective of many ultrasonic technologies, they may be 'high' from the perspective of the ear. This point is discussed further in Section 7.

As a final word on applications of ultrasound, those new to the area should be aware that, in addition to the established applications, there have always been candidate uses for ultrasound advocated with enthusiasm, but which have yet to stand the test of time.

This paper proceeds through a series of sections to provide an answer to the question 'what is ultrasound?'. Simple linear representations of acoustics waves, which are adequate for the vast majority of audio-frequency (20–20,000 Hz) acoustics, are often inaccurate for analyses in the ultrasonic frequency regime. This is because the ear is such a sensitive detector that the intensities *at the ear*[1] at which audio-frequency waves cause pain or even hearing damage, are in physical terms very low (see Section 7), and usually place those waves in the linear regimes: any nonlinearities in their propagation are usually too small to be easily detectable.

---

[1]Of course, amplitudes high enough to generate nonlinearities during propagation are often generated at audio-frequencies, by for example construction equipment and jet engines, but if human ears are close enough to the source to be in a region where amplitudes are this high, hearing protection should be worn to attenuate the wave before it reaches the ear.

However at ultrasonic frequencies the ear is not such a sensitive sensor. As a result, the higher amplitudes (needed for example, for food processing, or to provide strong SNRs during non-destructive testing) can be generated without, in the majority of cases, causing pain to the ear. Indeed, the need to generate such high amplitudes at the source becomes increasingly essential as the frequency increases. This is because of the need to maintain a satisfactory SNR, since the absorption of ultrasound by most media usually increases with frequency. However whilst they are strictly inaccurate in the nonlinear regime that such high amplitudes induce, if used cautiously the linear relationships can provide useful rough guides,[2] and so will be presented in Section 2 to demonstrate some of the basic features of acoustic waves.

The formulations of Section 2 assume that the wave propagates linearly. However in many applications, the amplitude of the ultrasound is sufficiently great, and the dissipation sufficiently low, for the inherent nonlinearity of the propagation to reveal itself. Such high amplitudes are very characteristic of ultrasonic applications: where MHz frequencies are used (for example to achieve tight spatial or range resolution, or focusing), the attenuation is so great that high source amplitudes are often used. At the lower ultrasonic frequencies, instrumentation often exploits the assumed insensitivity of the human ear to frequencies above 20 kHz to generate ultrasound (either directly or as a by-product of the vibration of some instrument, such as a dental scaler) which has an amplitude that is sufficiently high to cause acoustic processing of a material, in a way which would not be possible at audio frequencies without hearing hazard. Section 3 describes such nonlinear propagation and its effects.

Such nonlinearities need to be appreciated since their effects tend to run contrary to the 'common sense' expectations of those who have experience only with linear regimes (Section 5.2 illustrates examples where the author has been asked to solve problems with ultrasonic instrumentation which is not behaving as expected). Because of this, Section 4 describes perhaps the most potent source of nonlinearity, cavitation. This is not to say that other ultrasonic effects upon tissue (streaming and microstreaming, radiation forces, etc.), which have less than an entire section devoted to them, are less important: indeed, for foetal scanning, hyperthermia is very likely a more important issue than cavitation. However cavitation is also the most difficult to understand, perhaps because of its inherent propensity for nonlinearity, and hence is the topic of Section 4. After a discussion in Section 5 of the scales, in terms of space and time, encountered in typical ultrasonic applications, Section 6 describes the use of ultrasound in air, before Section 7 provides the conclusions of the paper.

2. Simple relationships

2.1. Description of a compressional acoustic wave

Acoustic waves can come in a variety of forms (Fig. 1). The energy contained in one form of wave can be converted to another, for example at interfaces between two media. These waves have different propagation characteristics (phase and group velocity, dispersion, attenuation, etc.). Indeed there are some forms of wave which do not propagate in the strict sense, such as evanescent waves and hydrodynamic pressure signals (the strength of which can readily be seen by moving one's head underwater when submerged in the domestic bath or swimming pool—the pressure signatures cause by flow at the pinna give rise to an apparently loud 'sound', but these do not propagate to distance and cannot be detected by a nearby observer).

However probably the most common and familiar forms of acoustic wave are the longitudinal compressional waves, in which the particles are displaced parallel to the direction of motion of the wave (Fig. 1(a)). It is important to note that in both cases, the particles themselves are merely displaced locally, or oscillate: it is the *wave* that travels from source to detector, not the particles. Therefore if one sings a loud, steady[3] note at a lighted candle from a distance of a few centimeters, the flame barely flickers, since it is local

---

[2]Rough guides like this are often useful because, in ultrasonics and acoustics in general, a measurement having an uncertainty ± 3 dB is often seen as sufficiently precise, and the range -3 to $+3$ dB covers an uncertainty in intensity of a factor of 4. The dB scale expresses, in logarithmic terms, the ratio of two intensities (I_1 and I_2), given in dB as $10 \log_{10}(I_1/I_2)$. Because there is a 6 dB difference between the minimum intensity (I_{min}) and the maximum intensity (I_{max}) in the ± 3 dB range, this equates to an uncertainty of I_{max}/I_{min} of $10^{6/10} \approx 3.98$. See Section 2.3.

[3]Avoid consonants as they introduce turbulence. For a quantitative demonstration of the small displacements associated with steady vowels, see Section 2.2.
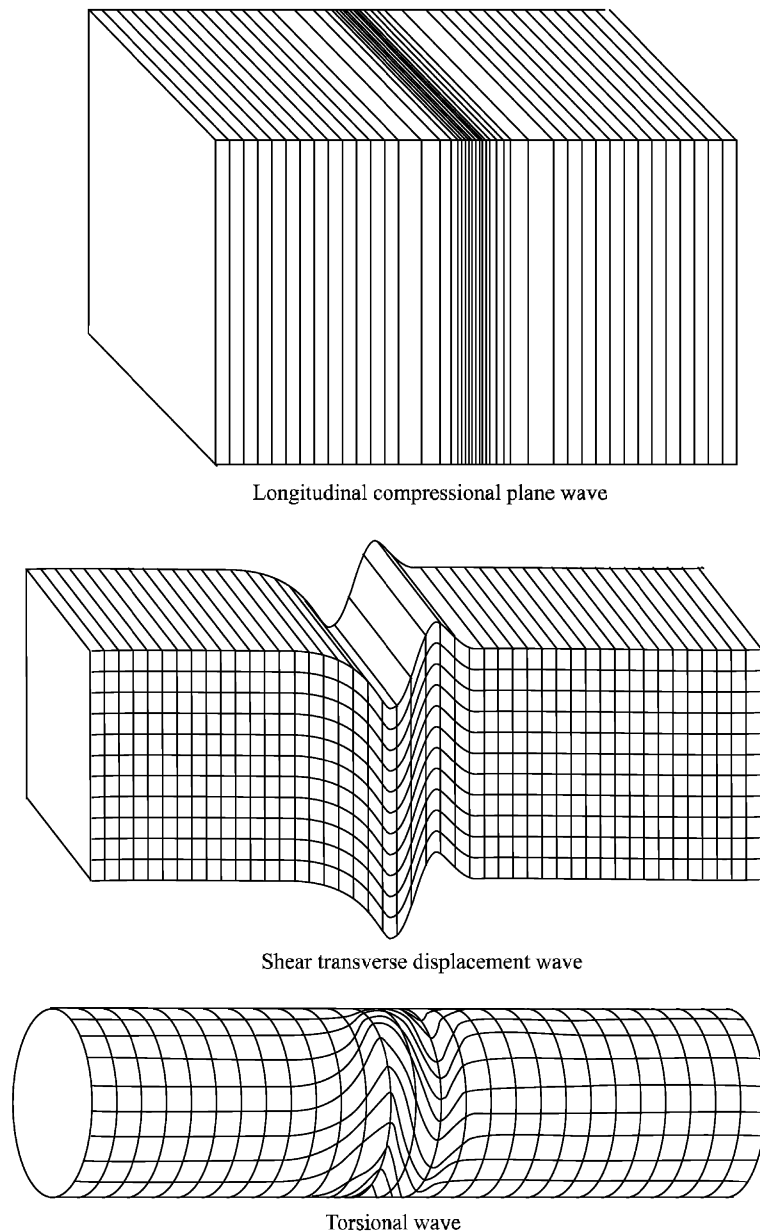
Fig. 1. Three examples of acoustic pulses, travelling from left to right. The media on either side of the wave pulse is in the equilibrium position: that on the right of the pulse has not yet been disturbed, and that on the left has returned to equilibrium after the oscillations associated with the pulse have damped down. The waves are: Longitudinal (compressional) plane wave: shear (transverse displacement) plane wave; and torsional wave. Wave types other than planar are common, spreading with other geometries, or focusing. Other wave types include Rayleigh waves, Lamb waves, Love waves, Stoneley waves (see Stephens and Bate, 1966) and Faraday waves (Faraday, 1831; Birkin et al., 2002; Leighton, 2004). In addition to propagating waves, evanescent waves exist, and can be important (e.g., in determining amplitudes close to the source).

vibrations which are transmitted: there is no net flow of air, which would correspond to an extinguishing 'blow'.

Fig. 1 shows a small subset of the types of acoustic waves that exist, and because there are so many types, it is useful first to consider a very simple analogue of a compressional longitudinal wave, shown in Fig. 2. This analogue consists of a series of bobs of equal mass, connected in a line by massless, lossless springs. The model
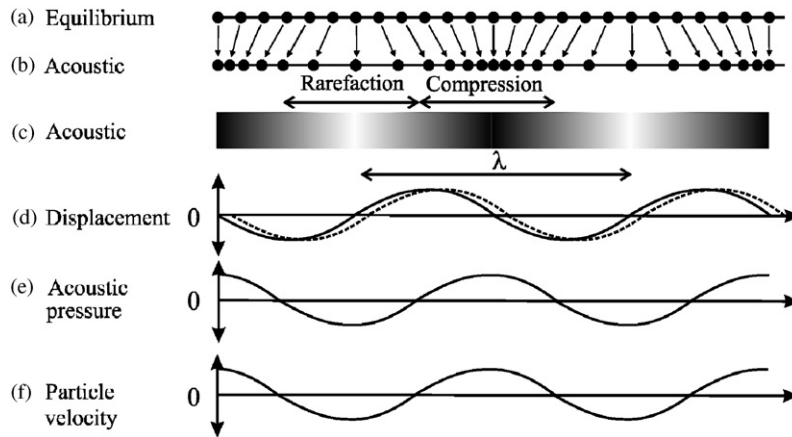
Fig. 2. Schematic of a one-dimensional single-frequency compressional longitudinal acoustic wave propagating linearly to the right, plotted as a function of the at-rest position in the material. See text for explanation.

therefore comprises the two necessary elements of any medium through which a sound wave will pass: inertia (invested in the bobs) and elasticity (invested in the springs). Only a section of the infinite line of bobs is shown.

Fig. 2(a) shows the bobs equally spaced in the equilibrium position. In Fig. 2(b) a one-dimensional single-frequency longitudinal wave is passing through the medium, and the bobs are shown frozen at an instant in time (as if photographed). Almost all of the bobs are displaced either to the left or right, the exceptions being those bobs at the centres of the rarefactions and compressions so created. The wavelength is much greater than the bob spacing and, in order to plot the particle velocity from this, we will need to know that the wave is travelling from left to right with a single phase speed (c_ϕ).

Arrows between parts (a) and (b) shows how each bob has been displaced. The bobs and springs in (a) and (b) represent the inertia and stiffness of a continuum, and interpolation between these bobs allows the characteristics of that continuum (through which the wave is passing) to be identified. Therefore in Fig. 2(c) we can represent the concentration of particles as a continuous change in density, the darker the regions the greater the density. This continuous change in density can be related to one in pressure, through the equation of state (Section 3.2), and this is plotted in Fig. 2(e). Regions of high pressure (*compressions*) in Fig. 2(e) correspond to points of high population density in Fig. 2(c). Similarly, low-pressure regions (*rarefactions*) occur at points with low concentrations of particles.

The solid line in Fig. 2(d) shows the displacement as a function of the equilibrium position for the continuum. This can be found by interpolating the discrete displacements required to go from Fig. 2(a) to Fig. 2(b), and plotting them (with right as positive, and left as negative, on the mantissa) as a function (on the abscissa) of the equilibrium position of the bob shown in Fig. 2(a). The displacement and pressure plots are in quadrature.[4] This schematic demonstrates an important point in acoustics, that one must take care to specify whether one is referring to pressure or displacement: in the figure, positions of zero displacement correspond to maximum or minimum pressure. If unqualified, common terms such as 'amplitude', 'node', or 'antinode' could apply to either displacement or pressure (Walton and Reynolds, 1984). An early example of one such ambiguity can be found by Paounoff (1939): "la lumière est plus intense aux plans nodaux des ondes stationnaires": one cannot tell from this phraseology whether the luminescence in the standing-wave field described by Paounoff occurred at the pressure nodes or the displacement nodes. For more on this topic, see Fig. 13(a).

Fig. 2 illustrates the concept of wavelength, that is the distance between two points on a wave (here, a sinusoidal wave) showing the same disturbance and doing the same thing (i.e. the disturbance is increasing in both, or decreasing, or stationary). The wavelength λ is shown on the figure, and is related to the phase speed

---

[4]That is, if one is a sine wave, the other is a cosine wave, such that they plot with a phase difference of $\pi/2$.

c_ϕ by $c_\phi = \Upsilon\lambda$ where Υ is the linear frequency (i.e., in Hertz). This is in turn related to the circular frequency ω (measured in radians per second) by $2\pi\Upsilon = \omega = c_\phi k$, where $k = 2\pi/\lambda$ is the wavenumber. Similarly, the group velocity c_g is defined as $c_g = \partial\omega/\partial k$ in the usual manner. For linear waves, a complex wavenumber can be used to describe the absorption of the wave by the medium for processes which convert the acoustic energy ultimately into heat. Such processes include viscous, ionic, etc. mechanisms. In contrast geometrical factors are incorporated by a range-dependence in the amplitude term. Other losses, such as diffraction losses and scatter, require application of some form of propagation model. These factors are discussed further in Section 2.2.

As stated above, this wave is travelling to the right, and a small time Δt later the displacement curve has moved to the dashed curve in Fig. 2(d). For each position along the wave x, the difference in the mantissa between the solid and dashed curves in Fig. 2(d) is proportional to the particle velocity v (it equals $v\Delta t$). The particles in the compressed regions are moving forwards, and those in rarefaction moving backwards. Particle speed is greatest at the regions of zero displacement, and reduces to zero at the points of maximum and minimum displacement. Comparison of the two curves of Fig. 2(d) in this way allows the particle velocity to be plotted, and this is shown in Fig. 2(f). Note that, the particle velocity and acoustic pressure are in phase, but they are in quadrature with the particle displacement. This finding for loseless linear waves will now be derived analytically as part of a discussion of the characteristics of waves which propagate linearly.

2.2. Simple relationships, impedance, and intensity in the linear limit

For the simple example discussed in the preceding section, the acoustic pressure P (Fig. 2(e)) and particle velocity v (Fig. 2(f)) are in phase. This would imply that the specific acoustic impedance of the medium Z is real, and for the moment this is the only type of wave which will be considered.[5] This particular impedance is defined through the ratio $Z = P/v$, and for such waves is numerically equal to the product of the mass density of a medium at equilibrium (ρ_0) and the phase speed of the compressional wave:

$$Z = P/v = \rho_0 c_\phi. \tag{1}$$

If the wave is linear, Eq. (1) allows unsophisticated estimations of the phase and magnitude relationships between displacement ε, acoustic pressure P and particle velocity v. If for example the displacement were a simple harmonic wave, of zero-to-peak displacement amplitude ε_0, then

$$\varepsilon = \varepsilon_0\,e^{j(\omega t - kx)},$$
$$v = \dot{\varepsilon} = j\omega\varepsilon_0\,e^{j(\omega t - kx)} = \omega\varepsilon\,e^{j\pi/2},$$
$$P = Zv = j\rho_0 c_\phi\omega\varepsilon_0\,e^{j(\omega t - kx)} = P_A e^{j(\omega t - kx)},$$
$$\ddot{\varepsilon} = -\omega^2\varepsilon, \tag{2}$$

where P_A is the acoustic pressure amplitude of the wave, recalling that the assumption is still maintained that Z is real. Eq. (2) confirms the deductions made in Section 2.1 using Fig. 2. That is to say, if the propagation is lossless and Z is real, then whilst acoustic pressure P and particle velocity v are in phase, they are in quadrature with the displacement (since $j = e^{j\pi/2}$).

Eq. (2) also allows the relative magnitudes of the various wave properties to be estimated in common materials. The basic properties of air, water and aluminium are shown in Table 1.

Table 1 also compares the properties of a sinusoidal ultrasonic wave of rms acoustic pressure amplitude 100 Pa in these three materials. From Eq. (2) it is simple to calculate the magnitudes of the particle velocity $|v| = |P|/|Z|$, the displacement $|\varepsilon| = |P|/(\omega|Z|)$ and the particle acceleration $|\ddot{\varepsilon}| = \omega|P|/|Z|$, and to see the roles that the different sound speeds and densities play in these calculations. Within a given material, the frequency dependence is important, which is illustrated by performing the calculations for Table 1 at 20 kHz and 1 MHz. As introduced qualitatively in Section 2.1, the reason why one can sing a vowel loudly at a candle flame and not perceive it to flicker is because the displacements are tiny: from Eq. (2), a sung note 'A' at

---

[5]In practice, there is a finite phase difference between P and v in lossy media, such as that for simple linear waves, Z is complex (see Eq. (8)). Such absorption will be introduced later in this section.

Table 1

A comparison of some of the acoustic properties of air, fresh water, and aluminium (all at sea surface normal conditions)

	Air at STP	Water	Aluminium
Density ($kg\,m^{-3}$)	1.2	1000	2700
Sound speed ($m\,s^{-1}$)	330	1480	6400
Specific acoustic impedance ($kg\,m^{-2}\,s^{-1}$)	400	1.5×10^6	1.7×10^7
For an acoustic wave with rms acoustic pressure amplitude of 100 Pa			
rms particle velocity amplitude at 10 kHz ($m\,s^{-1}$)	*0.25*	*6.7×10^{-5}*	*5.9×10^{-6}*
rms particle velocity amplitude at 1 MHz ($m\,s^{-1}$)	*0.25*	*6.7×10^{-5}*	*5.9×10^{-6}*
rms displacement amplitude at 10 kHz (m)	*4.0×10^{-6}*	*1.1×10^{-9}*	*9.4×10^{-11}*
rms displacement amplitude at 1 MHz (m)	*4.0×10^{-8}*	*1.1×10^{-11}*	*9.4×10^{-13}*
rms acceleration amplitude at 10 kHz ($m\,s^{-2}$)	*1.6×10^4*	*4.2*	*0.37*
rms acceleration amplitude at 1 MHz ($m\,s^{-2}$)	*1.6×10^6*	*420*	*37*
$(1-|R|^2) \times 100\%$ (interface to air)	100	0.107	0.0094
$(1-|R|^2) \times 100\%$ (interface to water)	0.107	100	29.8
$(1-|R|^2) \times 100\%$ (interface to aluminium)	0.0094	29.8	100

The first three rows of numbers show material properties. The next six rows of numbers (italicized) show the parameter values in each category for an acoustic wave having an rms acoustic pressure amplitude of 100 Pa. The final three rows form a matrix expressing the percentage of energy transmitted when a plane wave is normally incident at a plane interface between the medium shown in the row and the medium shown in the corresponding column (see text).

444 Hz, having an acoustic pressure amplitude of 0.02 Pa (0-peak, i.e. half the peak-to-peak amplitude in a sinusoidal wave) would generate displacement amplitudes in room air of only about 15 nm.

To return to the discussion of acoustic impedance, note that the specific acoustic impedance is just one of a range of impedances that can be defined in acoustics (depending, for example, on whether one uses the particle velocity or the volume velocity). These impedances take the usual role in physics in describing how simple waves are transmitted from one medium (where $Z = Z_1$) to another (where $Z = Z_2$), since they can be used to describe the constraining boundary conditions in a very simple form. For example if a plane compressional linear wave is normally incident on a plane boundary between two media, then continuity of the pressure gives us the first boundary condition, and continuity of the particle velocity gives us the second (Leighton, 1994, Section 1.1.5).

From these boundary conditions the pressure amplitude reflection coefficient for normally incidence plane compressional wave (note that it is important to have all these qualifications) is defined as the ratio $R = P_r/P_i$ where P_i is the acoustic pressure amplitude of the wave that is incident on the boundary, and P_r is the acoustic pressure amplitude of the wave that is reflected off it. It equals:

$$R = \frac{Z_2 - Z_1}{Z_2 + Z_1}. \tag{3}$$

Formulations for arbitrary angles of incidence exist (Kinsler et al., 1982; Leighton 1994, Section 1.1.5), which reduce to (3) at normal incidence. It should be remembered that the underlying model for (3) is based on a planar interface between two fluids, and that a fluid/solid or solid/solid boundary can give more complicated effects (such as the generation of shear waves) when a longitudinal wave is incident upon it at an arbitrary angle of incidence (Kinsler et al., 1982). It is however sufficient to illustrate to what degree differences in acoustic impedance between two media can lead to strong reflection of the incident wave. This process underlies a range of common practices in using ultrasonics, from the operation of range-finders in air, to the production of sonar and biomedical images (using the time-of-flight of the echo for range, and the intensity to indicate acoustic impedance mismatch at the reflecting boundary). Because the acoustic signal one expects to detect from reflection often resembles[6] the electrical signal used to drive the transmitter, to ensure that the

---

[6]The degree of resemblance depends on the transfer functions and ring-up/ring-down characteristics, but is often close enough to fool the unwary observer. There are techniques to increase the resemblance if ultrasonic high-fidelity systems are required (Doust and Dix, 2001).

detected signal is the result of acoustic propagation and not direct electrical pick-up of the driving signal, it is good practice in underwater ultrasonics to ensure that the detected signal disappears when the transducers are taken out of the water or, if that is not possible, when a sheet of expanded polystyrene is placed in the propagation path. This is because the impedances of air and expanded polystyrene are about 0.03% of the impedance of water, such that signals in water which are normally incident upon large sheets of expanded polystyrene exhibit values of R close to -1, indicating that the wave is almost entirely reflected with a π phase change. This type of interface is termed 'pressure release'. Waves in air which encounter walls of aluminium exhibit values of R close to $+1$ (the waves are almost entirely reflected, without a phase change), and the boundary is termed 'rigid' (Kinsler et al., 1982; Leighton, 1994, Section 1.1.5).

Whilst they do not hold for waves more complicated than the simple linear waves discussed in this section, relationships such as Eq. (2) are nevertheless frequently used to estimate the magnitude of various acoustic parameters in the manner used for Table 1. In similar vein, estimates are often made based on assumptions that the acoustic intensity of a wave is proportional to the square of its acoustic pressure, based on the correspondence for simple plane and spherical waves:

$$I = \frac{P_A^2}{2Z} = \frac{P_{rms}^2}{Z},$$ (4)

where P_A and P_{rms} are, respectively, the zero-to-peak and the rms acoustic pressure amplitudes of the wave (Leighton, 1994, Section 1.1.3, 3.2.1(c)(iii)).

Given that the intensities of the incident and reflected waves of the simple plane waves of Eq. (3) are, from (4), proportional to the square of their respective acoustic pressure amplitudes, then the intensity reflection coefficient for normally incidence plane compressional wave is R^2. The percentage of incident energy which is reflected by the boundary is $|R^2| \times 100\%$, and the percentage of energy which is transmitted is $(1-|R^2|) \times 100\%$, such that $1-|R^2|$ is known as the normal incidence intensity transmission coefficient. Insertion into Eq. (3) of the appropriate values from Table 1 provides the normal incidence values of the normal incidence intensity transmission coefficient in percentage terms (i.e. $(1-|R^2|) \times 100\%$) for interfaces involving boundaries between air, water and aluminium. Whilst 100% of the energy is transmitted, of course, for the trivial cases of perfect interfaces between a given material and itself (where the materials are said to be 'impedance matched'), the other cases calculated show considerable depreciation in the transmitted energy. It is particularly low for interfaces involving air, because of the low density of gas compared to fluid and solid. This is the reason for numerous phenomena in acoustics, including the use of coupling gel to eliminate air gaps when biomedical ultrasonic transducers are placed on skins for foetal scanning, physiotherapy, etc. The low transmission between liquid/soft tissue and gas also accounts for the restrictions on the use of ultrasound when large bodies of gas (in for example the lungs or gut) are present, which in part accounts for the advent of intracavity transducers. It accounts for the almost casual treatment of safety for many common aspects of industrial power ultrasonics: there can be little transmission of the ultrasound from an ultrasonic cleaning bath to the human body if an air gap is present between them. It also accounts for the way the assessment of hazard must change when contact is made, be it through hand contact with a transducer, or when whole body immersion occurs (in which case the close impedance matching between water and the human body can account for numerous transmission paths for acoustic energy to anatomical structure, e.g. from knees to ear). Therefore any assessments of the effect of ultrasound in a given circumstance must take account of (i) the various transmission paths to the organ in question, and (ii) the possibility that more than one organ should be considered. The discussion of dental ultrasonics in Section 6.2 illustrates these points.

The transmission losses calculated in Table 1 refer to that component of attenuation which is caused by the reflection of acoustic energy back from the interface. Again, this accounts for the efficacy with which diagnostic ultrasound detects structures with which the host medium forms a strong impedance mismatch (examples range from the detection of air-filled cracks in solids during ultrasonic non-destructive testing (NDT), to the clarity of bone structure in foetal scanning).

In general terms, the loss of energy from the propagating wave through reflection at interfaces enters the formulation through use of the reflection coefficients (themselves derived from the boundary conditions) to calculate the amplitudes of the reflected and transmitted waves from the amplitude of the incident wave. It is important to recall that there are other sources of loss, mentioned in Section 2.1. These enter the above

formulations through other routes. Other sources of loss would enhance the attenuation of the wave. Absorption (the conversion of acoustic energy ultimately into heat) can enter the formulation through use of a complex wavenumber. If now $k = q - jb$, then the above displacement becomes $\varepsilon = (\varepsilon_0/r)e^{j(\omega t - kr)} = (\varepsilon_0/r)e^{j(\omega t - qr + jbr)} = (\varepsilon_0/r)e^{j(\omega t - qr)}e^{-br}$, where in addition to the absorption loss e^{-br} the amplitude has been allowed to fall off as $1/r$ to incorporate inverse-square geometrical spreading losses in intensity with increasing range r (see later).

The parameter b characterises the absorption of the medium, and in general it increases strongly with frequency. For plane waves, absorption will contribute to attenuation an amount such that the amplitudes (pressure, displacement or particle velocity) decay with propagation distance x as e^{-bx} whilst, for propagation obeying (4), the wave intensity will fall off as e^{-2bx}. For example, the pressure and intensity for a plane wave could follow:

$$P = P_A\, e^{j(\omega t - qx)}\, e^{-bx} \Rightarrow \frac{dI}{I} = -2bx \Rightarrow I_2 = I_1\, e^{-2b(x_2 - x_1)}, \tag{5}$$

where x_1 and x_2 are the locations where the intensity takes values of I_1 and I_2 respectively. Two intensities can be compared via the decibel scale (Section 2.3), such that the logarithmic absorption coefficient α_{ab} is:

$$\alpha_{ab} = \frac{10 \log_{10}(I_1/I_2)}{x_2 - x_1} = 20b \log_{10} e \tag{6}$$

such that the choice of $x_2 - x_1$ determines the units of α_{ab} (e.g. dB/cm, dB/km). In turn the e-*folding distance* (the distance a wave must travel before its intensity decays to e^{-1} of its original value) is found by setting I_2/I_1 in Eq. (5) equal to e^{-1}, giving an e-folding distance for energy (L_e) of:

$$L_e = 1/(2b). \tag{7}$$

Values of the amplitude attenuation coefficient (in b and dB/m), along with the e-folding distance, are tabulated for fresh water, seawater and air at 10 kHz and 1 MHz for three materials in Table 2. The absorption increases with frequency, and in air it is very much greater than that in water (seawater being more attenuating than freshwater). Note that these are plane wave calculations, so that no amplitude changes associated with geometrical spreading or converging have been included (see below). The high absorption seen in air accounts for the fact that, whilst there are numerous devices which exploit the small wavelengths afforded by high frequency ultrasound to obtain good spatial resolution in water, tissue, and many homogeneous solids, applications of ultrasound in air are limited to the lower ultrasonic frequencies. For comparison, at 1 MHz the amplitude attenuation coefficient b for aluminium is 0.0207 neper m^{-1}, giving it an e-folding depth of 24 m.

Table 2
The acoustic absorption in fresh water, seawater and air (all at sea surface normal conditions), at 10 kHz and 1 MHz

	Water	Seawater	Air
10 kHz			
α_{ab} (dB m^{-1})	2×10^{-5}	4×10^{-4}	1×10^{-1}
b (Np m^{-1})	2×10^{-6}	5×10^{-5}	1×10^{-2}
e-folding distance for energy	250 km	10 km	50 m
1 MHz			
α_{ab} (dB m^{-1})	2×10^{-1}	3×10^{-1}	1×10^{3}
b (Np m^{-1})	2×10^{-2}	3×10^{-2}	1×10^{2}
e-folding distance for energy	25 m	17 m	5 mm

Symbols are defined in the text. *Sources*: Piercy et al. (1977), Leighton (1994), Medwin (2005). Whilst air has greater absorption than either type of water, the differences between fresh and seawater are revealing. These are not primarily due to the presence of sodium chloride, but rather to magnesium sulphate and boric acid. This illustrates two things. First, it shows the importance of properly characterising all of the sources of loss, even from structures or chemicals whose presence may at first sight be minor. Second, it illustrates the potential problems of using water as an in vitro medium for measurement. Whilst this is recognised for many traditional applications of ultrasound, and hence has led for example to derating procedures, we should remain aware of the potential problems as new methodologies and measurements are introduced (the interdependency of nonlinear propagation and absorption being one example).

In contrast, castor oil is often used as an absorber for MHz ultrasound, since at 1 MHz it takes a value of $b = 10.9$ giving it an e-folding depth of 46 mm.

Of the many sources of loss in an ultrasonic wave, one deserved special discussion. It is often (e.g. at low ultrasonic frequencies) called 'geometrical spreading loss' (although this is in some ways a misnomer—see below). It describes the loss in the locally measured wave amplitude as its energy is spread over a wider area, as the wave propagates away from the source. However unlike absorption, geometric spreading does not change the total energy invested in the wave: it simply changes the intensity or pressure measured at a single point depending on the location of that point with respect to the source.

However because of this, it is often considered to be a source of 'loss', particularly at low ultrasonic frequencies. This is because in many cases the wavelength is much greater than the size of the source (see Section 5.2). In such circumstances, in the free field it would be impossible to generate a plane wave (which has no geometrical spreading losses). Most sound fields would disperse away from the source, the wavefront expanding as it propagates and spreading the energy of the wave over an area which increases with distance from the source. Consider for example how such an effect is usually incorporated into the above formulation by use of a range-dependent amplitude. Spherical spreading from a monopole source would contribute an inverse square law to the loss in intensity with range r. As a result, the displacement in Eq. (2) would be characterised by an amplitude term which falls off as r^{-1} i.e. $\varepsilon = (\varepsilon_0/r)\,e^{j(\omega t - kr)}$. (Note that if intensity falls off as r^{-2}, then from (4) the pressure amplitude would fall off as r^{-1} and hence, from (2), so would the displacement amplitude).

Therefore at low ultrasonic frequencies (such as are used in much of sonar), users tend to discuss 'geometrical spreading losses'. However if the source size is large compared to the wavelength (as with MHz biomedical ultrasonics), geometrical factors are viewed very differently. With large values of ka (see Section 5.2), sources can produce focused fields. This is vital to the operation of many biomedical ultrasonics devices, both diagnostic (e.g. imaging) and therapeutic (e.g. HIFU, lithotripsy etc.). Under such circumstances the field tends first to undertake geometrical convergence (focusing), and only after the focus does geometrical spreading occur.

2.3. Reporting field amplitudes

The preceding discussion outlines the ways in which the amplitude of a wave can change, and because the magnitude of these changes can be so great, the decibel (dB) scale is commonly used. Misuse of this scale is responsible for errors, ambiguities and misreporting in the literature.

The amplitude of a wave will be attenuated through the absorption illustrated in Table 2, and also by scattering and diffraction (see Section 5.2 and Fig. 27). Loss at interfaces also occurs: only around 0.1% of the wave intensity would be transmitted across a plane air–water interface by a normally incident wave (Table 1). However we know from our experience with audio acoustics that we cannot set this value equal to zero, since a submerged person can hear sounds which originated from the air. Hence to cope with these large dynamic ranges it is usual to use a dB scale to express differences in amplitude or intensity. For two simple waves of the type described above, of intensities I_1 and I_2, the dB difference between them is $10\log_{10}(I_1/I_2)$. Footnote 2 used this when referring to the intensities at the limits of a ± 3 dB uncertainty range, and Eq. (6) used it to compare the intensities measured at two locations as the amplitude of a given propagating wave attenuated with distance. However more generally the dB scale can be used to compare any two intensities (one of which may, or may not, be a reference pressure, an important case which will be discussed below). The dB difference can also be used to compare two acoustic pressures (both being measured the same way, e.g. 0-peak amplitude, rms, etc.). Consider again the two simple waves discussed above, of intensities I_1 and I_2 and a dB difference of $10\log_{10}(I_1/I_2)$. Since for such waves the intensity is proportional to the square of the acoustic pressure amplitude (Eq. (4)), then the equivalent dB difference between them, in terms of their respective acoustic pressure amplitudes P_1 and P_2, is $20\log_{10}(P_1/P_2)$.

In acoustics it is not uncommon (although it is very bad practice) to cite the dB as if it were an absolute unit: in fact this is not the case, and the dB level cited is actually relative to some reference pressure. That is to say, in the formulation above, the dB level of the signal P_1 would be expressed by using for P_2 the appropriate reference level. Further confusion can be caused to the unwary by the fact that in common practice,

the reference level for waves in air[7] is different to that used for waves in liquids or liquid-like tissue (1 μPa rms). Therefore in this regrettably colloquial usage, the example acoustic wave in air used to discuss the implications of Eq. (2), having an rms acoustic pressure amplitude of 100 Pa, would by some be said to have an 'amplitude' of about 134 dB (i.e. $20 \log_{10}(100/20 \times 10^{-6})$). However were a wave of exactly the same acoustic pressure amplitude to be measured in water, colloquial usage would attribute to it an 'amplitude' of 160 dB (i.e. $20 \log_{10}(100/10^{-6})$). Proper usage would give these amplitudes, respectively, as 134 dB re 20 μPa, and 160 dB re 1 μPa. Failure to adhere to such a protocol, or indeed to appreciate that the dB is not an absolute unit and indeed has different reference pressures in different media, has led to some notable cases of inappropriate assessment of hazard. Chapman and Ellis (1998) discuss a current example, specifically the concern over the effect of sonar on marine mammals. They analyse a quote from The Economist (1998), which arose following scientific correspondence in Nature (Frantzis, 1998). Referring to a sonar source designed to produce low-frequency sound, The Economist stated that "It has a maximum output of 230 dB, compared with 100 dB for a jumbo jet." Chapman and Ellis (1998) criticise this phrase in the following way: "Regardless of the author's intention, the implication is that the whale would experience an auditory effect from the sonar that would be substantially greater than that of a person exposed to the jet aircraft." There are several reasons why this type of comparison is misleading.

First, the reference sound pressure for in-air acoustics (20 μPa rms) is not the same as that used in underwater acoustics and biomedical ultrasonics (1 μPa rms). This automatically means that a given rms acoustic pressure measured in water will have a level (in dB re 20 μPa rms) that is $20 \log_{10}(20/1) \approx 26$ dB greater than for the same rms acoustic pressure measured in air.

Indeed, many practitioners actually use a rule-of-thumb of subtracting 62 dB from intensity levels in water to estimate the intensities in air for the same acoustic pressure amplitude. This comes from the 26 dB to account for the different reference pressures, plus 36 dB to account for the differences in specific acoustic impedance required to compare intensities (see Eq. (4)):

$$10 \log_{10}(\rho_w c_w / \rho_g c_g) \approx 10 \log_{10}(1.5 \times 10^6 / 1.23 \times 343)$$
$$\approx 10 \log_{10} 3600 = 36 \text{ dB}.$$

To investigate the validity of this factor of 62 dB (or 61.5 dB, as some use), let us translate the underwater noise on a coral reef into an in-air equivalent as rated by the noise rating (NR) curves (a simplistic but widely used system for expressing the magnitude of ambient noise signals as a single number). The noise of snapping shrimp is the dominant source of underwater-sound in many tropical bays away from surf and man-made noise. It sounds like 'sizzling sausages' to snorklers swimming over tropical reefs (Ferguson and Cleary, 2001). Let us consider what these snorklers, with their human 20–20,000 Hz range, are hearing. Although the signal from the snapping shrimp contains energy at frequencies in excess of 100 kHz, the following analysis will consider the problem from the perspective of a standard NR (Noise Rating) calculation, which only considers energy up to the octave band centred on 8 kHz.

The white bars in Fig. 3 show the spectrum in this frequency range for the sound from the shrimp, as recorded in Kaneohe Bay, Hawaii (Everest et al., 1948). Similar levels have been confirmed internationally by Readhead (1997) and Au and Banks (1998). The spectrum over the frequency range of concern for calculating NR is shown in Fig. 3, both before (white bars) and after (black bars) the 62 dB air-sea "correction" recommended by many[8]. Fig. 3 also includes a spectrum of grey bars, indicating the intermediate step whereby the first 26 dB are subtracted to account for the difference in reference pressures.

---

[7]It is common to use a reference level in air of 20 μPa rms. This is based on I_{min}, the 10^{-12} W m^{-2} consensus minimum audible intensity at 1 kHz, which corresponds to an acoustic pressure amplitude of $\sqrt{2\rho_g c_g I_{min}} = 28.9$ μPa in terms of 0-peak acoustic pressure amplitude, or 20.4 μPa rms, such that 20 μPa rms is usually used. Here ρ_g and c_g refer respectively to the equilibrium density and sound speed in the gas (here, air); a similar notation will be used for other media, such that ρ_w and c_w will refer respectively to the equilibrium density and sound speed in water.

[8]http://www.pmel.noaa.gov/vents/acoustics/tutorial/8-conversion.html, the conversion of dB between air to water, in Underwater Acoustics Tutorial, US National Oceanic and Atmospheric Administration (NOAA) Vents Program. See also: Taking and importing marine mammals; Taking marine mammals incidental to navy operations of surveillance towed array sensor system low frequency active sonar; final rule, Federal register 2002 (67; 46712). See also: Final overseas environmental impact statement and environmental impact statement for surveillance towed array sensor system; Low frequency active (SURTASS LFA) sonar (Volume 1 of 2), US Department of the Navy, 2001.
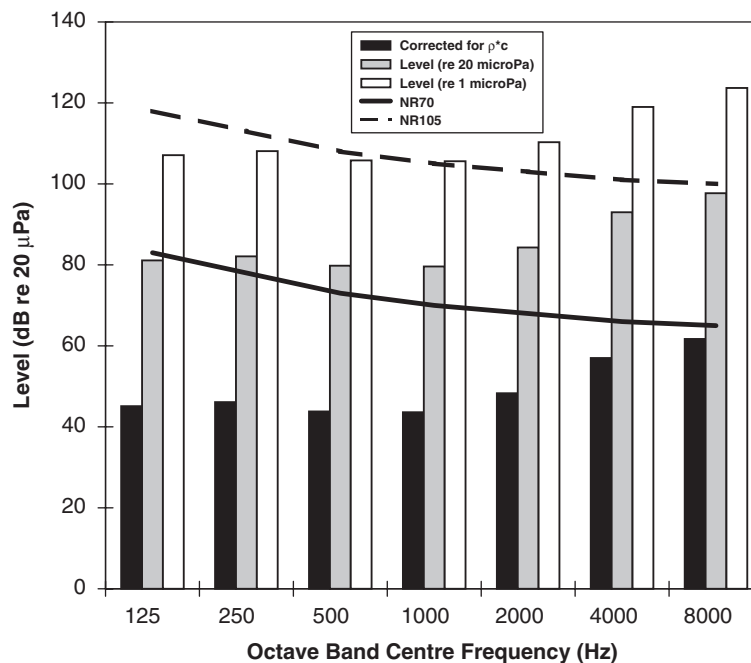
Fig. 3. This figure uses the noise rating curves to show why it might be inappropriate to suggest that subtracting 62 dB from an underwater sound pressure level ''converts'' that level to its aeroacoustic equivalent. To make this comparison as transparent as possible, the levels in each octave band are shown at three separate points during conversion. In white bars are shown unadjusted levels recorded in Kaneohe Bay, where the ambient acoustic spectrum is dominated by snapping shrimp. To account for the fact that most acoustic measurements performed in water are referenced to 1 μPa rms, while those performed in air are referenced to the nominal human threshold of hearing of 20 μPa rms, a sum of 26 dB is subtracted from the original levels to give the octave band levels illustrated by the grey bars (see text). To account further for the difference in the specific acoustic impedance from air to water, the octave band levels are reduced by an additional 36 dB, giving a net reduction of 62 dB per octave. These results are shown as black bars. The calculation indicates that according to the conversion method indicated, the audible crackle of a coral reef might be rated as NR70; a level prescribed as being the maximum allowable in the control space for a ship's machine room (figure by DC Finfer and TG Leighton).

The NR rating is determined by the NR curve which just envelopes the measured noise spectrum. Therefore this noise spectrum (the black histogram of Fig. 3) would be interpreted as a NR value of NR 70 (Bies and Hansen, 1996). For a human living space, NR 45 corresponds to the expected noise levels expected inside a living room in a domestic dwelling which is situated in an area of heavy industry. In exceeding this by 25, a rating of NR 70 would suggest that the acoustic environment near a coral reef is comparable to the maximum acceptable levels for the machine control room of a ship, as set forth by the UK Maritime and Coastguard Agency[9] for that environment. Snapping shrimp on a coral reef are certainly significant sources of sound. However it is difficult to accept the result of an NR calculation which subjectively likens the perceived acceptability of the noise to that found in a loud industrial setting. We know that, for the data in Fig. 3, in fact the snorkler in question would be hearing the natural acoustic environment that is commonly found away from sources of man-made noise during a shallow dive in say, Hawaii or the Caribbean.[10] This suggests that, as regards the acceptability of noise to humans, subtraction of more than 62 dB may be required in translating from water to air. This may be attributable in part to the differences in the way the ear operates in air and water (including questions of whether the ear canal is filled with water or air).

Although such subjective comparisons are not rigorous, they indicate that it is no simple matter to transfer 'annoyance' levels of sound from one medium to another, even when we restrict it to one species: to make such comparisons with an interspecies transfer included (as is frequently done between humans and cetaceans) is unwise.

---

[9]Code of Practice for Noise Levels in Ships, 1978. Crown Copyright.

[10]Indeed, since the snorkler would also hear the contributions made by the shrimp at >8 kHz, the reef environment would actually be perceived as 'louder'. However the trends in Fig. 3 above the 8 kHz band have not been included in the NR calculation.

Second, the values of many of the physical parameters (e.g. particle velocity, displacement, acceleration) associated with two acoustic waves which have the same rms acoustic pressure, one in air and one in water, are not the same. This can be seen from Eq. (2), and from rows 5–10 of Table 1, which are all calculated for a sinusoidal acoustic wave of 100 Pa rms acoustic pressure. It is by no means conclusive that the intensity alone is a sufficient measure of annoyance or hazard when transferring between physically different media.

Third, the quote in *The Economist* unwittingly compares the sonar sound level measured 'at the source' (which typically means at a distance of 1 m from an underwater sound source, where no listener, human or cetacean, is likely to be) with a level measured 'at the receiver' (i.e. at the position of the listener or microphone/hydrophone, which, for the aircraft case mentioned by *The Economist*, refers to the level averaged over several microphones ranged 100s to 1000s of metres away from the aircraft during take-off, where the intensity of the field has fallen off considerably as a result of geometrical spreading, absorption, scatter, etc. Chapman and Ellis, 1998). For this reason, just as no dB level should be used as an 'absolute' measure without quoting the reference level and the nature of the medium in which the measurement was taken, so too should it not be quoted without reference to the measurement position.

Fourth, as Chapman and Ellis (1998) point out, "there is no obvious connection between an annoying or harmful sound level for a human in air and an annoying or harmful sound level for a marine animal in water."

Finally, the frequency range to which the measurement refers, and the bandwidth of the signal generated by the source, is important. As discussed in footnote 11, the bandwidth of the signal is important when considering how its 'level' is interpreted. Furthermore, if the signal has a small bandwidth, as some sonar sources do, then concentrating the acoustic output over a narrow frequency range may hit, or miss, a particularly sensitive part of the spectrum for the subject. Furthermore, to state that a given signal is 'broadband' does not impart enough information to make a judgement as to the associated hazards. A pseudorandom sequence (or 'random' noise), a chirp, and an impulsive sound can all have the same bandwidth, and could all be designed to produce the same 'level' with respect to a given reference intensity or pressure, at the same range from a source. However the subjective effect on the listener of each could be very different.

This last point, regarding the spectrum of the emission, is particularly relevant when discussing infrasound and ultrasound. To be specific, there are particular problems associated with the assessment of potential hazard for humans when exposed to ultrasound and infrasound, because of reliance on the vast body of experience at audio frequencies. There is some overlap between the problems experienced in working with ultrasound and infrasound, but also each has specific problems based on the fact that, whilst the infrasound of interest tends to be treated as 'environmental noise', the ultrasound in question tends to be treated as 'signal'. This point will be discussed further below, using three example problems.

The first example issue relates to the A-weighted sound level, "the simplest and probably most widely used measure of environmental noise" (Kinsler et al., 1982). The measured sound spectrum is divided into frequency bands, and the energy in each band is weighted by a factor that reflects the sensitivity of the human ear to that frequency band (Bies and Hansen, 1996). These weighted energies are then combined to produce a single figure, given as dB(A), in an attempt to characterise the perceived loudness of a given environment. This procedure is so familiar that the steps behind producing a list comparing the 'noise levels' in various environments (ranking, for example, lawnmowers, rock concerts and aircraft on a single scale of A-weighted sound levels) are often ignored. As this weighting network was developed to protect against damage in the air due to sound within the audible frequency spectrum, A-weighting ignores energy which is transmitted within those third octave bands centred below 10 Hz or above 20 kHz. If therefore there is a 'significant' source of ultrasound (Grigor'eva, 1966; Acton, 1968, 1974, 1975, 1983; International Labour Office, 1977; International Non-ionizing Radiation Committee, 1984; auf der Maur, 1985; Damongeot and André, 1985, 1988; Lawton, 2001) or infrasound (von Gierke and Nixon, 1976) in the environment, then characterizing that environment by quoting the A-weighted decibel level will be inappropriate and misleading (see Section 6.2). The problems are further compounded when one considers what is meant by the word 'significant' in this context. For the purposes of the workshop with which this paper is associated, it should mean whether the 'measured field' can generate a potential hazard in humans.

This brings us onto our second problem: Both ultrasound and infrasound present difficulties in determining those 'measured fields' (Section 6). Furthermore, any past or current measurements of in-air ultrasound must

be critically questioned. This is because there is a lack of traceability for measurements in air at frequencies greater than 20 kHz. Although there is currently interest in increasing the upper frequency limit, primary standards for microphone calibration for sound in air have only been the subject of comparison between national measurement laboratories up to a frequency of 20 kHz. Measurements above this frequency cannot therefore be carried out in a traceable way using methods which have been the subject of international scrutiny and validation through the completion of formal comparisons, termed key comparisons (Zeqiri, 2005). Measurements in water can be traced to internationally validated standards in the frequency range 1–15 MHz, such that it is possible to measure the acoustic pressure amplitude at a given location and relate that back to a primary national standard. However, it is important to note that this does not tell us about the ultrasonic 'dose' given to humans in vivo, for example during foetal scanning (Duck, 1987; Duck and Martin, 1991; O'Brien, 1992; Siddiqi et al., 1995; Harris, 1999). Measurements of ultrasonic 'exposure' (which for example in the case of biomedical ultrasound refers to the measurements recorded in water) need to be undergo derating to allow estimation of the field levels which would occur in tissue (where acoustic pressure measurements are rarely made because of the invasiveness of hydrophones; Siddiqi et al., 1995). However the ultrasonic 'dosage' would refer to the quantitative determination of the interaction of ultrasonic energy with tissue, and this is currently not available. This point will be discussed further in Section 7.

Third, whilst it is not universally true, ultrasonic acoustic emissions tend to be dominated by man-made 'signals' (such as short pulses for diagnostic purposes, or the longer tone-burst or even continuous wave signals used for material processing). That is to say, their time-histories tend to be predictable. This is in contrast to emissions at audio or infrasonic frequencies, which tend to be viewed as environmental noise (even if they are impulsive in nature, such as can be generated by ordnance). As such it is very important to consider how the field is measured (and also, how it is then represented).[11] Consider for example a diagnostic ultrasound field used for foetal imaging. Here the sound field consists of a series of pulses, each with a centre oscillatory frequency of a few MHz, and duration of a microsecond or so (the 'on-time'). The interval between consecutive pulses consists of an 'off-time' of around 1 ms, such that there is a pulse repetition frequency (PRF) of about 1 kHz. Even at one specific location, this field has no single 'intensity', because (despite the rather loose use of the term 'instantaneous intensity') the measurement of intensity requires some time window for the measurement, and the result is an average over the duration of that time window τ. For example, a plane wave with time-dependent pressure field P over a given surface, would have an associated power per unit area based on the time-average (say from t_1 to t_2) of the product of the acoustic pressure and the particle velocity (Leighton, 1994, Section 1.1.7). Therefore using Eq. (1) to substitute for the particle velocity, the intensity at the given surface can be based on the product of the Real parts of the complex acoustic pressure and complex particle velocity:

$$
\begin{aligned}
I &= \frac{1}{t_2 - t_1} \int_{t_1}^{t_2} \mathrm{Re}(P)\,\mathrm{Re}(v)\,\mathrm{d}t \\
&= \frac{1}{t_2 - t_1} \int_{t_1}^{t_2} \left(\frac{P + P^*}{2}\right)\left(\frac{v + v^*}{2}\right)\mathrm{d}t \\
&= \pm \frac{1}{4(t_2 - t_1)} \int_{t_1}^{t_2} (Zv + (Zv)^*)(v + v^*)\,\mathrm{d}t,
\end{aligned}
\tag{8}
$$

---

[11]When plotting a spectrum from the voltage V time history output of a sensor, there are a number of conventions. With the frequency usually plotted on the abscissa, the four most common options for the mantissa are: $V\,Hz^{-1}$; $V^2\,Hz^{-1}$; V; V^2. Clearly the representations that use V^2 in preference to V are plotting a parameter which reflects the energy of the signal, as opposed to the amplitude. The advantage of using Hz^{-1} comes from the common interpretation of a spectrum as a histogram, since the frequency bins will be finite. If this is the interpretation, then changing the width of these bins should affect the amplitude of the spectral level plotted. This is certainly appropriate for broadband signals. Environmental noise can fall into this category. However this methodology is problematic if the signal is a sine wave. Whilst not purely sinusoidal, some common ultrasonic fields can be sufficiently close for this to be an issue, for example the field used for ultrasonic physiotherapy or material processing. For a sine wave, the energy in the bin is independent of the bin width, since all the energy is at a single frequency, i.e. it has zero bandwidth. Only one of the bins will contain non-zero energy. Division of the energy of that bin by the bandwidth of the bin simply causes the spectral peak corresponding to the sine wave to reduce in amplitude as the bin width increases. As a result, the parameters V and V^2 are sometimes used in preference to $V\,Hz^{-1}$ and $V^2\,Hz^{-1}$ (a quantity resembling power), if the signal is perceived to more closely resemble a sinewave than a broadband signal (Leighton et al., 2005b)
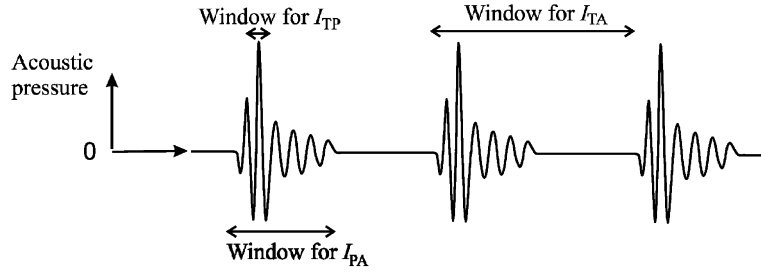
Fig. 4. Schematic of the pressure time history of some ultrasonic pulses. Three possible intensities can readily be defined from it (the pulse average intensity I_{PA}, the temporal average intensity I_{TA}, and the temporal peak intensity I_{TP}). The arrows indicate an appropriate approximate time window for each to be calculated over via Eq. (8).

where the * symbol indicates the complex conjugate. If the wave were sinusoidal[12] this would quickly reduce to:

$$I = \pm \frac{Z + Z^*}{4} vv^*$$
$$= \pm \frac{vv^*}{2} \operatorname{Re}\{Z\}. \tag{9}$$

The intensity of a plane wave can also be interpreted in terms of the mean energy density of the wave, $\phi_V = \rho_0 vv^*/2$ (Leighton, 1994, Section 1.1.3). In time Δt, a plane wave travelling at speed c_0 will carry energy $\phi_V \Xi c_0 \Delta t$ across a plane of area Ξ whose normal is aligned with the direction of propagation. Since the intensity equals the rate at which energy crosses a unit area of such a plane, then

$$I = \frac{\phi_V \Xi c_0 \Delta t}{\Xi \Delta t} = \phi_V c_0$$
$$= \pm \frac{\rho_0 c_0}{2} vv^*, \tag{10}$$

which, when compared with (9), indicates that:

$$\operatorname{Re}\{Z\} = \rho_0 c_0. \tag{11}$$

Therefore, when Z is real, (9)–(11) reduces to (1) and (4) for the simple harmonic wave discussed there. Fig. 4 shows a schematic of the pressure time history of some ultrasonic signal. Three possible intensities can readily be defined from it, with horizontal arrows to show their corresponding time windows (such that the left extremity of each arrow corresponds to a time which would be used as t_1 in Eq. (8), whilst the right extremity occurs at the time which would be used as t_2). To calculate the pulse average intensity (I_{PA}), the time window (and subsequent average) is taken over the duration of the pulse. There is the temporal average intensity (I_{TA}), where the window is taken over many pulses. Hence $I_{PA} > I_{TA}$ for the foetal imaging field under discussion, since the average which makes up I_{TA} will include measurement during the off-time. In turn, because the pulse takes time to ring up and ring down, the temporal peak intensity I_{TP} will be greater than the I_{PA}. It is therefore important to quote which intensity is being used, not only to avoid ambiguity, but because one time window might be far more relevant than another to the process under discussion. For example, probably the two main physical processes of interest relating to hazard during ultrasonic foetal scanning are hyperthermia and the bubble-based activity known as inertial cavitation (see Section 4.3) (Miller and Ziskin, 1989; AIUM/NEMA 1992, 1998; AIUM 1993; Barnett et al., 1998). Hyperthermia is a relatively slow process (compared to the period of a single cycle of the insonifying field), with the potential for significant tissue heating occurring only over many pulses of the foetal imaging field discussed above. Therefore I_{TA} would be the more relevant intensity to use in discussion of the hyperthermia hazard. In contrast, whilst there are issues (such as the

---

[12]Given that $\cos^2 \omega t = (\cos 2\omega t + 1)/2$, then if the interval $(t_2 - t_1)$ covers an whole number of oscillatory cycles, the integral of $\cos 2\omega t$ over this window is zero, giving $\int_{t_1}^{t_2} \left(\frac{\cos^2 \omega t}{t_2 - t_1} \right) dt = \frac{1}{2} \int_{t_1}^{t_2} \frac{\cos 2\omega t \, dt}{t_2 - t_1} + \frac{1}{2(t_2 - t_1)} \int_{t_1}^{t_2} dt = \frac{1}{2}$.

persistence of cavitation nuclei) which carry over from one pulse to the next (Leighton, 1994, Section 5.3), on the whole the cavitation effect is a far more rapid response than hyperthermia and, what is more, is a threshold phenomenon. Therefore, if only these three intensities were available, I_{TP} would probably be the more useful than either I_{PA} or I_{TA} in discussion of the cavitation hazard. It is therefore no coincidence that the peak rarefaction pressure, the most widely accepted amplitude measurement for the discussion of cavitation hazard at a known frequency, contains much more information in common with the I_{TP} than it does with either I_{PA} or $I_{TA.}$

Of course there are numerous other ways of measuring intensities, and indeed it is important to include spatial as well as temporal information into measurement of intensity. This is not only because ultrasonic fields are often focused (leading for example to the use of the subscripts SA or SP to indicate spatial average or spatial peak measurements). It is also because, at all frequencies, acoustic waves have the propensity to be changed by the environment (Table 1 illustrates the propensity for reflection through the presence of small values for $(1 - |R|^2) \times 100\%$), which can lead to highly anisotropic fields, a feature which will be discussed further in Section 3.5.

3. Nonlinear propagation

3.1. The loss of linearity

The preceding section illustrated how complex notation can readily be used to describe several important features of linear acoustic wave propagation (as it can for waves of other types). This formulation is very widespread in acoustics because, such is the sensitivity of the human ear at audiofrequencies (Section 7), a great deal of the acoustic propagation that has been modelled is of low enough amplitude to allow for the use of linear theory. However at ultrasonic frequencies, the amplitudes used can be sufficiently high that nonlinear propagation occurs. One reason for this is because high source levels are often used to ameliorate signal-to-noise problems when ultrasonic absorption is high, and it does tend to increase with increasing frequency (see Section 2.2 and Table 2). In addition, without the constraint to avoid pain and hearing damage, ultrasound can be exploited to process the medium, which almost always requires higher acoustic pressure amplitudes than encountered at audio frequencies, where the response of the ear is the primary consideration.

Of course when such high source levels generate fields which propagate nonlinearly, the use of complex representation for a wave (which is ubiquitous throughout linear acoustics[13]) is invalid. This can be simply illustrated through the quadratic process, which is probably the simplest and most common order of nonlinearity that is considered mathematically (consider the early terms of a Taylor Series). Whilst the square of the complex representation gives signal only at twice the original frequency (i.e. $(e^{j\omega t})^2 = e^{j2\omega t}$), trigonometric representation shows there are additional components in the signal, as can be seen from footnote 12. Indeed comparison with that footnote explicitly shows that the convention of using the real component of the complex entity to represent the measurable quantity is flawed if the process is nonlinear, since it reveals the errors in the above complex example (i.e. $(\text{Re}(e^{j\omega t}))^2 = \cos^2 \omega t \neq \text{Re}(e^{j2\omega t}) = \cos 2\omega t$). Higher powers act in a similar manner, e.g.

$$(\text{Re}(e^{j\omega t}))^3 = \cos^3 \omega t = (\cos 3\omega t + 3 \cos \omega t)/4 \neq \text{Re}(e^{j3\omega t}) = \cos 3\omega t. \tag{12}$$

If the regime is indeed nonlinear, then one loses not only the ability to use complex representation of waves, but also a plethora of the most useful mathematical techniques in wave physics, including small amplitude expansions, Green's function, Fourier transforms, superposition and addition of solutions.

---

[13]Consider a parameter u_1 that is a function of the time t (the argument applies equally to the spatial coordinates). Say that an operation G transforms u_1 into w_1, so that $G(u_1) = w_1$. Similarly the operator might act on a second parameter, u_2, such that $G(u_2) = w_2$. If G is a linear operator, then $G(u_1 + u_2) \propto w_1 + w_2$. Thus examples of linear operations on $e^{j\omega t}$ are: multiplication by a real constant, (i.e. $G(u_1) = \chi u_1$); differentiation by time ($G(u_1) = \partial u_1/\partial t$); double-differentiation by time ($G(u_1) = \partial^2 u_1/\partial t^2$); and displacement in time ($G(u_1(t)) = u_1(t + \tau)$) where χ and τ are real constants. However important operations which are *not* linear include taking the square of a parameter ($G(u_1) = u_1^2$) and related functions.

3.2. The source of the nonlinearity

Perhaps the most important equation in acoustics is the one which defines the sound speed in terms of the equation of state for the medium $p = p(\rho, S)$ where S is the entropy and p is the sum of all steady and unsteady pressures in the medium. In an infinite body of material that contains no dissipation, the sound speed c may be defined through

$$c^2 = \frac{\partial p(\rho, S)}{\partial \rho},\tag{13}$$

which in turn describes the adiabatic or isentropic bulk modulus B_S, and the isothermal bulk modulus B_T, of the material[14]:

$$B_S = \rho \left(\frac{\partial p}{\partial \rho}\right)_S, \quad B_T = \rho \left(\frac{\partial p}{\partial \rho}\right)_T.\tag{14}$$

Nonlinearity in the relationship between reversible, adiabatic variations in pressure p and density ρ in a medium of constant composition, can be characterised at small amplitudes through a Taylor series expansion of the equation of state along the isentrope for which the specific entropy S takes the value S_0 (Beyer, 1998):

$$p - p_0 = \left.\frac{\partial p}{\partial \rho}\right|_{S,0} (\rho - \rho_0) + \frac{1}{2!} \left.\frac{\partial^2 p}{\partial \rho^2}\right|_{S,0} (\rho - \rho_0)^2 + \frac{1}{3!} \left.\frac{\partial^3 p}{\partial \rho^3}\right|_{S,0} (\rho - \rho_0)^3 + \cdots,\tag{15}$$

where p_0 and ρ_0 are the unperturbed values of pressure and density, respectively. The subscript 0 on the partial derivatives indicates that they are evaluated at the unperturbed state (ρ_0, S_0) (Hamilton and Blackstock, 1998). Equating the perturbation $(p - p_0)$ to the acoustic pressure P, and writing the density variation as $\Delta\rho = \rho - \rho_0$ Eq. (15) can be rewritten as:

$$p - p_0 = P = A\left(\frac{\Delta\rho}{\rho_0}\right) + \frac{B}{2!}\left(\frac{\Delta\rho}{\rho_0}\right)^2 + \frac{C}{3!}\left(\frac{\Delta\rho}{\rho_0}\right)^3 \cdots,\tag{16}$$

where

$$A = \rho_0 \left.\frac{\partial p}{\partial \rho}\right|_{S,0}, \quad B = \rho_0^2 \left.\frac{\partial^2 p}{\partial \rho^2}\right|_{S,0}, \quad C = \rho_0^3 \left.\frac{\partial^3 p}{\partial \rho^3}\right|_{S,0}.\tag{17}$$

Through (13) we can interpret the description of A in (17) as describing the isentropic speed of sound for small amplitude signals, c_0:

$$c_0 = \sqrt{\left.\frac{\partial p}{\partial \rho}\right|_{S,0}} = \sqrt{\frac{A}{\rho_0}}.\tag{18}$$

This is the sound speed at which the linear waves inherent in the descriptions of Section 2 propagate. Those wave descriptions stem from the fact that solutions to the plane wave equation, used for most of audio acoustics, are of the form $P = g(t \pm x/c_0)$ for the acoustic pressure and $v = f(t \pm x/c_0)/(\rho_0 c_0)$ for the particle velocity. The particular forms $e^{j(\omega t - kx)}$, used for the example of Eq. (2), form a subset of these general solutions. The $(t - x/c_0)$ argument represents waves travelling towards $x \to \infty$ whilst the $(t + x/c_0)$ argument represents waves travelling in the opposite direction, towards $x \to -\infty$.

Substitution shows that $P = g(t \pm x/c_0)$ and $v = f(t \pm x/c_0)/(\rho_0 c_0)$ are satisfactory solutions of the one dimensional linearised plane wave equation (often called the 'plane wave equation' by acousticians because of

---

[14]The bulk modulus in turn is simply a three-dimensional form of the stiffness familiar from simple spring-bob oscillations, where the negative sign makes the bulk modulus positive for most (but not all) materials, specifically those which are compressed by an increase in pressure. The bulk modulus serves a stiffness-like role, in that the square root of the ratio of it to an inertial term, provides a characteristic time^{-1} parameter for the material (that parameter being the sound speed for an acoustic wave (m s^{-1}); in the spring-bob, the root of the ratio of the stiffness to the bob mass provides the natural frequency (rad s^{-1})).

the dominance of the assumption in acoustics that the propagation is linear), which is given below for pressure

$$\frac{\partial^2 P}{\partial t^2} = c_0^2 \frac{\partial^2 P}{\partial x^2} \tag{19}$$

and again for particle velocity:

$$\frac{\partial^2 v}{\partial t^2} = c_0^2 \frac{\partial^2 v}{\partial x^2}. \tag{20}$$

Such substitutions are readily undertaken, given that

$$
\begin{aligned}
\frac{\partial P}{\partial t} &= \frac{\partial g}{\partial(t \pm x/c_0)} \frac{\partial(t \pm x/c_0)}{\partial t} = g' \frac{\partial(t \pm x/c_0)}{\partial t} = g', \\
\frac{\partial^2 P}{\partial t^2} &= \frac{\partial g'}{\partial(t \pm x/c_0)} \frac{\partial(t \pm x/c_0)}{\partial t} = g'' \frac{\partial(t \pm x/c_0)}{\partial t} = g'', \\
\frac{\partial P}{\partial x} &= \frac{\partial g}{\partial(t \pm x/c_0)} \frac{\partial(t \pm x/c_0)}{\partial x} = g' \frac{\partial(t \pm x/c_0)}{\partial x} = \pm \frac{g'}{c_0}, \\
\frac{\partial^2 P}{\partial x^2} &= \pm \frac{1}{c_0} \frac{\partial g'}{\partial(t \pm x/c_0)} \frac{\partial(t \pm x/c_0)}{\partial x} = \pm \frac{g''}{c_0} \frac{\partial(t \pm x/c_0)}{\partial x} = \frac{g''}{c_0^2},
\end{aligned}
\tag{21}
$$

where $g' = \partial g / \partial(t \pm x/c_0)$. Similarly, given $f' = \partial f / \partial(t \pm x/c_0)$ then:

$$
\begin{aligned}
\frac{\partial v}{\partial t} &= \frac{1}{\rho_0 c_0} \frac{\partial f}{\partial(t \pm x/c_0)} \frac{\partial(t \pm x/c_0)}{\partial t} = \frac{f'}{\rho_0 c_0} \frac{\partial(t \pm x/c_0)}{\partial t} = \frac{f'}{\rho_0 c_0}, \\
\frac{\partial^2 v}{\partial t^2} &= \frac{1}{\rho_0 c_0} \frac{\partial f'}{\partial(t \pm x/c_0)} \frac{\partial(t \pm x/c_0)}{\partial t} = \frac{f''}{\rho_0 c_0} \frac{\partial(t \pm x/c_0)}{\partial t} = \frac{f''}{\rho_0 c_0}, \\
\frac{\partial v}{\partial x} &= \frac{1}{\rho_0 c_0} \frac{\partial f}{\partial(t \pm x/c_0)} \frac{\partial(t \pm x/c_0)}{\partial x} = \frac{f'}{\rho_0 c_0} \frac{\partial(t \pm x/c_0)}{\partial x} = \pm \frac{f'}{\rho_0 c_0^2}, \\
\frac{\partial^2 v}{\partial x^2} &= \pm \frac{1}{\rho c_0^2} \frac{\partial g'}{\partial(t \pm x/c_0)} \frac{\partial(t \pm x/c_0)}{\partial x} = \pm \frac{f''}{\rho_0 c_0^2} \frac{\partial(t \pm x/c_0)}{\partial x} = \frac{f''}{\rho_0 c_0^3}.
\end{aligned}
\tag{22}
$$

The following analysis will demonstrate two features. First, that the linearised plane wave equation is not valid for waves of finite amplitude, and hence, if we are strictly accurate, linear acoustic waves of the form of (19) and (20) never propagate in fluids (gases and liquids). Most of audiofrequency acoustics, of course, operates on the assumption that the wave amplitude is so small that the linear representation is accurate to within our ability to measure it. As discussed in Section 7, this is often not the case in ultrasonic work. Hence the second purpose of the following analysis is to illustrate the important terms which must be small in order for linear propagation models to be adequate.

The characterization of the propagation of an acoustic wave in a fluid requires three fundamental inputs enshrined in equations reflecting: first, the conservation of mass in a fluid; second, the fluid dynamic properties relating such motions to the pressure gradient which causes them; and third, an equation which shows that pressure gradient to be part of a longitudinal wave. Stated in one-dimensional form, these three equations are, respectively: the equation of continuity:

$$\frac{\partial \rho}{\partial t} + \frac{\partial(\rho v)}{\partial x} = 0, \tag{23}$$

where v is the particle velocity, and ρ the fluid density; Euler's equation for an inviscid fluid:

$$v \frac{\partial v}{\partial x} + \frac{\partial v}{\partial t} = -\frac{1}{\rho} \frac{\partial p}{\partial x}, \tag{24}$$

where p is the sum of all steady and unsteady (assumed here to be purely acoustic) pressures; and an equation which relates the wavespeed to the equation of state (Eq. (13)).

Combination of these three equations allows formulation of the propagation of acoustic longitudinal waves in a fluid, linearisation allowing the generation of what is generally termed the (linearised) plane wave equation. In the small amplitude regime where this is applicable, the sound speed is represented by the phase speed in the linear limit c_0, and the approximation[15] made that $\rho^{-1} \approx \rho_0^{-1}$ where ρ_0 is the equilibrium density:

$$\rho = \rho_0(1 + \Delta\rho/\rho_0) \Rightarrow \rho^{-1} = \rho_0^{-1}(1 + \Delta\rho/\rho_0)^{-1} \approx \rho_0^{-1}(1 - \Delta\rho/\rho_0 + \cdots)$$

$$\Rightarrow \rho^{-1} \approx \rho_0^{-1} - \Delta\rho/\rho_0^2 + \cdots$$

$$\Rightarrow \Delta\rho/\rho \approx \Delta\rho/\rho_0 - (\Delta\rho/\rho_0)^2 + \cdots$$

$$\Rightarrow \Delta\rho/\rho \approx \Delta\rho/\rho_0 \Rightarrow \rho^{-1} \approx \rho_0^{-1}, \quad \left(\frac{\Delta\rho}{\rho_0} \ll 1\right). \tag{25}$$

In this linear limit Eq. (13) gives

$$c_0^2 \frac{\partial\rho}{\partial t} = \frac{\partial p}{\partial t}, \quad c_0^2 \frac{\partial\rho}{\partial x} = \frac{\partial p}{\partial x} \tag{26}$$

and substitution of the first equation of (26) into (23), with (25) (i.e. $\rho^{-1} \approx \rho_0^{-1}$), gives:

$$\frac{1}{c_0^2} \frac{\partial p}{\partial t} + \frac{\partial(\rho v)}{\partial x} = 0 \Rightarrow \frac{\partial v}{\partial x} + \frac{v}{\rho_0} \frac{\partial\rho}{\partial x} = -\frac{1}{\rho_0 c_0^2} \frac{\partial p}{\partial t}. \tag{27}$$

Similarly, if from (25) we have $\rho^{-1} \approx \rho_0^{-1}$, then Euler's Eq. (24) becomes:

$$v \frac{\partial v}{\partial x} + \frac{\partial v}{\partial t} = -\frac{1}{\rho_0} \frac{\partial p}{\partial x}. \tag{28}$$

Linear acoustics are based on the assumption that two of the terms in the above series of equations are negligible, specifically that $|(v/\rho_0)(\partial\rho/\partial x)| \ll |\partial v/\partial x|$ when calculating $(\partial p/\partial t)/(\rho_0 c_0^2)$ using (27); and that $|v(\partial v/\partial x)| \ll |\partial v/\partial t|$ when calculating $(\partial p/\partial x)/\rho_0$ using (28). Differentiation of (27) with respect to t, and of (28) with respect to x, gives the one dimensional linearised plane wave equation for pressure (19) if the equivalence $(\partial^2 v/\partial x\partial t) = (\partial^2 v/\partial t\partial x)$ is made. As discussed above, Eq. (19) describes a linear pressure wave propagating at speed c_0, and has solutions $P = g(t \pm x/c_0)$, proven using the substitutions of (21) into (19).

Similarly differentiation of (27) with respect to x, and of (28) with respect to t, with the same two terms deemed to be negligible, gives the one dimensional linearised plane wave equation for particle velocity (20), with solutions $v = f(t \pm x/c_0)/(\rho_0 c_0)$, proven using the substitutions of (22) into (20).

If the linear solutions $P = g(t \pm x/c_0)$ and $v = f(t \pm x/c_0)/(\rho_0 c_0)$ are valid, then the conditions which make them valid (i.e., which ensure $|v(\partial v/\partial x)| \ll |\partial v/\partial t|$ and $|(v/\rho_0)(\partial\rho/\partial x)| \ll |\partial v/\partial x|$) are readily found. Taking the first inequality, $|v(\partial v/\partial x)| \ll |\partial v/\partial t|$, substitution from (22) gives

$$\frac{\partial v}{\partial t} = f' \quad \text{and} \quad v \frac{\partial v}{\partial x} = \pm \frac{v}{c_0} f' \Rightarrow v \frac{\partial v}{\partial x} / \frac{\partial v}{\partial t} = \pm \frac{v}{c_0}. \tag{29}$$

Consider the second inequality $|(v/\rho_0)(\partial\rho/\partial x)| \ll |\partial v/\partial x|$ in the same linear limit, where (26) is valid, and recall that all perturbations in pressure are assumed to be acoustic. Since neglect of the nonlinear term in (28) implies

---

[15]Linear acoustics requires the approximation $\rho^{-1} \approx \rho_0^{-1}$ which, as Eq. (25) shows, is obtained by ignoring the quadratic (and higher) terms (e.g. $(\Delta\rho/\rho_0)^2 + \ldots$). It is not sufficient to say that, given $\rho = \rho_0 + \Delta\rho$ and $\Delta\rho/\rho_0 \ll 1$, we can in turn make the approximation that $\rho \approx \rho_0$, since that would be to ignore the first order perturbation, an incompressible assumption which is at odds with the concepts behind linear acoustics (Fig. 2) and would, for example, imply infinite sound speeds.
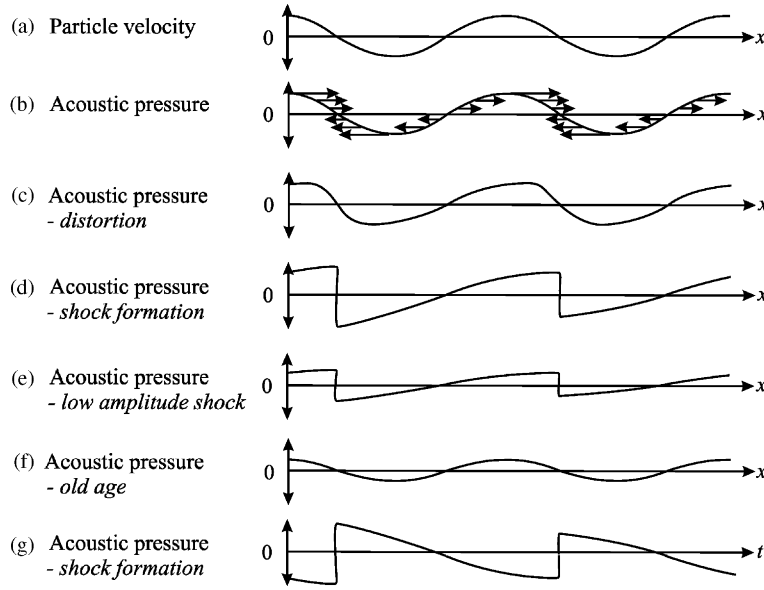
Fig. 5. Schematic showing the development of an infinite, sinusoidal plane wave during nonlinear propagation. The first two graphs (repeated from Fig. 2) show the initial sinusoidal waveform in terms of (a) particle velocity and (b) pressure. They are both plotted as a function of position x, with the particle velocities are superimposed as vector arrows on the pressure plot of (b). Unlike during the linear propagation of Fig. 2, these waveforms propagate nonlinearly, such that as it propagates away from the source, the pressure waveform distorts (c), and if dissipation is not too great, can eventually form a shock (d). Enhanced absorption of the higher frequencies then causes the amplitude to decrease (e), until eventually the 'old age' waveform is sinusoidal once more (f). Parts (a) to (f) of the figure plot the pressure waveforms as a function of x; Part (g) plots the pressure waveform of (d) as a function of time t.

that $\partial v/\partial t = \left(-\partial p/\partial x\right)/\rho_0$, then substitution from (26) and (18) reduces the second ratio to

$$
\begin{aligned}
\frac{v}{\rho_0}\frac{\partial \rho}{\partial x}\Big/\frac{\partial v}{\partial x} &= \frac{v}{\rho_0 c_0^2}\frac{\partial p}{\partial x}\Big/\left(\pm f'/\rho_0 c_0^2\right) \\
&= -v\rho_0\frac{\partial v}{\partial t}\Big/\left(\pm f'\right) \\
&= -v\rho_0\left(f'/\rho_0 c_0\right)/\left(\pm f'\right) \\
&= \mp\frac{v}{c_0}.
\end{aligned}
\tag{30}
$$

Hence the linear limit is approached as the acoustic Mach number (v/c_0)f becomes small and the two nonlinear terms become negligible. The consequence of finite acoustic Mach numbers is that Eqs. (19) and (20) no longer hold, and a waveform which is initially sinusoidal will not remain so because of two nonlinear effects which act co-operatively. Both can be readily understood through the realization that, if dissipation is small, then P and v would be in phase (Leighton, 1994, Section 1.2.3(a); Fig. 2). First, there is a *convection* effect. In simple terms, if v/c is not negligible, then parts of the wave tend to propagate as $c+v$. The particle velocity varies throughout the wave, and so the greater the local acoustic pressure, the greater the velocity of migration of that section of the wave. Consider the case when P and v are in phase (as occurs if the impedance is real— see Section 2.1). This was shown in Fig. 2, and the particle velocity and pressure plots from there are repeated in Figs. 5(a) and (b). However the particle velocities are superimposed as vector arrows on the pressure plot of Fig. 5(b). Unlike the linear propagation of Fig. 2, during the nonlinear propagation of Fig. 5 the regions of compression (where the v and c are in the same direction) would tend to migrate faster than the regions of

rarefaction (where v is opposite to c). The pressure peak propagates with the greatest speed, the trough with the least (Fig. 5(b)).

Second, there is an effect which arises because, when a fluid is compressed, its bulk modulus and stiffness increase. This results in an increase in sound speed, and this effect too will cause the pressure peaks to travel at greater speed than the troughs, and tend to try to catch up and encroach upon them (Fig. 5(c)).

A continuous wave that is initially sinusoidal (Fig. 5(a) and (b)) will therefore distort. The compressional parts of the wave 'catch up' on the rarefaction components as the propagation progresses, such that it becomes distorted[16] (Fig. 5(c)). Such distortion of course is accompanied by the appearance in the spectrum of energy at harmonics of the driving frequency. Balancing this tendency is, of course, the absorption of the medium: if it is very great, the wave amplitude will decrease so rapidly that, even at high source levels, high Mach numbers will not be maintained for much of the propagation path away from the source, and the nonlinear distortion is negligible. However where absorption is not so great, such distortion can proceed until a shock wave develops (Fig. 5(d)). The discontinuity length (or shock-formation distance, L_{dis} see Eq. (42)) is taken to be the distance propagated by acoustic plane waves in a lossless medium when an infinite slope first appears in the waveform. For a shock to develop in this way, the absorption must not have been so great as to dissipate the energy in the wave before the shock can develop. Just as the discontinuity length is characteristic of the distance over which the wave would propagate *in the absence of dissipation* in order to exhibit this strong nonlinear feature, so the e-folding length of Eq. (7) typifies the distance over which the wave will propagate *in the absence of nonlinearity* in order to show the effects of absorption strongly. The competition between the influences of nonlinearity and viscothermal absorption is characterised by the dimensionless Gol'dberg number Γ_G (Gol'dberg, 1956), equal to:

$$\Gamma_G = \frac{1}{bL_{dis}} = \frac{2L_e}{L_{dis}}, \tag{31}$$

where b is the attenuation coefficient for small amplitude waves (Eq. (5)), and L_e is the e-folding distance for energy (Eq. (7)). Since for the waves of Section 2.2, the length $2L_e$ equals the e-folding distance for the amplitudes of acoustic pressure, displacement and particle velocity, then the Gol'dberg number can be thought of as the ratio of two lengths, one characterising the dissipation and the other characterising the nonlinearity. Both lengths pertain to the distance through which the wave would have to propagate, in the absence of the competing effect, for their characteristic effect to manifest itself strongly. A large value of the Gol'dberg number indicates that the nonlinearity has generated a shock long before the wave has been strongly absorbed.

In Fig. 5(d), the Gol'dberg number has been sufficiently great for a shock to develop. However, as discussed above, the process of nonlinear distortion is, in the frequency domain, associated with the 'pumping' of energy from the fundamental frequency up to higher frequencies where the absorption is greater (for most but not all materials—see Fig. 15). There is therefore enhanced absorption of this energy, such that further propagation is accompanied by a decrease in wave amplitude. The waveform amplitude decreases (Fig. 5(e)). Eventually this hypothetical wave is sinusoidal once more, as the only unabsorbed energy is at the fundamental (Fig. 5(f)). If the absorption is greater at higher frequencies, then whilst this 'old age' waveform might resemble the sinusoid that would have been detected had only linear propagation occurred, its amplitude is less than would have been found at equivalent distances from the source had the same initial wave propagated only linearly. Similarly the higher absorption would mean more acoustic energy has been converted to heat during this propagation path, than would have occurred had only linear propagation of the same initial waveform taken place.

Fig. 5(g) plots the shocked waveform as a function of time t, instead of position x (as was used for the rest of Fig. 5 and for Fig. 2). This is because the explanations in both Fig. 2 and Fig. 5 are easier with respect to the spatial coordinate. However most measurements are made with respect to the temporal coordinate. In comparing Figs. 5(d) and (g), note that the appearance of the waveform is reversed: this is because that

---

[16]An additional feature (not apparent in Fig. 5 because it illustrates the distortion in an infinite plane wave) arises from the action of dissipation and diffraction, which cause phase shifts in the various frequency components of the wave. As a result, the distorted waveform is not symmetrical about the zero-line: in general the trough, which corresponds to negative values of the acoustic pressure, becomes rounded whilst the positive peak is augmented.

portion of a waveform which arrives first at a fixed measuring point in the medium (such as a fixed microphone or hydrophone) is plotted at the earliest arrival times in Fig. 5(g). This has important uses: for example, whilst explanation of nonlinear propagation is most easily done by referring to waveforms plotted as a function of x, the waveforms appear to be reversed when monitored using a fixed hydrophone and
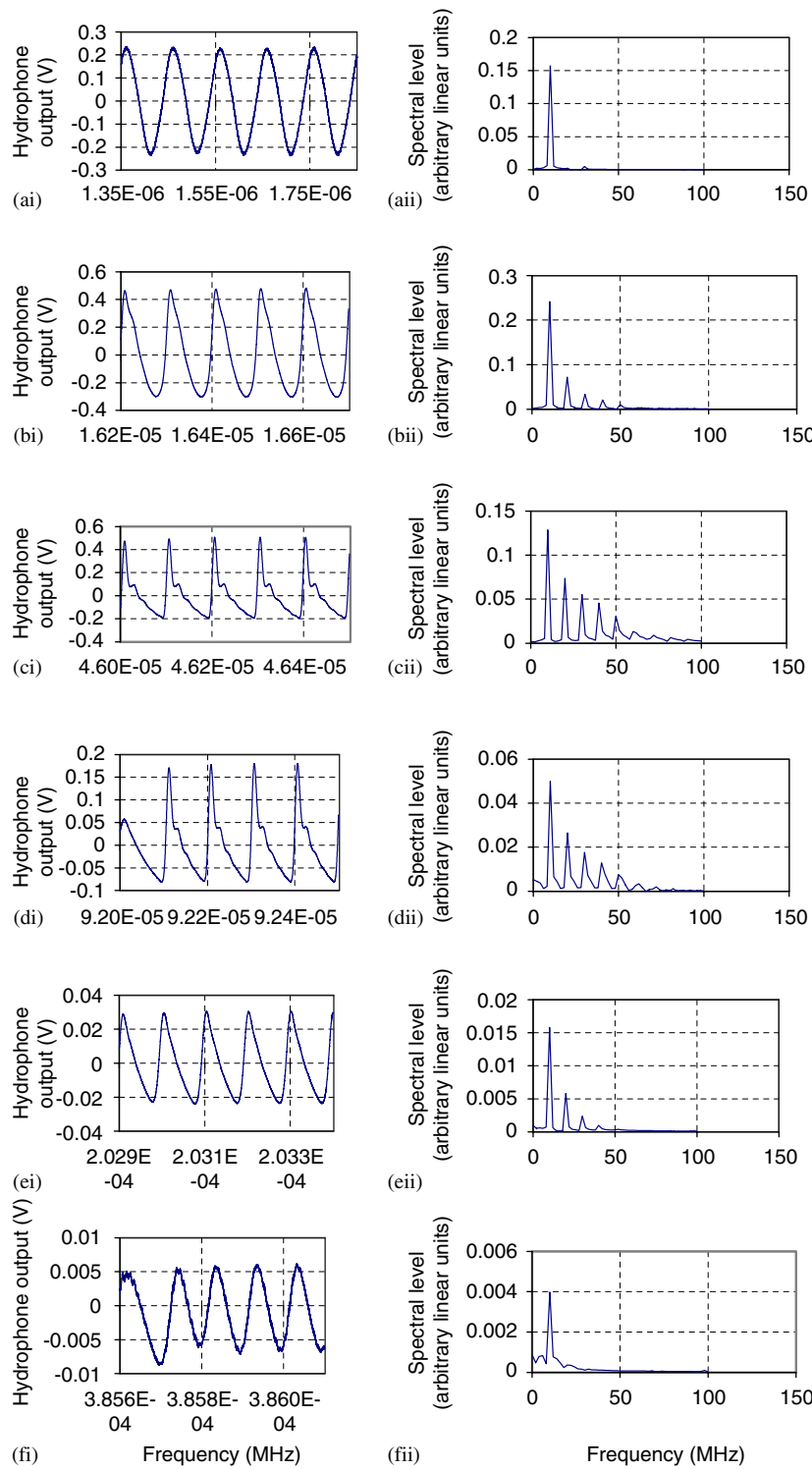
oscilloscope (which plot as a function of t). This, with the asymmetry described in Footnote 16, can be exploited in measuring the polarity of hydrophones, i.e., in determining whether it is a compression or a rarefaction which causes a positive increase in voltage.

Fig. 5 therefore explains the data in Fig. 6, where the waveform is detected by a fixed hydrophone and displayed on an oscilloscope. The real data in (i) illustrate the time history of the wave, measured at increasing distances ((a)–(f)) from these sources. The corresponding spectra are shown in (ii). Close to source, the waveform is initially nearly sinusoidal (a(i)) and single frequency (a(ii)). As it propagates through the medium, each compressive region gains upon the preceding rarefactive half-cycle, the peak positive acoustic pressure appearing earlier and earlier in the time history compared to the peak rarefaction. An accumulated steepness of the waveform between the two develops (b(i)) and harmonics appear in the spectrum (b(ii)). After propagating a distance corresponding to the discontinuity length, the waveform includes a discontinuity, in that a shock wave develops (c(i)). A continuum component may increase in the spectrum (c(ii)). The contribution of higher harmonics to the waveform is clearly visible (c(i)). Note that the amplitude after this time decreases, because any further compressional advance leads to dissipation and results in a reduction in the amplitude of the shock. This is because the waveform distortion has been equivalent to transferring some of the energy of the initial wave to higher frequencies, which are more strongly absorbed (d,e) The energy transfer is not sufficient to maintain the shock, and the wave approaches a low-amplitude sinusoidal form (termed 'old age') (f).

The vastness of the frequency range covered in underwater ultrasonics has several implications (see Section 5.1). No one hydrophone can span it (Fig. 7), and the calibration of hydrophones (which may themselves be invasive, directional etc.) requires very great skill. The nonlinear propagation described in the preceding paragraph is one tool which is exploited to decrease the time taken for a hydrophone calibration. A standard calibrated hydrophone is placed sufficiently far from the source to detect energy at many harmonics (as in Fig. 6(d)). If the sound field remains constant when the calibrated sensor is replaced by the unknown sensor and monitors the same positioning the sound field, comparison of the two measured signals allows many frequencies to be calibrated simultaneously.

To summarise the effect on signal-to-noise ratios (SNRs) during nonlinear propagation, energy is pumped from lower to higher frequencies, where it is preferentially absorbed. This means that the net attenuation over distance will be greater if nonlinear propagation occurs, than if conditions were linear. Furthermore, a narrow band detector tuned to the frequency of the emitted pulse might fail to detect energy in the returned signal which is outside of its bandwidth (and hence 'invisible' to it). Both of these will act to reduce the signal-to-noise of the received signal, a problem which may not be alleviated by simply increasing the amplitude of the emitted pulse (since this enhances the nonlinear effects, a phenomenon known as "acoustic saturation"—see Section 3.4).

Propagation such as that described above is just one of the possible sources of nonlinearity: others include the transducer itself, and entities within the water column (see Section 4). As the earlier discussion of the Gol'dberg number showed, the degree to which the effects occur for a given acoustic signal in a given environment of course depends not only on the nonlinearity (and hence the rate at which energy is transferred from lower to higher frequencies) but also on the absorption. Some features, such as bubbles, increase both, and it may be that the absorption is so great that nonlinearity is not present in the received signal (although the fact that acoustic absorption by a bubble population tends to peak, rather than simply increase with

Fig. 6. The signal from a 0.25″ diameter Panametrics plane transducer, driven by a 10-cycle 10 MHz tone burst. Part (i) shows the oscilloscope voltage (V) against the timebase (s). The overall system sensitivity (hydrophone plus amplifier, minus loading correction) at 10 MHz was 378.65 nV/Pa, so the peak positive pressures are around 1.2 MPa. Part (ii) shows the amplitude spectral level against frequency (MHz). Measurements were made with a $2 \times 9 \, \mu m^2$ bilaminar membrane hydrophone (Marconi, with a high gain, 100 MHz bandwidth preamplifier). This had an active element of diameter 0.5 mm, separated from the transducer face by (a) 2 mm, (b) 24 mm, (c) 68 mm (the position of the last axial maximum, i.e., the ratio of the square of the faceplate radius to the acoustic wavelength; see Eq. (69)), (d) 136 mm, (e) 300 mm, (f) 570 mm, determined from the time relative to the transducer firing. Data were recorded by a Tektronix TDS 784D DPO oscilloscope (50 ns/div, 5000 point waveforms). The experimental system was aligned according to IEC 61102 prior to measurement (International Electrotechnical Commission, 1991): the water temperature was 18.7 °C. (Measurements taken at the request of the author by M. Hodnett and B. Zeqiri, National Physical Laboratory, UK).
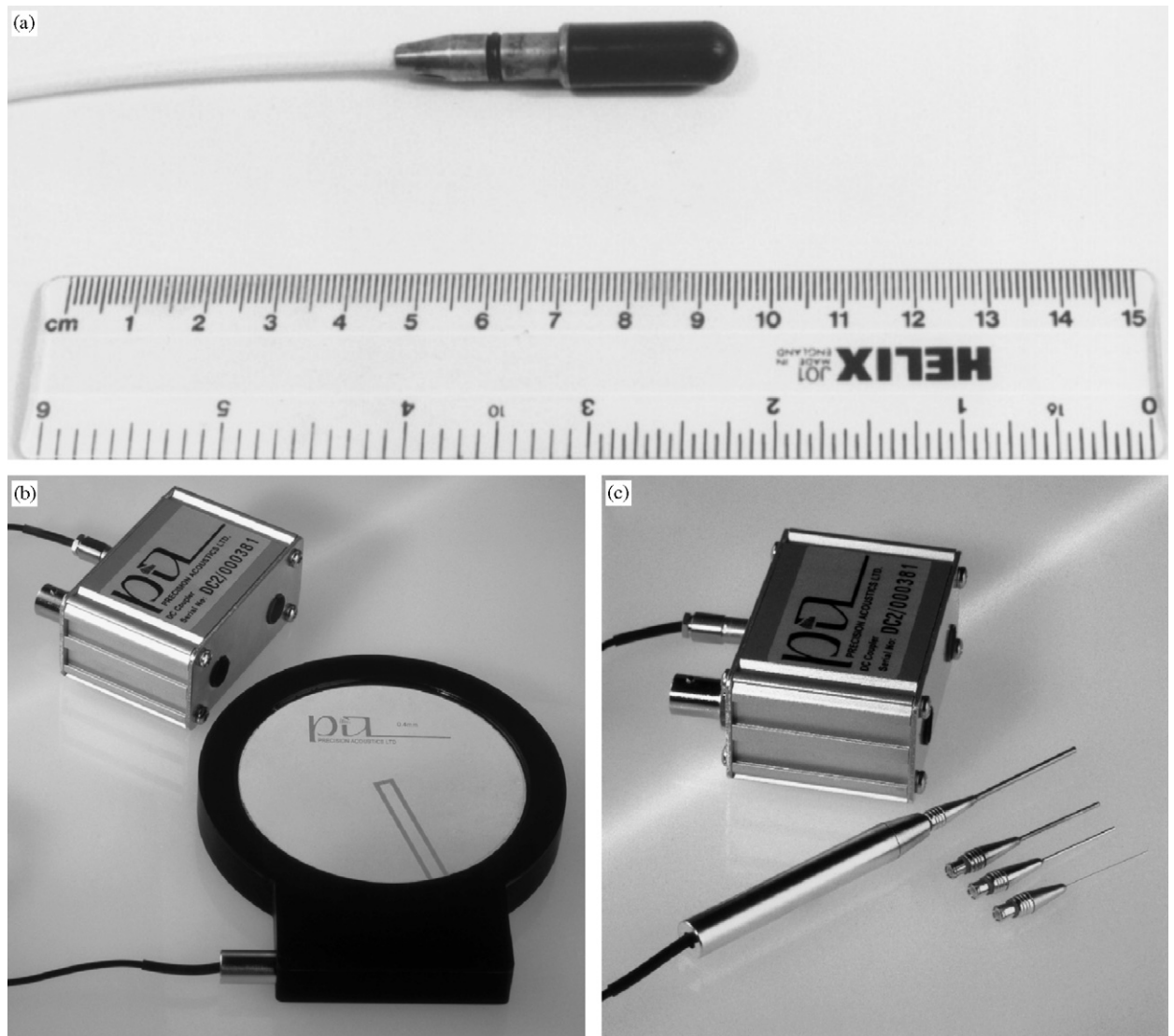
Fig. 7. Three common types of hydrophone. (a) Bruel and Kjaer 8013 miniature hydrophone, suitable for measurements from roughly 50 Hz–200 kHz. (b) Polyvinylidene fluoride (PVDF) coplanar shielded membrane hydrophone (Precision Acoustics Ltd, Dorchester UK, Hydrophone type CPM04/1) with 0.4 mm active element, calibrated from 1 MHz to 60 MHz (all active element dimensions refer to diameters). The preamplifier is partially inserted in the hydrophone housing, and a DC Coupler box is also shown. (c) Selection of PVDF needle hydrophones (Precision Acoustics Ltd, Dorchester UK, Hydrophone type HPM1/1, HPM05/3, HPM02/2, HPM075/1) with 1.0, 0.5, 0.2 and 0.075 mm active elements, respectively. Each hydrophone attaches onto the preamplifier shown (in the figure only the HPM1/1 is attached to the preamplifier). A DC Coupler box is also shown Taken together, this range of needle hydrophones cover a range from 10 kHz to 60 MHz, with each individual needle hydrophone being calibrated across a subset of this (e.g., the 1 mm hydrophone is calibrated from 10 kHz to 20 MHz, whereas the 0.075 mm hydrophone is calibrated from 1–60 MHz). In the photographs of (b) and (c) (obtained courtesy of A. Hurrell and T. Gill, Precision Acoustics Ltd.), the preamplifier is 60 mm long and has a diameter of 9 mm, and the DC Coupler measures $60 \times 45 \times 30$ mm^3.

frequency, may hold opportunities for exploitation of nonlinear effects; see Fig. 15(c)). However its possibility during propagation must be appreciated. This is not only because nonlinear propagation might cause enhanced absorption, or may make some energy in the received signal 'invisible' if it is outside the bandwidth of the detector, but also because it might be exploited. The ability of the propagating medium to generate multiple frequencies, as illustrated in Fig. 6, could not only be used to diagnose the properties of that medium (e.g., bubbly water). It could also be used to generate a signal containing harmonics across a wide frequency

range for simultaneous testing of the scatter at many frequencies from the seabed or a target (the propagation after scattering, being of lower amplitude, would tend to be linear and so preserve the frequency characteristics of the target within the usual linear constraints of absorption, etc.).

A simple model for the transference of some energy from lower to higher frequencies (which does not include the critical absorption component) can be found in the Taylor series expansion (16). This is adequate to demonstrate the generation of harmonics through a nonlinear process (including propagation). If the nonlinear fluid element (in this case the liquid) is subjected to single-frequency insonification $P(t) \propto \cos \omega t$, then the second and third harmonics are generated by the quadratic B and cubic C terms of Eq. (16), with of course additional frequencies as indicated by the trigonometric expansions in footnote 12 and Eq. (12).

There are many ways in which the nonlinearity has been exploited in biomedical ultrasonics (Duck, 2002). The next section however will concentrate on only one application, that of parametric sonar, since it directly shows use of the quadratic nonlinearity, and also provides the background for one of the in-air applications of ultrasound. This is important because, as will be shown in Section 6, most of the in-air applications of ultrasound tend to be based rather on the generation of high signal amplitudes rather than cogent understanding and exploitation of the nonlinearities so generated.

3.3. Parametric sonar

The Taylor series description of the nonlinearity (16) can also be used to illustrate what happens if the medium responds nonlinearly to insonification by an acoustic field consisting of two coherent frequencies. For example, the initial waveform $P(t) \propto \cos \omega_1 t + \cos \omega_2 t$ can generate combination-frequency signals at $\omega_1 \pm \omega_2$, as well as at $2\omega_1$, $2\omega_2$, $\omega_1 \pm 2\omega_2$, $2\omega_1 \pm \omega_2$, etc. since the quadratic terms alone gives $2 \cos \omega_1 t \cos \omega_2 t = \cos(\omega_1 + \omega_2)t + \cos(\omega_1 - \omega_2)t$. Because of this, nonlinear propagation can be exploited to generate a beam of sound far narrower than would be possible for a given source size, were the propagation to behave linearly. In general, to obtain a highly directional acoustic beam, the size of the source must be very much greater than a wavelength (see section 5). Conversely, if the wavelength is much larger than the acoustic source, the sound field tends to be emitted in an omnidirectional manner. This leads to a number of problems and solutions. For example, if one wishes to produce a narrow beam of 'low' frequency sound (i.e., sound for which the wavelength is not significantly less than the source size), linear techniques are precluded by the source size required. For example, a 500 Hz sonar beam would have wavelengths in bubble-free water of ~3 m, and clearly mounting a source much larger than this on, say, the front of a ship is not feasible. Similarly if one has museum exhibits (e.g., paintings) spaced every 2 m and one wishes to direct a beam of sound from the ceiling to a 1 m^2 region in front of each exhibit in order to carry recorded spoken information about that exhibit, the source size would have to be much greater than the wavelength of, say, 500 Hz in air, which is ~0.7 m.

Nonlinear acoustics offers a possible solution to these problems (Bennett and Blackstock, 1975; Yomeyama et al., 1983). Consider two sources, one driven at ω_1 and the other at ω_1, which are physically big enough to generate narrow ultrasonic beams. These two beams (called the 'primaries') are directed such that they overlap in the medium. In the region where they overlap, they can generate a highly directional propagating wave which contains the various frequencies listed above, and more. The signal at the 'difference frequency' $\omega_1 - \omega_2$ is of particular interest,[17] for several reasons. First, the directionality of the emission is far greater than could be obtained with a source of the same size operating at this frequency directly. Second, depending on the medium, the higher frequencies can be more strongly absorbed, so that only the difference frequency propagates to distance (the use of parametric sonar in the oceans in a good example of this). Third, in many practical situations, only the difference frequency is within the bandwidth of the detector (the museum scenario cited above would provide an apt example, the detector here being the human ear). Probably the

---

[17]Note that this generation of a propagating wave at the difference frequency is distinct from the purely linear process of generating beats, which occurs when waveforms are superimposed at the detector. Another distinct process by which difference frequencies (and other signals) can be generated is through nonlinearities in the receiver (e.g. the ear, preamplifier, or microphone; see Section 6.4). These can act without necessarily there being nonlinearity present in the propagation, as can nonlinearities in the transmitter or the data acquisition process.

major drawback of this application, which has implications for the safe use of ultrasound, is that it is in general very difficult to generate high intensities at the difference frequency using this system (because it is a second-order process, based for example on the quadratic term in Eq. (16)). This could lead to the use of very high levels for the primary signals in such applications. Given the paucity of information on the safe levels for human exposure to ultrasound in air (Section 6), and the lack of traceability for the measurement of such fields (see Section 2.3), this could be a safety issue.

There are in fact many commercial systems available which probably exploit nonlinear ultrasonic interactions to generate localised audiofrequency sound.[18] HyperSonic Sound[TM] advertise: "This ability to direct or focus sound into a tight beam has a wealth of applications. Imagine: directing narration in a museum only to the people standing in front of a specific display; capturing and holding customers' attention to advertise a product or promote a brand at the point-of-purchase, without disturbing employees or causing unwanted noise pollution; providing information or messages that can offer direction to shorten wait times to people standing in line; directing an alarm or alert only to the intended operator in a control room environment to assist them in making timely, critical decisions." They cite the following applications: "Digital Signage/NarrowCasting; In-Store Advertising; Museums; Trade Shows; Kiosks; Corporate Lobbies; Command & Control Room; Automotive Dealerships". As the use of other acoustic technologies (such as active noise control and virtual acoustic systems) increases, there may be a proliferation in the application of such parametric technology (to provide, for example focused control sources) to implement them more effectively. This topic of human exposure to high levels of ultrasound is discussed further in Section 6.

3.4. The material and convective nonlinearities

As outlined in Section 3.2, there are two contributions to the change in phase speed of the wave, the change in stiffness (or bulk modulus) and the convection. These are called the *material nonlinearity* and the *convective nonlinearity*, respectively, and are formulated as follows (Leighton, 1994, Section 1.2.3). The propagation velocity of a point in the wave having particle velocity v is

$$\text{Propagation velocity}\big|_{v=\text{constant}} = \frac{\mathrm{d}x}{\mathrm{d}t}\bigg|_{v=\text{constant}} = v + c, \tag{32}$$

where a convection component v is added to c, the local speed of sound. This local speed has in turn been affected by the change in bulk modulus, and is related to c_0, the sound speed for waves of infinitesimal amplitude. This effect can be determined by substituting Eq. (16) into (13) to give:

$$\frac{c}{c_0} = \sqrt{1 + \frac{B}{A}\left(\frac{\Delta\rho}{\rho_0}\right) + \frac{C}{2A}\left(\frac{\Delta\rho}{\rho_0}\right)^2 + \cdots}$$
$$\approx 1 + \frac{B}{2A}\left(\frac{\Delta\rho}{\rho_0}\right) + \frac{1}{4}\left(\frac{C}{A} - \frac{1}{2}\left(\frac{B}{A}\right)^2\right)\left(\frac{\Delta\rho}{\rho_0}\right)^2 + \cdots \tag{33}$$

assuming isentropic conditions and that it is valid to perform this binomial expansion. The ratio B/A is called the second-order nonlinearity ratio of the liquid and characterises the potential size of the nonlinearity. Following Beyer (1998), we make use of the simple relationship for progressive plane linear waves, in isentropic conditions, that follows from Eq. (1) and (18) by, for example, retaining only the first term of the expansion (16)

$$\frac{\Delta\rho}{\rho_0} \approx \frac{P}{A} \approx \frac{p_0 c_0 v}{\rho_0 c_0^2} = \frac{v}{c_0} \tag{34}$$

---

[18]See HyperSonic Sound (http://www.atcsd.com/hss.html); holosonics (http://www.holosonics.com). Note that the web-based material currently available on such products does not allow the author fully to assess the mechanisms or compare the levels with guidelines (Section 6.4), and until this is done any assessment of the potential or otherwise for hazard cannot be made.

using (18) to substitute for A. Retaining only the first two terms in the expansion (33) and substituting for $\Delta\rho/\rho_0$ from (34) gives:

$$c \approx c_0 + \frac{B}{2A}v \tag{35}$$

The equivalent expression for an isentropic gas can readily be obtained by noting that the expansion of the equation state along an isentrope for a perfect gas gives:

$$\frac{p}{p_0} = \left(\frac{\rho}{\rho_0}\right)^\gamma = \left(1 + \frac{\Delta\rho}{\rho_0}\right)^\gamma$$

$$= 1 + \gamma\left(\frac{\Delta\rho}{\rho_0}\right) + \frac{\gamma}{2!}(\gamma - 1)\left(\frac{\Delta\rho}{\rho_0}\right)^2$$

$$+ \frac{\gamma}{3!}(\gamma - 1)(\gamma - 2)\left(\frac{\Delta\rho}{\rho_0}\right)^3 + \ldots \tag{36}$$

where γ is the ratio of the specific heat at constant pressure to that at constant volume. Term-by-term comparison with (16) gives (Beyer, 1998):

$$A = \gamma, \quad \frac{B}{A} = \gamma - 1, \quad \frac{C}{A} = (\gamma - 1)(\gamma - 2) \tag{37}$$

Substitution of (37) into (35) indicates that:

$$c = c_0 + \frac{\gamma - 1}{2}v \tag{38}$$

for a perfectly isentropic gas. Therefore, using (35) and (38), Eq. (32) can be rewritten to include both the material and convective nonlinearities explicitly:

$$\text{Propagation velocity}\big|_{v=\text{constant}} = \frac{\mathrm{d}x}{\mathrm{d}t}\bigg|_{v=\text{constant}} = v + c$$

$$= c_0 + \left(1 + \frac{\gamma - 1}{2}\right)v \ \text{ for a perfectly isentropic gas, and}$$

$$= c_0 + \left(1 + \frac{B}{2A}\right)v \ \text{ for a liquid.} \tag{39}$$

In the brackets in Eq. (39), the unity term corresponds to the contribution from the convective nonlinearity, and the other term to that from the material nonlinearity. For water the ratio $B/2A$ equals 2.5, whereas for air the isentropic gas equivalent is $(\gamma-1)/2 = 0.2$. Therefore in water the dominant cause of the waveform distortion is nonlinearity of the equation of state (the material nonlinearity), whereas in air the distortion arises mainly through convection.

The sum of the material and convective nonlinearities is given by the 'coefficient of nonlinearity' ς, where from Eq. (39):

$$\text{Propagation velocity}\big|_{v=\text{constant}} = \frac{\mathrm{d}x}{\mathrm{d}t}\bigg|_{v=\text{constant}} = c_0 + \varsigma v, \tag{40}$$

where

$$\varsigma = \frac{\gamma + 1}{2} \ \text{ for a perfectly isentropic gas, and}$$

$$\varsigma = 1 + \frac{B}{2A} \ \text{ for a liquid.} \tag{41}$$

For air $\varsigma = 1.2$, and for water $\varsigma = 3.5$. From this one might expect the distortion to be more obvious in water than in air; however one must take into account attenuation of high frequencies. The discontinuity length is given by
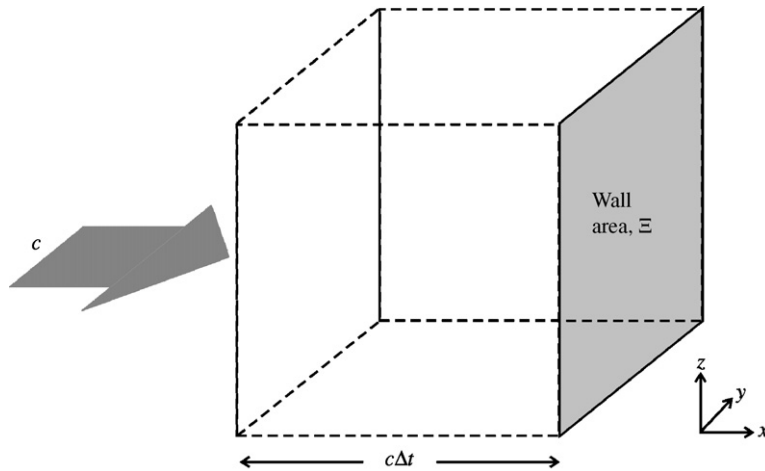
$$L_{\text{dis}} = \frac{1}{\varsigma M k}, \tag{42}$$

Fig. 8. A plane wave, travelling along the x-axis at speed c, approaches a wall of area Ξ (aligned with the yz plane).

where k is the wavenumber and where M is the peak acoustic Mach number of the source, the ratio of the amplitude of the particle velocity at the source to c_0. Thus (assuming large Gol'dberg numbers; Eq. (31)) the shock forms closer to the source as the coefficient ς, which indicates the degree of nonlinearity, increases. It also forms sooner as the amplitude increases, because the speed differential between the peaks and the troughs increases. Similarly L_{dis} decreases with increasing frequency, since this signifies decreasing wavelength, and so the peaks have to travel a shorter distance to catch up with the troughs. If the point of observation is at a distance greater than L_{dis}, then as either amplitude or frequency are increased the discontinuity length decreases, the point where the shock forms moving closer to the source. This means that increasing amounts of energy can be dissipated at the shocks beyond L_{dis} before the wave arrives at the point of observation. If the energy supplied to the wave at the source is continually increased, there comes a point at which the increased dissipation between the discontinuity point and the point of observation outweighs the increase in energy supplied to the wave at the source. Beyond this critical source power, the wave ceases to be dependent upon the source amplitude: any additional energy supplied to the wave by the source is lost at the shock front, and *acoustic saturation* is said to have occurred (Leighton, 1994, Section 1.2.3; Leighton, 1998; Duck, 1999; Duck, 2002).

3.5. Other phenomena

Consider a plane wave, travelling in the $+x$ direction at speed c, approaching a wall in the yz plane of area Ξ (Fig. 8). The wave energy is completely absorbed by the wall. If the wave has intensity I, then the energy absorbed by the wall in a time Δt is $I\Xi\Delta t$. The wall must have applied a force F_r in the $-x$ direction to stop the wave motion, which in time Δt acted over a distance $c\Delta t$. Therefore the work done by the wall on the wave is $F_r c\Delta t$. Equating this to the energy absorbed, we obtain $F_r = \Xi I/c$. From Newton's third law of motion, this must be equal and opposite to the force exerted by the wave on the wall. Therefore upon absorption the wave exerts a *radiation pressure* ($p_{rad,abs}$) in the direction of its motion of magnitude

$$p_{rad, abs} = I/c \tag{43}$$

for normal incidence of plane waves.[19] The force F_r exerted by the wall can also be thought of as acting upon the wave to absorb its momentum. In time Δt the wall absorbs a length $\Delta L = c\Delta t$ of the wave, exerting an

---

[19]Demonstrations of radiation pressure are not confined to acoustics laboratories, but can frequently be seen in science fiction films, where ray guns appear to have the ability to impart a force capable of making the victim (usually a *Star Wars* Imperial stormtrooper) stagger backwards. Likening this motion to that observed when catching a 5 kg bag of potatoes, suggests the radiation force is 50 N. This implies that, during firing, the ray gun would need to project power W equal, from Eq. (43), to a force of $(50c)$ N, where c is the wavespeed. Were the ray-gun to project electromagnetic radiation, such as a laser beam, the power of the gun would have to be $50 \times 3 \times 10^8 = 1.5 \times 10^{10}$ W. This is more than ten times the combined power output of the two 600 MW turbines at the Torness

impulse $F_r \Delta t = \Xi I \Delta L / c^2$ upon the wave, causing a change in momentum of $\Delta \Gamma$. Since after absorption the momentum of wave is zero, then the momentum associated with one wavelength of the wave (setting ΔL equal to λ in the above) is:

$$\Delta \Gamma_\lambda = I \Xi \lambda / c^2. \tag{44}$$

If this normally incident wave is reflected, instead of being absorbed, this momentum must be not simply absorbed but reversed. The wall must exert twice as much force upon the wave, and so the radiation pressure felt by the reflector is:

$$p_{\text{rad,refl}} = 2I/c \tag{45}$$

for total reflection of normally incident waves back along the line of incidence (Leighton, 1994, Section 1.1.4).

As the acoustic wave travels through the medium, it will be absorbed (Section 2.2). However the momentum absorbed from the acoustic field manifests as a flow of the liquid in the direction of the sound field, termed *acoustic streaming* (Lighthill, 1978, Leighton, 1994, Section 1.2.3; Trinh and Robey, 1994). Several potential beneficial uses of this phenomenon have been investigated (Nightingale et al., 1995; Rife et al. 2000; Shi et al., 2002), and it has also been assessed for its possible adverse effects (Starritt et al;., 1991; Barnett et al., 1998). Since it is more usual to consider energy than momentum in the context of acoustic waves, the process is conventionally thought of as the setting up of an energy gradient in the direction of propagation when energy is absorbed from the beam during its passage through an attenuating liquid. A gradient in energy corresponds to a force, and when this acts upon the liquid a streaming flow is generated. The force per unit volume (F/V) equals the gradient in pressure (Δp_{stream}) which causes the liquid to accelerate in the direction of propagation:

$$\Delta p_{\text{stream}} = F/V = 2bI/c. \tag{46}$$

From this equation it is clear that if both intensity and attenuation can vary spatially throughout a sound beam in a uniform medium, then so will the streaming forces and flows. An increase in either parameter will increase the streaming. As will be evident from the preceding section, the pumping of energy into higher frequencies, which are more strongly absorbed than the fundamental, means that attenuation may vary spatially in an acoustic field of finite amplitude. Finite amplitude effects will also affect streaming through the formation of shocks. Starritt et al. (1989) observed the enhancement of streaming in high amplitude diagnostic pulsed ultrasonic fields which have formed shocks in water.

Streaming speeds of up to around 10 cm/s can be demonstrated from clinical ultrasonic equipment. Fig. 9 shows a plan view of dye, carried along by the streaming flow, in three clinical underwater ultrasound beams. The visualisation technique is described by Merzkirch (1987), utilising the electrolysis of water containing dissolved thymol blue indicator. Through the insertion of acoustically-transparent 'clingfilm' windows in the diagnostic *B*-scan field, Starritt et al. (1991) demonstrated that, in addition to local energy absorption, there is a more significant contribution to unimpeded flow in the far-field region beyond the focus. To be specific, this comes from a narrow jet of flowing liquid which is generated near the focus and flows onwards from there with much the same speed. They therefore concluded that the acoustic stream is powered significantly by a near-focus 'source pump', which results from the enhanced absorption of the high-frequency components of the distorted finite amplitude pulses there. In materials, such as tissue, which are not free to flow, stresses may still be set up by these processes, and consideration must be given to the response of the medium (Starritt et al., 1991).

There is a second type of streaming associated not with the spatial attenuation of a wave in free space, but which instead occurs near small obstacles placed within a sound field, or near small sound sources, or vibrating membranes or wires (Leighton, 1994). It arises instead from the frictional forces between a boundary and a medium carrying vibrations of circular frequency ω. Unlike the streaming described earlier, this time-independent circulation occurs only in a small region of the fluid, being generally confined to an acoustic boundary layer of thickness:

$$L_{\text{ms}} = \sqrt{2\eta/\rho\omega}, \tag{47}$$

(*footnote continued*)
nuclear power station in Scotland. However since the speed of sound is lower than that of light, the equivalent power requirements would be only 17 kW in air and 75 kW in water.
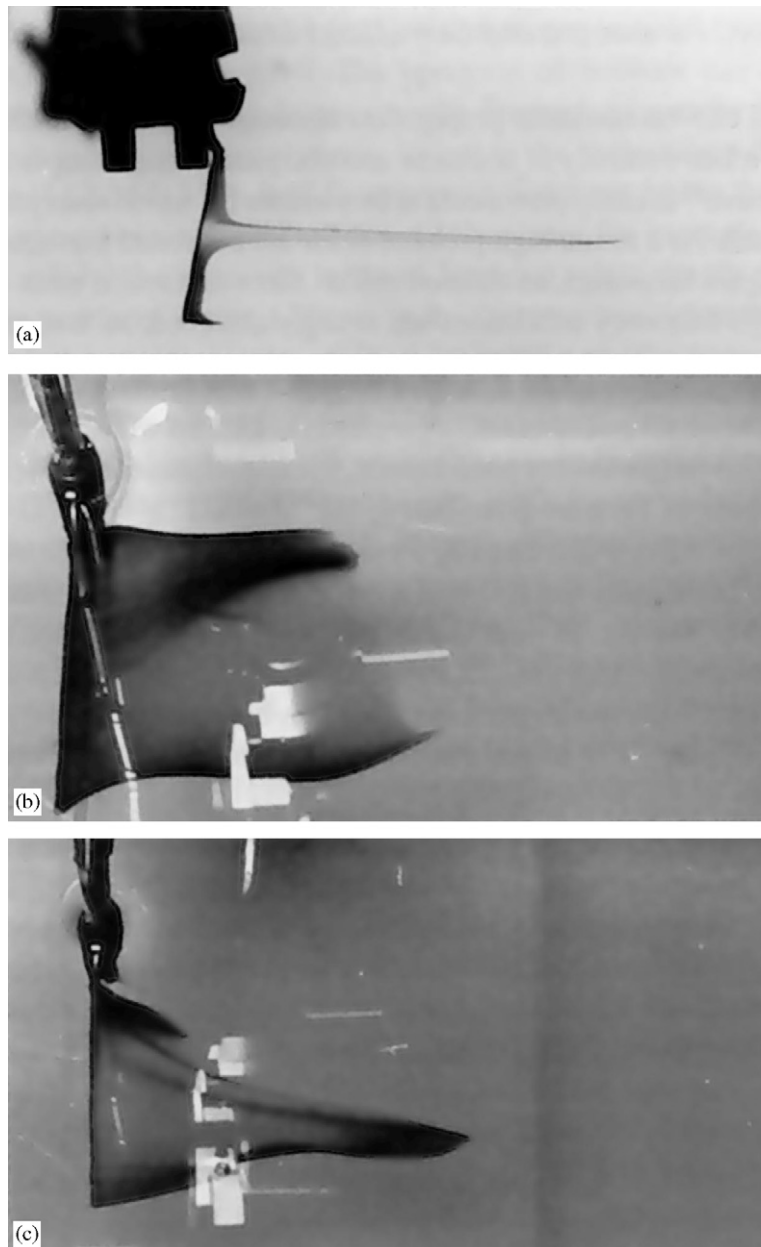
Fig. 9. Streaming visualized using thymol blue indicator for (a) a diagnostic *B*-scan transducer, (b) a scanned diagnostic array and (c) a physiotherapy transducer. From Starritt et al. (1991).

where η and ρ are the shear viscosity and density respectively of the liquid (Nyborg, 1958). Because of the restricted scale of the circulation, it is commonly termed *microstreaming* (Fig. 10). Microstreaming can bring about a number of important effects. The shear forces set up within the liquid may disrupt DNA (Williams, 1974), disaggregate bacteria (Williams and Slade, 1971), disrupt human erythrocytes and platelets in vitro and in vivo (Williams et al., 1974; Williams, 1977), and other bioeffects (Rooney, 1972). Microstreaming can specifically occur as a result of the oscillations of an acoustically driven bubble in a sound field, which can also lead to bioeffects (Leighton, 1994, Section 4.4.3c(iii), Section 4.4.4, Section 5.4.2; Clarke and Hill, 1970).

The nonlinear propagation discussed earlier may be indirectly responsible for the relative scarcity of nonlinear acoustic phenomena, compared to optical ones. This is because, in many pure media, the sound
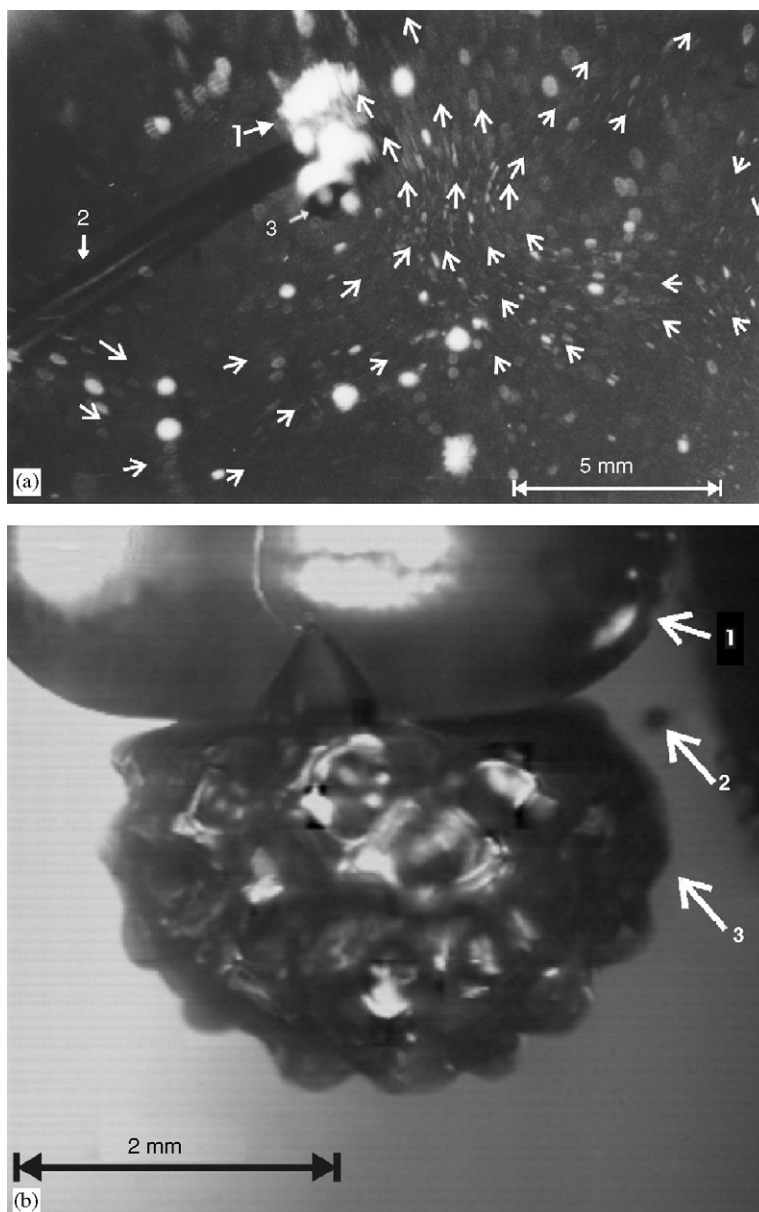
Fig. 10. (a) A microtube (labelled 2) is inserted into a 10 kHz sound field of approximate 0-peak acoustic pressure amplitude 0.2 MPa in tap water, and air is injected into the tube, generating bubbles at the tip of the nozzle (labelled 3). One, labelled 1, displays the characteristic rippled surface shimmer of surface waves (including the Faraday wave), which can pinch off microbubbles from the main bubble (Leighton, 1994, Section 4.4.1(b)). The result of such 'pinching off' can be seen in (b). The arrows in (a) follow the flow of such small bubbles as they are transported within the microstreaming circulation: and their motion is evident through the streaks they produce in the picture under the 1 ms flash exposure. Arrows are aligned with the local streaks to show more clearly the local direction of the microstreaming flow. Given that streaks of up to 0.6 mm are made during the 1 ms flash, flow speeds of up to about 0.6 m s⁻¹ are evident, and can reverse direction over a span of 4 mm (see upper right corner), giving rise to shear. (Picture: Leighton TG). (b) Picture showing the fragmentation of a gas bubble (of radius ∼2.1 mm) driven at 1.5006 kHz (139 Pa). The bubble is held against buoyant rise against the base or a vertical glass rod (labelled 1). Microbubbles (labelled 2 and 3, the latter being much smaller) are arrowed. They have been caused by fragmentation at the tips of the peaks of the surface waves (Leighton, 2004). (Picture: Birkin PR, Watson YE, Leighton TG).

speed is non-dispersive at frequencies for which absorption is small over the distance of a wavelength. As a result, high-pressure fields are converted into shock waves as energy is pumped into the higher harmonics, as outlined earlier. Since absorption tends to be greater at higher frequencies, the high frequency oscillations are
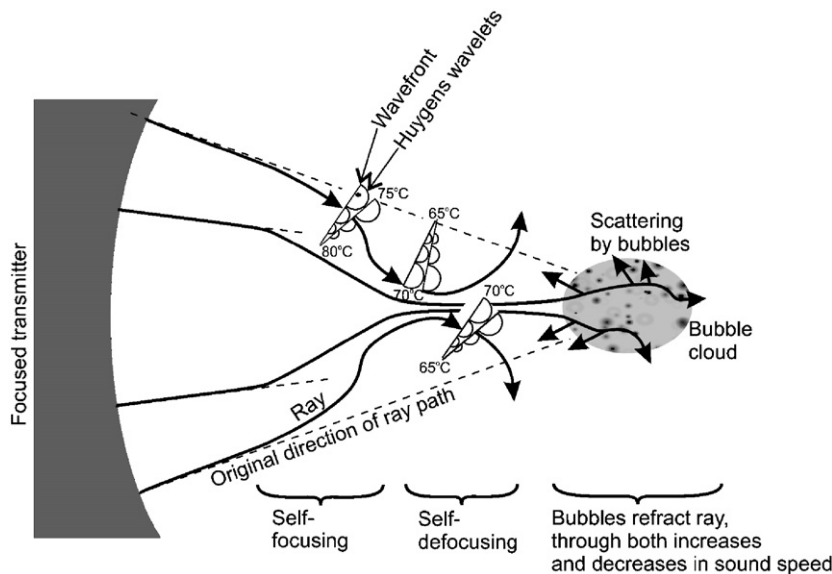
Fig. 11. A hypothetical scenario which illustrates both self-focusing and self-defocusing, as a result of both temperature and bubble effects. Consider a focused transducer emitting into hot water. Selected ray paths (solid lines) are shown. The dashed lines show the original angles with which four rays propagate away from the transducer. Because of the beampattern, at a given range from the faceplate the temperature of the water close to the transducer axis is greater than that further from the axis. However the absolute temperature varies with range. The transducer itself is very hot, and heats the water close to it to $>74\,°C$, and in this spatial region self-focusing occurs because the sound speed decreases with increasing temperature at $>74\,°C$ (Fig. 12). Consider the uppermost ray, and its associated wavefront (labelled). The region of that wavefront closest to the axis is warmer ($80\,°C$) than the region further from the axis, which is at $75\,°C$ (the temperatures are indicated for each region on the plot). Hence the wavefront tends to turn towards the transducer axis (which might be envisaged through the greater radii attained in a given time by the Huygens wavelets further from the axis). A similar process happens with all the other rays, and self-focusing occurs: the rays become more concentrated than they would have been had they followed their original trajectories (the dashed lines). However they then enter a region further from the hot transducer where self-defocusing occurs, because the water temperatures are $<74\,°C$ ($70\,°C$ on axis, and $65\,°C$ off-axis, such that the sound speed decreases as one moves off-axis). As a result the wavefront turns away from the axis, and self-defocusing occurs. The rays then reach an area of bubbly water. These bubbles backscatter some acoustic energy, and could cause either focusing or defocusing because they can both increase and decrease the sound speed. Whilst the inclusion of so many strong effects in a single figure is for illustrative purposes only, the complexity of intense sound fields should not be underestimated. For example, the focus could in time move closer to the transducer, leaving a bubble cloud trapped in tissue at greater ranges (as shown in the figure), through a variety of mechanisms. These include temperature changes induced in tissue near the transducer as the device heats up, and backscatter by the cloud (which itself could have been generated through cavitation, rectified diffusion, outgassing, etc.).

strongly absorbed, so that strong sound waves are rapidly dissipated in the liquid. This effect can be reduced by engineering dispersion into the medium, for example by propagating the sound through a waveguide, or by introducing gas bubbles. Nevertheless there are several other nonlinear effects associated with the propagation of ultrasound, such as self-interaction and parametric phenomena, stimulated scattering and phase conjugation (Leighton, 1994, Section 1.2.3). Examples of some of these are given below.

A variety of self-interaction effects are shown in (Fig. 11). One is the *self-focusing* of acoustic beams. Thermal self-focusing is a consequence of the heating which occurs in a medium as a result of acoustic absorption. In most liquids such heating causes the sound-speed to fall (or equivalently causes the acoustic refractive index to increase) so that the beam is focused in towards the axis as a result of total internal reflection at its perimeter. In water, however, the sound speed passes through a maximum at $74\,°C$ (Fig. 12), so that thermal self-focusing only occurs at temperatures in excess of this. At lower temperatures, the inverse phenomenon of self-defocusing occurs. Acoustic streaming imparts a defocusing effect by increasing the acoustic propagation speed near the beam axis.

There are mechanisms other than thermal which can bring about self-focusing and self-defocusing. Because the presence of bubbles can strongly affect sound speed (Section 4.2), an inhomogeneity in the distribution of
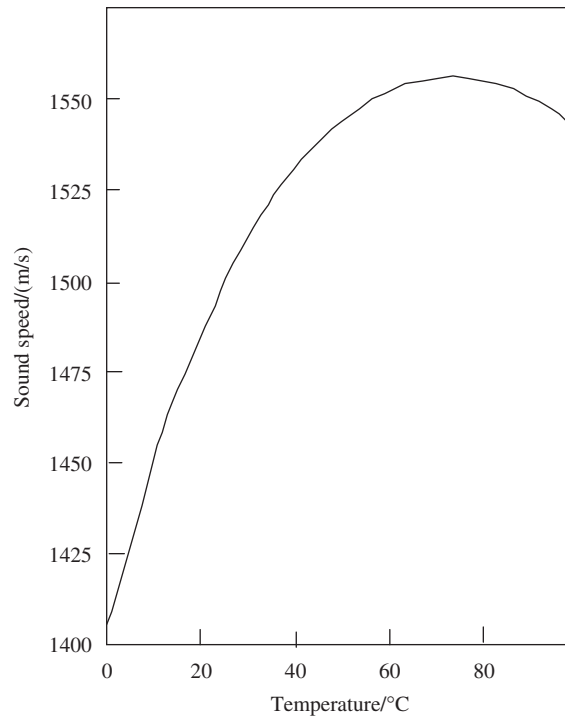
Fig. 12. A plot of the sound speed as a function of temperature in pure water under 1 atmosphere of static pressure.

bubbles can cause self-focusing and self-defocusing, and other spectacular refractive effects (as exploited by humpback whales—Leighton, 2004). In addition, since the acoustic impedance of bubbly water can be very different from that of bubble-free water, reflection can occur at the boundary between bubbly and bubble-free water. These phenomena become self-interaction effects when the sound field itself shapes the distribution of bubbles, which then modify the sound field (also shown in Fig. 11). Self-interaction effects involving bubbles are very common in liquids, because of the potency of the interaction between bubbles and sound (see the discussion of Fig. 19 in Section 4.2). For example, Bjerknes forces (Stephens and Bate, 1966; Leighton, 1994, Section 4.4.1) cause bubbles to accumulate at regions where the time-varying pressure oscillations are greatest or least, depending on bubble size. In Fig. 13, the clustering of bubbles at the acoustic pressure amplitudes of a standing wave field is indicated by the bands of sonoluminescence measured there. These bands can in turn modify the sound field through scattering. A similar effect is illustrated in Fig. 11, where the bubbles cluster at the focus, scattering and refracting the sound. The presence of bubbles can also bring about self-transparency, where the absorption decreases with increasing intensity, though this can arise in bubble-free media, such as glycerin, owing to the temperature-dependence of the absorption coefficient.

Self-focusing can occur not just in the bulk of a liquid, but at an interface between two media where, for example, distortion of the surface of a water sample by the beam can lead to a focusing effect simply as a result of local angling of the reflecting surface (Leighton, 1994, Section 1.2.3). In the extreme case, when the reflected beams are directed upwards, it can lead to *acoustic self-concentration* and the formation of a fountain.

Therefore both heating and bubbles can affect beam focusing, and of course can affect each other (Section 4). It would be important to consider these effects in circumstances where a tight beam focus is required, but where conditions promote both heating and bubble activity, and nonlinear propagation (Frizzell et al., 1983; Hynynen, 1987, 1991; Lee and Frizzell. 1988; Billard et al., 1990). One example of where such conditions occur, for example, is HIFU (High Intensity Focused Ultrasound, or Focused Ultrasound Surgery, FUS—Yang et al., 1993; Vaezy et al., 1998; Wu et al., 2002). Having grown from a long history of experiment and
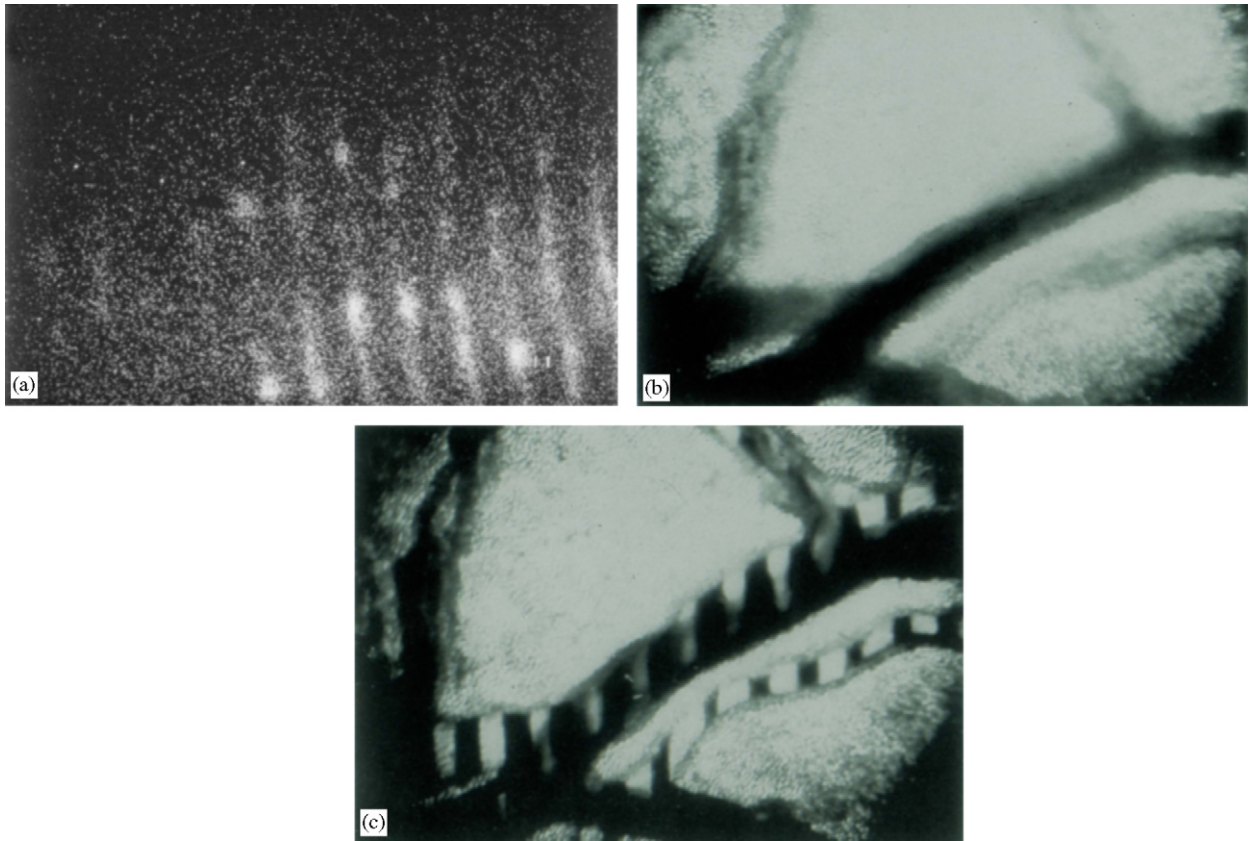
Fig. 13. (a) Primary Bjerknes forces produce bands of sonoluminescence, emitted from thousands of bubbles which cluster at the acoustic pressure antinodes in a standing wave field generated using the 1 MHz signal from a physiotherapeutic ultrasonic generator ($I_{TA} = 3.3$ W cm^{-2}, 22 °C). Hydrophone measurements confirm that the bands of luminescence are aligned with the acoustic pressure antinodes (Leighton et al., 1988), and that the band separation is ~0.7 mm, equivalent to half a wavelength (Leighton, 1994, Section 4.2.4). Placement of layers of in vitro cells (mouse tumour line EMT6/Ca/VJAC) in such a field showed preferential cell death at the antinodes (Pickworth et al., 1989). (b) Blood vessels of the area vasculosa of a 3.5-day-old chick embryo in the absence of ultrasound. (c) Red blood cell banding in the blood vessels of a 3.5-day-old chick embryo in the presence of an ultrasonic standing wave field (3 MHz, $I_{TA} = 1$ W cm^{-2}, band separation = 0.25 mm, equivalent to half a wavelength). There were no hydrophone measurements to determine whether the bands occurred at pressure nodes or antinodes (ter Haar and Wyard, 1978).

research[20] (ter Haar, 1986; ter Haar, 2001; Leighton 1994, Section 4.4.2 (b)(i)), this technology (as other papers in this issue will describe) has grown to a therapy where the sound field of high I_{TA} (e.g. continuous-wave) is focused into a region which is scanned across a tumour (Kennedy, 2005). The typical size of this focus is a few millimetres in each dimension. Tissue destruction is the result of heating (Barnett 1980a, b), and the generation of bubble activity can occur and can enhance heating (Holt and Roy 2001; Bailey et al., 2001; Thomas et al., 2005; Rabkin et al., 2005). Treatment times might be reduced if this effect could be controlled in the clinical environment.

---

[20]Experiments of the effects of high I_{TA} focused ultrasound on tumours have been ongoing from the 1950s (Herrick 1953, Nightingale 1959, Fry and Johnson 1978, ter Haar et al. 1991; Hand et al., 1992). Research into the possible use in other clinical procedures has a similar long history. Early experiments (dating from the 1950s) were on neurosurgical research (Fry et al., 1954; Fry and Dunn 1956; Bausauri and Lele 1962; Warwick and Pond, 1968), then in ophthalmology work (Lizzi et al., 1978, 1984, 1992; Coleman et al., 1986; Polack et al., 1991) and studies of the nervous system (Fry et al., 1970; Lizzi and Ostromogilsky, 1987), Meniere's disease (Kossof et al., 1967; Barnett, 1980a, b) and the reduction of bleeding through ultrasonic haemostasis (Hwang et al., 1998; Vaezy et al., 1999, 2001).

4. Acoustic cavitation

The previous section demonstrated the presence of nonlinearity during acoustic propagation, and ended with discussion of examples of how it can affect focusing. By far the most effective way of generating a nonlinearity, and of focusing acoustic energy both in terms of time and space, is through the interaction of acoustic waves with bubbles, a phenomenon known as acoustic cavitation.

Gas bubbles are the most potent naturally occurring entities that influence the acoustic environment in liquids. Upon entrainment under breaking waves, waterfalls, or rainfall over water, each bubble undergoes small amplitude decaying pulsations with a natural frequency that varies approximately inversely with the bubble radius, giving rise to the 'plink' of a dripping tap or the roar of a cataract. When they occur in their millions per cubic metre in the top few metres of the ocean, bubbles can dominate the underwater sound field. Similarly, when driven by an incident sound field, bubbles exhibit a strong pulsation resonance. Acoustic scatter by bubbles can confound sonar in the shallow waters which typify many modern maritime military operations. If they are driven by sound fields of sufficient amplitude, the bubble pulsations can become highly nonlinear. These nonlinearities might be exploited to enhance sonar, or to monitor the bubble population. Such oceanic monitoring is important, for example, because of the significant contribution made by bubbles to the greenhouse gas budget (Haugan and Drange, 1992; Stewart, 1992; Broecker and Siems, 1984; Farmer et al., 1993; Deane and Stokes, 1999; Leighton et al., 2004). In industry, bubble monitoring is required for sparging, electrochemical processes, the production of paints, pharmaceuticals and foodstuffs. At yet higher amplitudes of pulsation, gas compression within the collapsing bubble can generate temperatures of several thousand Kelvin whilst, in the liquid, shock waves and shear can produce erosion and bioeffects. Not only can these effects be exploited in industrial cleaning and manufacturing, and research into novel chemical processes, but moreover we need to understand (and if possible control) their occurrence when biomedical ultrasound is passed through the body. This is because the potential of such bubble-related physical and chemical processes to damage tissue will be desirable in some circumstances (e.g., ultrasonic kidney stone therapy), and undesirable in others (e.g., foetal scanning) (Leighton, 2004).

This list of example applications illustrates the distinctions which are made between the different forms of cavitation. The sound of a breaking wave, mentioned below, is generated through the pulsations of bubbles, decaying in amplitude following their entrainment. However when driven by a sound field, the pulsations, rather than decaying, can persist, the bubble pulsating in what is termed 'stable cavitation'. Associated with such behaviour are the effects of bubbles on the sound speed, and the scattering of the sound field (Section 4.2). A range of other behaviours can affect the medium. These include Bjerknes forces (Fig. 13), which are radiation forces associated with bubble oscillation, and cause translational movements of bodies suspended in the liquid (Leighton, 1994, Section 4.4.1). For example, platelets might be caused to accumulate
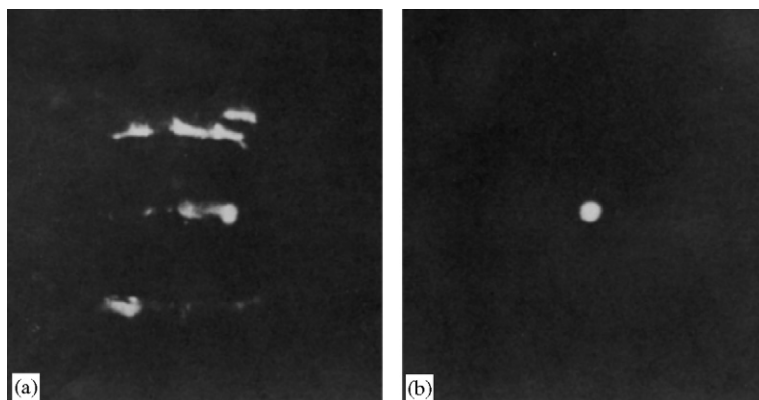

Fig. 14. (a) Image-intensified photograph of multibubble sonoluminescence in tap water, placed in a rectangular vessel and driven by an ultrasonic horn at 20 kHz. (b) As for (a) but with the source driven at higher amplitudes. In this instance, cavitation at the tip of the horn (indicated by the spot of luminescence there) is so intense that it shields the rest of the liquid from the ultrasonic field, suppressing cavitation there. (From Walton and Reynolds, 1984).

around a pulsating bubble (Miller et al., 1979); bubbles might group together, forming acoustic 'shields' which hinder the penetration of sound further into the liquid (Leighton, 1994, Section 5.3; Leighton, 1995; Fig. 14); and bubbles may translate through the medium generating hydrodynamic shear which can cause cell lysis (Miller and Williams, 1989). Microstreaming currents generated in the liquid close to the oscillating bubble wall can cause cell lysis (Vivino et al., 1985). These examples illustrate an important point: such is the potency of the interaction of bubbles with acoustic waves that the presence of bubbles can drastically affect the lengthscales, timescales, and magnitudes of the effects we expect from that wave. In the free field, diffraction limits the lengthscales over which we might expect significant stresses to be exerted on tissue, because it determines the lengthscales one must travel in order to see significant differences in particle velocity or displacement. However when bubbles are present, such changes can occur over much smaller distances (Fig. 10).

During *rectified diffusion* (Leighton, 1994, Section 4.4.3) the equilibrium radius of the bubble grows as the pulsations draw previously-dissolved gas out from the surrounding liquid into the bubble interior. This could conceivably cause a bioeffect through mechanical action or depletion of the gas reservoir, but probably is most important in that it affects the size distribution of bubbles in the population, which can affect the type of cavitational behaviour they undertake.

For many decades the term 'stable cavitation' was taken to imply, not only the fact that the bubbles pulsate over many cycles and remain physically intact, but also to imply that the physical effects generated by these pulsations are characteristic of 'low energy' sources. Therefore whilst nonlinear acoustic emissions from stable cavitation could be detected, shocks and luminescence could not. Similarly, whilst vigorous stable cavitation might cause rupture of delicate membranes (through microstreaming or radiation forces), erosion of steel does not occur. Whilst delicate long-chain polymers might be fragmented by microstreaming associated with stable cavitation, free radicals were not produced. Such 'high energy' effects were rather associated with a phenomenon known as 'transient' cavitation, so-named because the bubble pulsation which generated these effects was thought always to result in break-up of the bubble. Clearly it is unsatisfactory to have a definition which depends on two factors (stability of bubble and whether the effects caused by the cavitation were 'high energy' or not). This is because the scheme would break down when 'high energy' phenomena were observed from bubbles which pulsated stably over many cycles. Indications (specifically the observation of sonoluminescence from a stable bubble) that this might occur were first reported by Saksena and Nyborg (1970), but definitive proof was not forthcoming until later (Gaitan and Crum, 1990; Gaitan et al., 1992). Following this, a new scheme was adopted, whereby most of 'stable' cavitation (i.e., excluding the type which could produce sonoluminescence) was renamed 'non-inertial cavitation'; all cavitation which generated the afore-mentioned 'high-energy' effects was termed 'inertial cavitation'. Whilst this provided a useful working definition (primarily because researchers rarely observed the 'cavitation' itself, or could even agree on a definition, but rather worked with the observed effects of cavitation), a rigorous definition was found by re-examining the work of Flynn (1975a, b). The acceleration term in the equation of motion of the bubble is divided into two parts, a pressure function (PF) and an inertial function (IF), such that:

$$\ddot{R} = \mathrm{IF} + \mathrm{PF}. \tag{48}$$

The inertial function is so-called since it is reminiscent of a kinetic energy gradient, in that it represents the effect of inertial forces in the liquid. For a free collapse, for example, it would be negative, representing the spherical convergence of the liquid. The PF represents the acceleration which is due to the summed pressure forces, as will now be shown.

Non-inertial cavitation is said to occur when PF dominates the dynamics of the collapse: inertial cavitation is said to occur when IF dominates. Approximate forms (e.g., ignoring radiation an thermal losses—see below) of the PF and IF are:

$$\mathrm{IF} = -\frac{3\dot{R}^2}{2R}$$

$$\mathrm{PF} = \frac{1}{\rho_0 R}\left\{\left(p_0 + \frac{2\sigma}{R_0} - p_\mathrm{v}\right)\left(\frac{R_0}{R}\right)^{3\kappa} + p_\mathrm{v} - \frac{2\sigma}{R} - \frac{4\eta\dot{R}}{R} - p_0 - P(t)\right\}, \tag{49}$$

which are found by comparing (48) with the well-known Rayleigh–Plesset equation for bubble dynamics:

$$R\ddot{R} + \frac{3\dot{R}^2}{2} = \frac{1}{\rho_0}\left\{\left(p_0 + \frac{2\sigma}{R_0} - p_v\right)\left(\frac{R_0}{R}\right)^{3\kappa} + p_v - \frac{2\sigma}{R} - \frac{4\eta\dot{R}}{R} - p_0 - P(t)\right\} + O(\dot{R}/c),$$ (50)

where p_0 is the static pressure in the liquid outside the bubble, σ is the surface tension (causing the $2\sigma/R$ Laplace pressure term—Leighton 1994, Section 2.1.1), and p_v is the vapour pressure. The mass density of the liquid (ρ_0) is assumed to be incompressible. This is indicated by the neglected terms $O(\dot{R}/c)$, which indicates that acoustic radiation losses are not included in this equation. Given that thermal losses are also not included (see the comments on κ, below), the only dissipation mechanism in this equation is through the shear viscosity η.

The term κ is the so-called polytropic index. This engineering term is not a fundamental quantity, but takes an intermediate value between γ (the ratio of the specific heat of the gas at constant pressure to that at constant volume) and unity, depending on whether the gas is behaving adiabatically, isothermally, or in some intermediate manner (such that the ideal gas relationship between the bubble volume (V) and its gas pressure (p_g) can vary between $p_g V^\gamma = $ constant and $p_g V^1 = $ constant). Note that the use of a polytropic law only adjusts the way gas pressure changes in response to volume changes to account for heat flow between the gas and its surroundings. In most bubble acoustics models where it is used, κ takes a constant value over the oscillatory cycle and, used in this way, can never describe net thermal damping during the oscillatory cycle of a bubble (Leighton et al., 2004). However the polytropic index does adjust the bubble stiffness for this heat flow.

The following sections will explain typical bubble dynamical behaviour, progressing from its oscillator characteristics (Section 4.1) through non-inertial cavitation (Section 4.2) to inertial cavitation (Section 4.3).

4.1. The bubble as an oscillator

The ideal spherical pulsating bubble acts as a damped oscillator: the stiffness comes from the bubble gas; and the inertia is invested primarily in the surrounding liquid, which is set into motion when the bubble wall moves. Viscous, thermal and acoustic radiation losses contribute to the damping.

For spherical bubbles, at least four possible classes of equation of motion can be constructed, depending on the 'frame' (Leighton, 1994, Section 3.2.1(a)) chosen in which to represent the system (i.e. whether the position of the bubble wall is expressed in terms of bubble volume $V(t)$ or radius $R(t)$, and whether the external driving field is expressed in terms of the acoustic pressure $P(t)$ or force $F(t)$). In the radius/force frame, if the displacement of the bubble wall is R_ε, such that

$$R(t) = R_0 + R_\varepsilon(t)$$ (51)

then the equation of motion is:

$$m_{RF}^{rad}\ddot{R}_\varepsilon + b_{RF}^{tot}\dot{R}_\varepsilon + k_{RF}R_\varepsilon = -F(t) = -4\pi R_0^2 P(t),$$ (52)

where the force $F(t)$ is assumed to come from an applied pressure field $P(t)$ which gives uniform pressure over the bubble wall at any instant (e.g. as occurs if all the wavenumbers k associated with $P(t)$ are such that $kR_0 \ll 1$). The negative sign ensures that a quasi-static reduction in pressure produces an increase in the radial coordinate (r) of the wall. The stiffness in this frame is $k_{RF} \approx 12\pi\kappa p_0 R_0$ (Leighton, 1994, Section 3.2.1(b)) and the inertia (the so-called "radiation mass") is $m_{RF} = 4\pi R_0^3 \rho_0$ (Leighton, 1994, Section 3.2.1(c)(iii)) The term b_{RF}^{tot} summarises all the dissipation mechanisms (Leighton, 1994, Section 3.4).

As linear oscillators at low amplitudes of pulsation, gas bubbles in liquids are abundant, and responsible for many of the sounds we associate with liquids in the natural world. When driven by external sound fields, a bubble exhibits a powerful pulsation resonance, plus numerous resonances associated with higher order spherical harmonic shape perturbations. At finite amplitudes, bubbles will not only 'process' the driving sound field by generating harmonics, subharmonics and combination frequencies; they will also process the surrounding medium, producing physical, chemical, and biological changes. Furthermore, all these phenomena are not simply interesting in their own right: they can be exploited as tools. As a result,

problems in bubble acoustics can sometimes lead to complete solutions, starting with the fundamental physics and ending with a product or device in the clinic, laboratory, or market.

To examine the stiffness element in detail, note that the gas, if slowly compressed, exerts a force which resists that compression, and would tend to make the bubble expand (and vice versa).[21] Potential energy is stored in the gas as the bubble volume changes. When the bubble wall moves, the surrounding liquid must also move: If the system has spherical symmetry, then the velocity of an incompressible liquid falls off as an inverse square law away from the bubble wall (Minnaert 1933). Therefore there is a kinetic energy associated with bubble pulsations which is characterised by the moving matter. Since the liquid is so much denser than the gas, this is primarily invested in the liquid (though motion of the gas contributes to a much smaller extent Leighton et al., 1995). Comparison of the potential and kinetic energies (which is in effect a consideration of the relative effects of the gas stiffness and the liquid inertia) allows the formulation of the natural frequency Υ_0 of the oscillator. A simple calculation, based on the linear pulsations of a spherical air bubble of equilibrium radius R_0 in water, which is assumed to be incompressible and inviscid, gives

$$\Upsilon_0 R_0 \approx 3.3\,\text{Hz\,m}, \quad R_0 > \sim 10\,\mu\text{m} \tag{53}$$

assuming one atmosphere of static pressure. Eq. (53) neglects surface tension, making this formulation less valid for smaller bubbles. Throughout this paper, the long wavelength limit $kR_0 \ll 1$ is assumed.

Eq. (53) is found by substituting sea surface parameters (for water and air) into the resonance frequency, found by a small-amplitude expansion of Eq. (50):

$$\Upsilon_0 = \frac{\omega_0}{2\pi} = \frac{1}{2\pi R_0 \sqrt{\rho_0}} \sqrt{3\kappa\left(p_0 - p_v + \frac{2\sigma}{R_0}\right) - \frac{2\sigma}{R_0} + p_v - \frac{4\eta^2}{\rho_0 R_0^2}} \approx \frac{1}{2\pi R_0}\sqrt{\frac{3\kappa p_0}{\rho_0}}, \tag{54}$$

where ω_0 is the natural circular frequency of the bubble, and where the final approximation neglects the effects of vapour pressure p_v, surface tension σ and shear viscosity η.

The bubble is of course displaying the features expected of a single-degree-of-freedom linear resonance (Leighton, 1994, Section 4.1). For example, in steady-state, the amplitude of pulsation tends to be largest close to the resonance condition. Bubbles just larger than the size which is resonant with the sound field will pulsate in antiphase to those just smaller than resonance size. This leads to somewhat unusual features, such that for most separation distances, bubbles which are either both larger than, or both smaller than, resonance size, tend to attract; whilst repulsion occurs if one bubble is greater than resonance size and the other is smaller (Leighton, 1994, Section 4.4.1). However in order to calculate the frequency-dependence of any of these resonant effects, the bubble damping must be known.

The characteristic values in Eq. (53) are responsible for the ubiquitous nature of the bubble acoustics when sound is passed through liquids. Take for example a breaking ocean wave: this can generate bubbles having radii typically ranging from millimetres to microns (Leighton et al., 2004). From Eq. (53), these provide pulsation natural frequencies in the frequency range of at least ~1–500 kHz, respectively (with commensurate quality factors of roughly 30–5). Similarly, a biomedical sound field of a few MHz might resonate with a micron-sized bubble.

Eq. (54) does not incorporate thermal or acoustic radiation losses, which require more sophisticated models (Leighton, 1994, Section 4.2), bubble–bubble interactions (Foldy, 1945; Kargl, 2002) reverberation (Leighton et al., 2002), or the fact that the bubble may be constrained by surrounding structures, such as pipes, tissue, etc. (Miller, 1985; Quain et al., 1991; Leighton et al. 1995; Oguz and Prosperetti, 1998; Geng et al., 1999; Miller and Quddus, 2000; Leighton et al., 2000; Symons, 2004; Yang and Church, 2005.). Indeed, whilst the integral which expresses the inertia associated with bubble expansion converges in three-dimensions (e.g. for the pulsation of a bubble in free space), if the bubble is constrained to expand along the length of a uniform pipe without fracturing it, the 'radiation mass' is proportional to the length of the pipe and so can become very great indeed (Leighton et al., 1995). Therefore, for example, conceptual models of the ultrasonically-induced expansion of bubbles contained within blood vessels, to sizes sufficiently large that the liquid flow becomes more 1D than 3D, could well be precluded by the associated liquid inertia, causing wall rupture (although of

---

[21]Outside of this quasi-static limit, the phase relation between the driving force and the bubble volume of course changes in the expected manner in the pseudolinear limit (Leighton, 1994, Section 4.1).
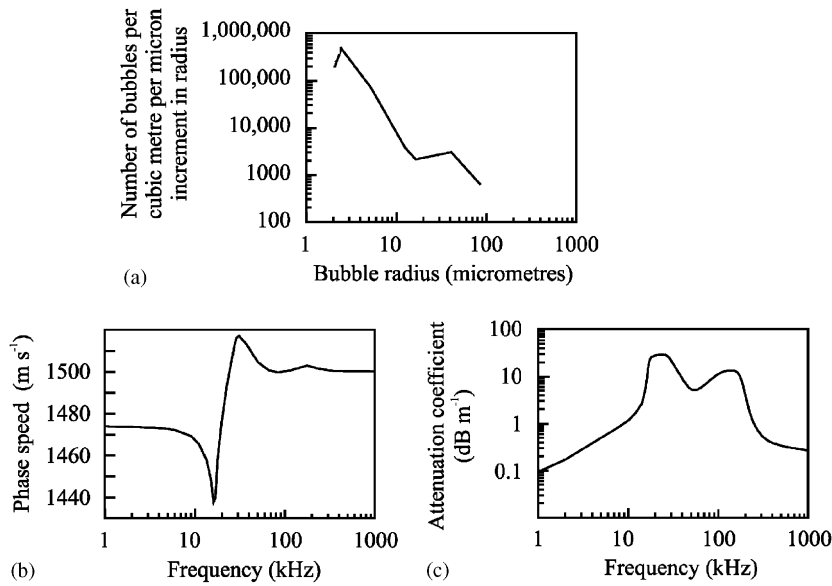
Fig. 15. (a) A bubble distribution function taken from a sea trial by the author and students. The mantissa plots the number of bubbles per cubic metre, per micron increment in radius. (b) Phase speed variations with frequency derived for the bubble population shown in (a). (c) The excess attenuation (i.e. that component of attenuation for which bubbles are responsible) with frequency derived for the bubble population shown in figure (a) (data from TG Leighton, SD Meers).

course cavitation need not always be the main cause when such effects are observed (O'Brien and Frizzell, 2000)).

Section 4.2 examines the effect which bubbles have on acoustic propagation, and Section 4.3 discusses inertial cavitation. Of all the bubble-based phenomenon, this is the one which has historically attracted most interest with respect to ultrasonic bioeffect (Carstensen 1987). This fact, and its complexity, warrants a devoted section. However in the last decade interest has increased in other bubble-based phenomena, such as the use of ultrasonic echocontrast agents (Cosgrove, 1996, 1997). Many of these are engineered forms of microbubbles. From initially being an agent designed to enhance the echogenicity of blood during ultrasonic imaging (Yeh et al., 2004), the technology is now being investigated for use in ultrasonically medicated targeted drug delivery (Shortencarier et al. 2004; Pitt et al., 2004; Zhao et al., 2004; Postema et al., 2004; Dayton et al., 2004).

4.2. The effect of bubbles on acoustic propagation

Fig. 15(a) shows a bubble size distribution, measured in the ocean, along with the associated sound speed (Fig. 15(b)) and the component of attenuation for which bubbles are responsible (Fig. 15(c)). Although a wide range of bubble sizes are present (from at least microns to millimetres) in the ocean, the population as a whole tends to impart to the ocean characteristics such that, for frequencies below about 20 kHz, the bubbles reduce the sound speed to less than that of bubble-free water ($\sim$1480 m s^{-1}), whilst for frequencies above about 40 kHz, the bubbles may tend to increase the sound speed (Fig. 15(b)). The magnitude of the change to sound speed increases the closer the insonifying frequency is to the critical 30–50 kHz range. The additional attenuation caused by bubbles (over and above that which occurs in bubble-free water) also peaks in this range (Fig. 15(c)).

These features are caused by the oscillatory behaviour described in Section 4.1. Bubbles may either increase or decrease the sound speed compared to that of bubble-free liquid, because of the characteristics imparted by the distinction between a stiffness-controlled and an inertia-controlled regimes. In short, the bubble pulsation

undergoes a π phase change (compared to the phase of the driving pressure field) in passing from one regime to the other, and this imparts a sign change to the perturbation of the sound speed.

Consider a volume V_c of bubbly water, which is made up of a volume V_w of bubble-free water and a volume V_g of gas (distributed in an unspecified way between an unspecified number of bubbles of arbitrary size). Conservation of volume gives:

$$V_c = V_w + V_g, \tag{55}$$

where the subscripts will be taken to refer to the gas (g), bubble-free water (w) and the cloud (c). Mass conservation is simply expressed by multiplication of the volumes with the respective densities (of cloud, ρ_c; bubble free water, ρ_w and gas, ρ_g), i.e.

$$\rho_c V_c = \rho_w V_w + \rho_g V_g. \tag{56}$$

Assume that the bulk moduli and sound speeds of the components can be defined through Eqs. (13) and (14), such that for example

$$c_\varepsilon^2 = \frac{B_\varepsilon}{\rho_\varepsilon} = \left(\frac{\partial p(\rho, S)}{\partial \rho}\right)_\varepsilon, \quad \varepsilon = w, g, \tag{57}$$

where the subscript ε can refer to application to gas (g) or bubble-free water (w). Differentiation of Eq. (55) with respect to the applied pressure gives, with (57), the relationship between the bulk moduli

$$\frac{1}{B_c} = \frac{V_w}{V_c}\frac{1}{B_w} + \frac{V_g}{V_c}\frac{1}{B_g} \tag{58}$$

and hence, noting Eq. (57), we define a function (which is not an inherent property of the bubble cloud in the thermodynamic sense), equal to the root of the ratio of the bulk modulus of the cloud to its density (Leighton et al., 2004):

$$\xi_c = \sqrt{\frac{B_c}{\rho_c}} = \sqrt{\left(\frac{V_c}{\rho_w V_w + \rho_g V_g}\right)\bigg/\left(\frac{V_w}{V_c B_w} + \frac{V_g}{V_c B_g}\right)} \approx c_w\left(1 + \frac{B_w V_g}{V_c B_g}\right)^{-\frac{1}{2}} \approx c_w\left(1 - \frac{B_w V_g}{2V_c B_g}\right), \tag{59}$$

where use is made of the small-perturbation approximations: $1/\rho_c \sim 1/\rho_w$ (Eq. (25)) and $\rho_c V_c = \rho_w V_w + \rho_g V_g \sim \rho_w V_w$ and $V_c \approx V_w$. Finally, the substitution $c_w = \sqrt{B_w/\rho_w}$ is made from Eq. (57) and a binomial expansion performed under the assumption that $B_w V_g(t) \ll B_g V_c(t)$. This is valid if the void fraction V_g/V_c is very low If the cloud were not dissipative, this function would equal the sound speed in the cloud. However since dissipation does occur there, such an identity would not be rigorous. How therefore sound speeds can be estimated from this function is discussed below.

To simplify the expression further, assume that all the bubbles are of the same size (i.e. the population is monodisperse). Note that it is not a difficult extension to include a polydisperse population (Leighton et al., 2004), although that is not necessary for the illustrative purposes of this section. Assume that the bubble population is monodisperse, containing N_b bubbles each of volume V_b and equilibrium radius R_0. The instantaneous bubble radius is R, and the bubble number density is $n_b = N_b/V_c$. Applying Eq. (57) to the gas and water, and noting that $V_b \propto R^3$, implies that $B_w = \rho_w c_w^2$, that $V_g = n_b V_c V_b$, and that under these conditions $B_g = \partial P/(\partial \rho_g/\rho_g) = -\partial P/(3\partial R/R)$. Substitution of these into Eq. (59) gives:

$$\begin{aligned}\xi_c &\approx c_w\left(1 + \frac{3\rho_w c_w^2 N_b V_b}{2RV_c}\frac{dR}{dP}\right) \approx c_w\left(1 + \frac{3\rho_w c_w^2 n_b V_b}{2R}\frac{dR}{dP}\right) \\ &\approx c_w\left(1 + 2\pi\rho_w c_w^2 n_b R_0^2 \frac{dR}{dP}\right),\end{aligned} \tag{60}$$

where the use of the differential symbol d here implies an intention to calculate the result numerically (Leighton et al., 2004). The importance of the dR/dP (or, equivalently, the dV/dP) term of Eq. (60) in determining the sound speed can be explained using plots of the applied pressure P against bubble volume V (Leighton et al., 2004).
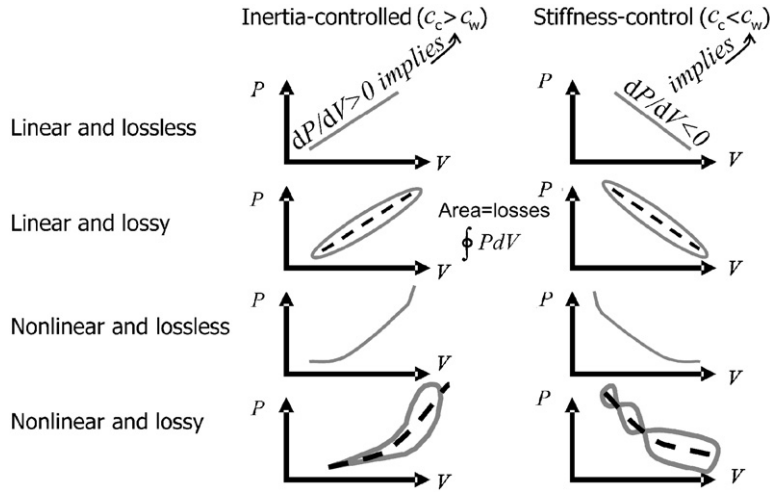
Fig. 16. Schematics of applied pressure versus steady-state bubble volume oscillations. The left column shows the result for the inertia-controlled regime ($\omega > \omega_0$), and the right column corresponds to the stiffness controlled regime ($\omega < \omega_0$). The four rows correspond to conditions which are (from top downwards): linear and lossless; linear and lossy; nonlinear and lossless; nonlinear and lossy. Dash lines are used to identify the 'characteristic spines' of loops (see text).

First consider a monodisperse bubble population (i.e. all bubbles have the same equilibrium radius) pulsating in the linear steady state when driven by an acoustic field of circular frequency ω. If the propagation were linear and lossless, the graphs of applied pressure (P) against bubble volume (V) would take the form of straight lines, the location of the bubble wall being plotted by the translation of the point of interest up and down these lines at the driving frequency (Fig. 16, top row). Since a positive applied pressure compresses a bubble in the stiffness-controlled regime, here $dP/dV < 0$ (Fig 16, top row, right). However since a phase change of π radians occurs across the resonance, the opposite is true in the inertia-controlled regime ($dP/dV > 0$, Fig. 16, top row, left) (Leighton, 2004; Leighton and Dumbrell, 2004).

The behaviour of the top row of Fig. 16 reflects the trend indicated at the start of Section 4.2, and because of this the sound speed in bubbly water (c_c) is increased in the inertia-controlled regime, and decreased under stiffness-control. Obviously, a bubble which is driven in the inertia-controlled regime will be expanding during the compressive half-cycle of the driving pulse, which contributes a component increase in volume to the bubbly water during compression. The sign of $dP/dV > 0$ implies, through (60), that inertia-controlled bubbles will increase the sound speed in bubbly water (c_c) above that found in bubble-free water (c_w). In the stiffness-controlled mode, the bubble will compress to a greater extent than the volume of water it replaces during this compressive half-cycle. Hence through (60), the usual phase change which occurs across resonance means that, in the stiffness-controlled regime, $dP/dV < 0$. This in turn changes the sign of the contribution made by the bubbles to the sound speed in the mixture, and $c_c < c_w$. If the bubble population contains a range of equilibrium radii, an appropriate summation is required (Leighton et al., 2004).

If conditions are linear and lossy (Fig. 16, second row), each acoustic cycle in the steady-state must map out a finite area which is equal to the energy loss per cycle from the First Law of Thermodynamics. The sound speed can be estimated using the dP/dV gradient of the spine of the loop (shown in Fig. 16 as a dashed line). Assume the gas is perfect. Its internal energy U is a state function, such that whenever an orbit crosses its previous path, at both moments represented by the intersection the value of U is the same. More specifically, consider that:

$$dU = \bar{d}Q + \bar{d}W = \bar{d}Q - P\,dV, \tag{61}$$

where the notation indicates that both the incremental heat supplied to the bubble ($\bar{d}Q$) and the work done on the bubble ($\bar{d}W$) are not exact differentials, while dU is.

Because Fig. 16 (and later, Fig. 17) use the applied acoustic pressure $P(t)$, the area mapped out by any loop represents the energy subtracted from the acoustic wave by the bubble in the time interval corresponding to the perimeter of the loop. This is because the bubble dynamics (such as used here) may be interpreted simply as
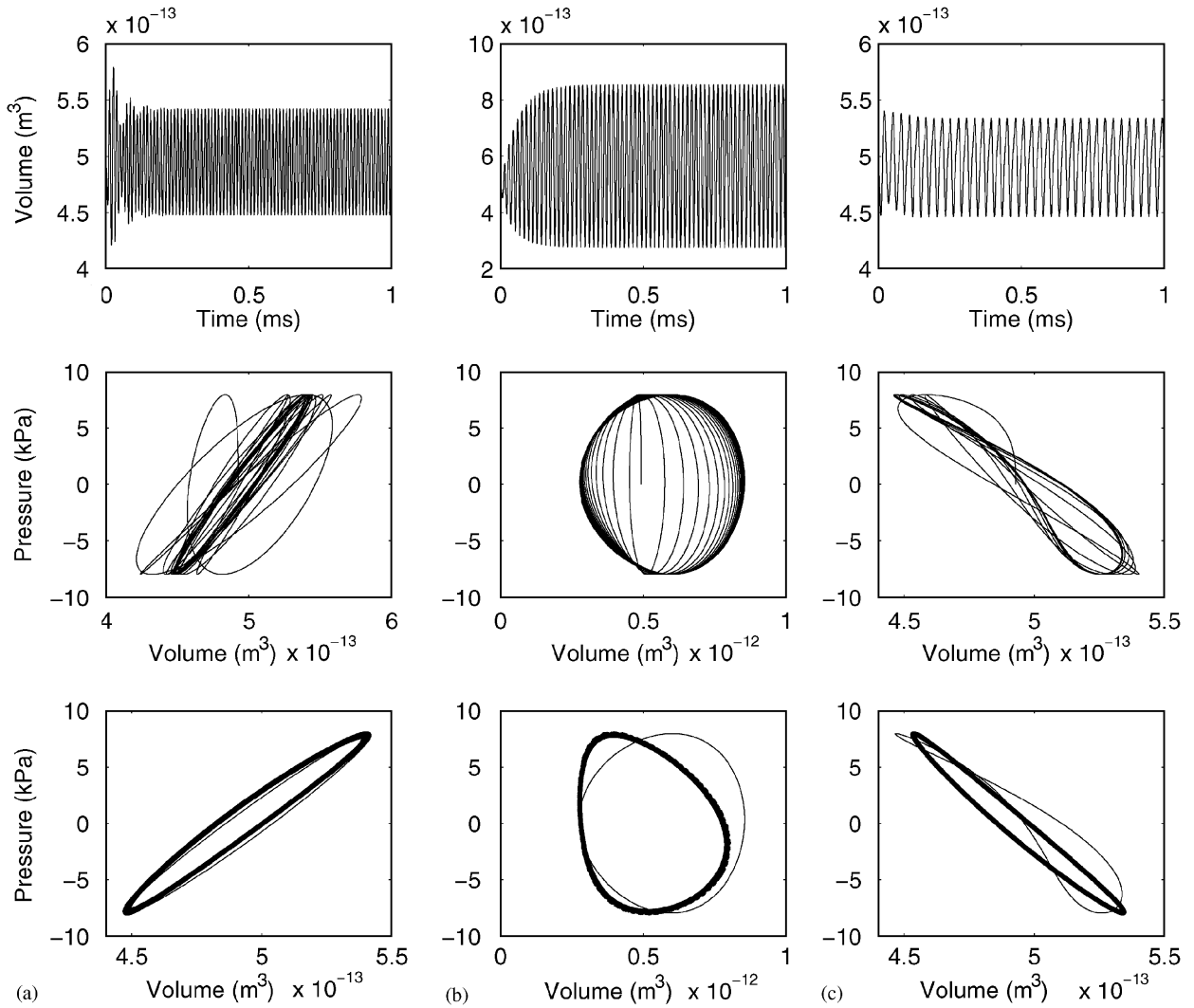
Fig. 17. Bubble responses for a 49 μm bubble insonified by a semi-infinite pulse starting at $t = 0$ with an amplitude of 7.95 kPa at (a) 84.2 kHz (b) 65.7 kHz and (c) 31.5 kHz. The top graph in each case shows the volume time history calculated using the a nonlinear equation of motion for a bubble with appropriate damping (Leighton et al., 2004). The middle graph in each case shows the corresponding pressure–volume curve (applied pressure vs. bubble volume). The darker area in each P–V curve shows the steady state regime, where the successive loci overlap each other. Nonlinear components will cause crossovers in a loop (as in part (c) where a second harmonic arises from driving the bubble close to half resonance frequency). In calculating the energy dissipated by the bubble through integration of such pressure–volume maps, the areas of the clockwise loops will be subtracted from those of the anticlockwise. The bottom row superimposes the steady-state loops of the middle row (thin line) with the corresponding linear solution using the steady-state linear formulation (thick line). (After Leighton et al. 2004).

a statement of the equality between that pressure difference (Δp) which is uniform across the entire bubble wall, and a summation of other. These terms relate to the pressure within the gas/vapour mixture inside the bubble (p_i), surface tension pressures (p_σ), and the dynamic terms resulting from the motion of the liquid required when the bubble wall is displaced, which will here be termed p_{dyn}. Thus

$$\Delta p = p_i - p_{\mathrm{dyn}} - p_\sigma. \tag{62}$$

The energy E_{loop} subtracted from the sound field by the pulsating bubble in each circuit of a loop is given by

$$E_{\mathrm{loop}} = - \oint p_i \, \mathrm{d}V + \oint p_{\mathrm{dyn}} \, \mathrm{d}V + \oint p_\sigma \, \mathrm{d}V, \tag{63}$$

noting that the details of the chemistry on the bubble wall may make the final integral non-zero. However Δp equals the spatial average over the bubble wall of the blocked pressure $\langle p_{\text{blocked}} \rangle$, which in the long-wavelength limit equals the applied acoustic pressure $P(t)$ that would be present at the bubble centre were the bubble not present. Substituting Eq. (62) into (63) therefore shows that the area mapped in a loop in the applied pressure-volume plane is the energy subtracted from the acoustic wave in the time interval corresponding to that loop:

$$E_{\text{loop}} = -\oint \Delta p \, \mathrm{d}V = -\oint \langle p_{\text{blocked}} \rangle \, \mathrm{d}V \approx -\oint P \, \mathrm{d}V. \tag{64}$$

Therefore, the rate at which the acoustic field does work on the bubble can be found by integrating the area in the pressure–volume plane enclosed by the loops formed by the intersections described above, and dividing energy so obtained by the time interval taken to map out that loop. In this way the rate at which the bubble subtracts energy from the driving acoustic field can be calculated.

Traditionally in bubble acoustics, researchers have found greatest imprecision and difficulty in defining a sound speed near resonance. The second row of Fig. 17 illustrates how this will coincide with conditions where not only is the area mapped out very large, but the characteristic gradient of $\mathrm{d}P/\mathrm{d}V$ is very difficult to identify (in keeping with known through-resonance behaviour of sound speed of the type shown in Fig. 15(b).).

If conditions are nonlinear and lossless (Fig. 16, third row), in steady-state the P–V plots must encompass zero area, but they will depart from straight-lines (for example because the degree of compression cannot scale indefinitely). The gradient $\mathrm{d}P/\mathrm{d}V$ varies throughout the acoustic cycle in a manner familiar from nonlinear acoustic propagation, and this can appropriately describe nonlinear propagation and the associated waveform distortion in the usual manner (Morse and Ingard, 1986). As before, if the bubble population contains a range of equilibrium radii, an appropriate summation is required (Leighton et al., 2004). Furthermore, since such a summation would provide an approximation for the relationship between pressure and density for the sample of bubbly water, treating it as an effective medium would provide the information required, (through Sections 3.2 and 3.3) to predict the effectiveness of bubbles in enhancing parametric sonar, an observed effect which has previously been modelled using analysis which assume finite-amplitude expansions of the bubble pulsation and simplified models for damping (Kozyaev and Naugol'nykh, 1980; Kustov et al., 1982; Lerner and Sutin, 1983; Kotel'nikov and Stupakov, 1983).

If conditions are nonlinear and lossy (Fig. 16, bottom row), finite areas are mapped out, and whilst the characteristic spines may present significant challenges, nonlinear propagation may again be identified (the example of the right of the bottom row in Fig. 16 illustrates a strong third harmonic, where the steady-state volume pulsation undertakes three cycles for each period of the driving field).

This scheme can now be used to interpret Fig. 17, which uses a nonlinear model (see Leighton et al., 2004) to predict the response of a single air bubble (of equilibrium radius 49 μm) in water, subjected to a semi-infinite sinusoidal driving pulse (starting at $t = 0$). Under linear sea surface conditions this bubble has a resonance of 65.7 kHz. The left column, (a), corresponds to insonification at 84.2 kHz, a frequency greater than resonance, i.e. the inertia-controlled regime. The middle column, (b), corresponds roughly to a bubble at resonance (65.7 kHz). The column on the right, (c), shows insonification at 31.5 kHz, a frequency less than resonance (i.e. the stiffness-controlled regime).

The top row shows the volume time history of the bubble, as predicted by a nonlinear model (see Leighton et al., 2004). The middle row plots the same data in the plane of the applied pressure versus bubble volume. The locus of this plot consists of a single point until the onset of insonification. From this moment on, the locus describes orbits until reaching steady-state, after which it repeatedly maps out a given orbit. The time-dependent rate at which each bubble in the population subtracts energy from the driving acoustic field can be calculated in the manner described for Fig. 16, with steady state being achieved as $t \to \infty$ (Fig. 17, middle row).

Of particular interest is the bottom row of Fig. 17, which superimposes the steady-state nonlinear loops of the middle row (thin line) with the corresponding linear steady-state solution; thick line). At frequencies much greater than or less than resonance (not shown), both models predict loci indistinguishable from straight lines (dissipation and nonlinearities being negligible at such extremes, the area mapped out by each loop is very small). The gradients of these lines have opposite signs, in keeping with the phase change of π radians which takes place between the stiffness- and inertia-controlled regimes.

Closer to resonance, increasing dissipation imparts finite areas to the loops, and the sound speed must be inferred from the spine of the loop. While in some cases the nonlinear model would impart a similar spine to its loop as would that of linear theory (Fig. 17(a), bottom row), closer to resonance identification of the optimum spine becomes more difficult (Fig. 17(b), bottom row; be aware that the conditions for resonance in the nonlinear and linear models are slightly different). The increasing dissipation and indistinct nature of the spine near resonance may lead to inaccuracies, as discussed above. The different losses predicted by linear and nonlinear theories in the steady state are readily determined by comparing their respective loop areas in the bottom row of Fig. 17. Of particular interest is Fig. 17(c), where the nonlinear model displays a second harmonic (which is of course not apparent in the linear result). In calculating the losses, the area of the clockwise loops must be subtracted from the anticlockwise loops (Leighton et al., 2004). Clearly when bubbles undergo nonlinear pulsations, the propagation conditions may be very different from the predictions of linear theory, and indeed this may be exploited by dolphins and porpoises (Leighton, 2004; Leighton et al., 2004; Leighton et al., 2005b)

This method of visualising the losses from the sound field through the areas of the P–V loops provides a method, not only of calculating the losses during steady state, but also during the ring-up period (an alternative method must be used during ring-down - Leighton et al., 2004; Leighton and Dumbrell, 2004). The exact loss mechanisms included, and the accuracy with which they predict losses, depends on the quality of the terms in the equation of motion for the bubble which encapsulate these processes (the plots in Fig. 17 include thermal, viscous and acoustic radiation losses which encapsulate the nonlinearity; the more commonly used Rayleigh–Plesset equation only includes viscous losses, and whilst there have been attempts to add radiation and thermal losses by augmenting the viscous terms, these can only be partially successful). If linear bubble oscillations only are assumed to occur, and only steady-state oscillations are to be considered, then analytical expressions for the power lost to acoustic radiation, viscous and thermal effects can be readily derived (Leighton, 1994, Section 4.1.2(d)).

The ability of bubbles to affect the sound speed is evident in Fig. 19, where the acoustic modes of a vessel are made manifest by the ability of ultrasonically induced chemiluminescence to reveal the position of acoustic pressure antinodes. Since for a vessel of fixed geometry and boundary conditions, the frequency of the modes depends on the sound speed (Birkin et al., 2003a). Therefore the frequency at which the various modes occurs can be used to give the sound speed (e.g. between 868 and 1063 m s^{-1}—compared to ~1500 m s^{-1} for bubble-free water-in the study of Birkin et al., 2003a).

However, whilst we might exploit such patterns as Fig. 19 to estimate sound speeds, the existence of such patterns and 'characteristic sound speeds' is in some ways very strange. This is because the bubble population in Fig. 19 was generated by a 'power ultrasound' transducer. As such, it therefore contained not just non-inertial cavitation, but also inertial cavitation. The number, dynamics, and locations of such bubbles are in large parts governed by the random conditions of the nucleation (Church, 2002), and so the actual bubble population will be rapidly changing on the scale of an acoustic cycle. Furthermore, the distribution of the cavitation is clearly highly inhomogeneous on the scale of a wavelength. How therefore this inhomogeneous, rapidly changing and stochastic population manages to generate a highly stable characteristic sound speed for the medium is not entirely clear. It is surprising that there appears to be present a bubble population, the statistics of which have sufficient longevity to give a sound speed that could lock the insonification into a specific mode of the vessel with a mode. This is another example of a self-interaction effect, as introduced in Section 3.5. The phenomenon of inertial cavitation is the topic of the next section.

4.3. Inertial cavitation

When induced by a changing pressure field, inertial cavitation requires that the bubble undergo significant expansion, prior to a more rapid collapse, and then a rebound (which emits a pressure pulse). This can generate a range of effects, both chemical and biological, but perhaps the earliest observables attributed to inertial cavitation were erosion (see Fig. 18), as noted in the 'pitting' in ship propellers, and the associated generation of cavitation noise (primarily the rebound pressure pulses). Here the changing pressure field which causes cavitation is generated hydrodynamically, not acoustically, but the principles are the same. An interesting observation in the behaviour of submariners illustrates well the importance to inertial cavitation of
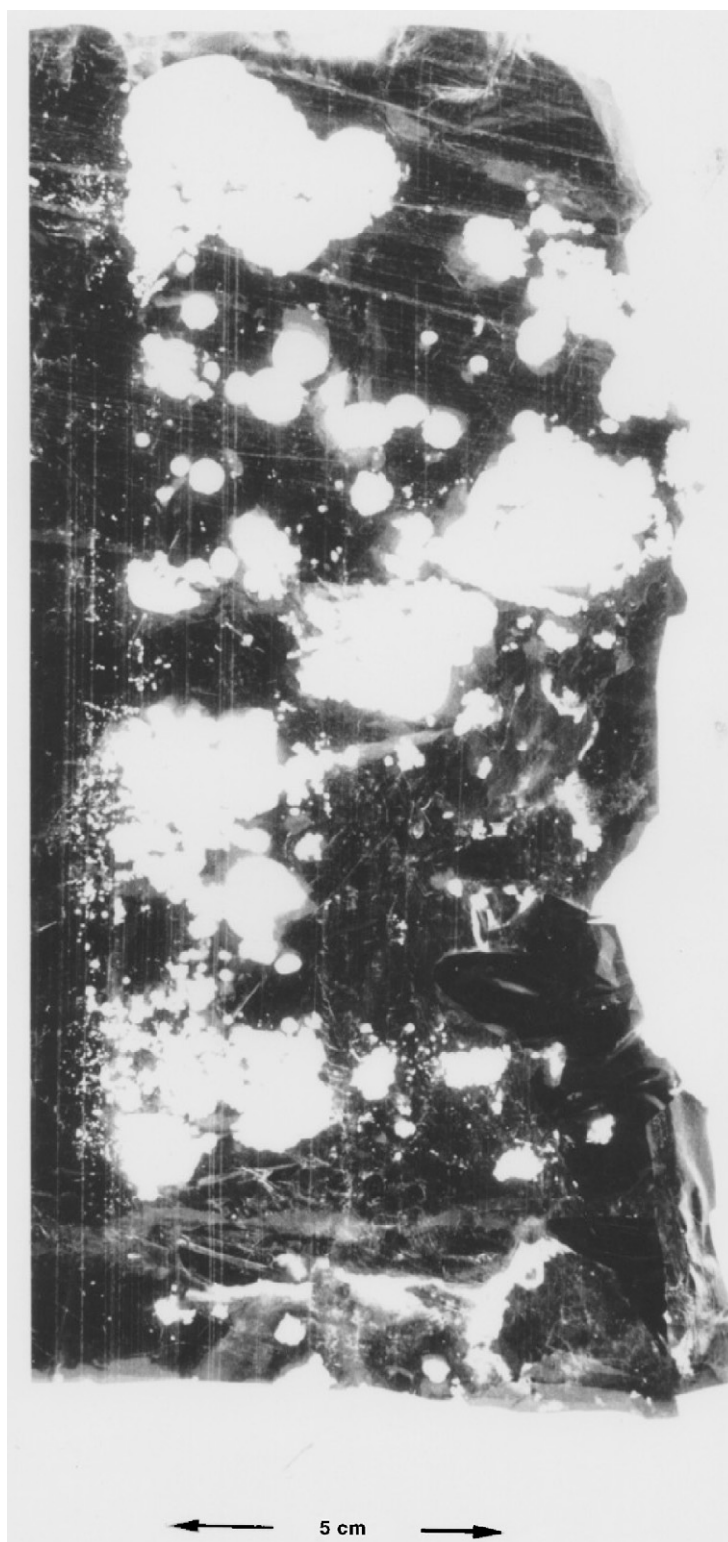
Fig. 18. A back-lighted sample of aluminised mylar sheet, which has been placed for about one minutes in a cavitating field (acoustic pressure amplitude ~0.2 MPa, 10 kHz). The dark regions show where the sheet is intact. Large light circles indicate where the aluminium has been removed through cavitation erosion (Leighton, 1994).
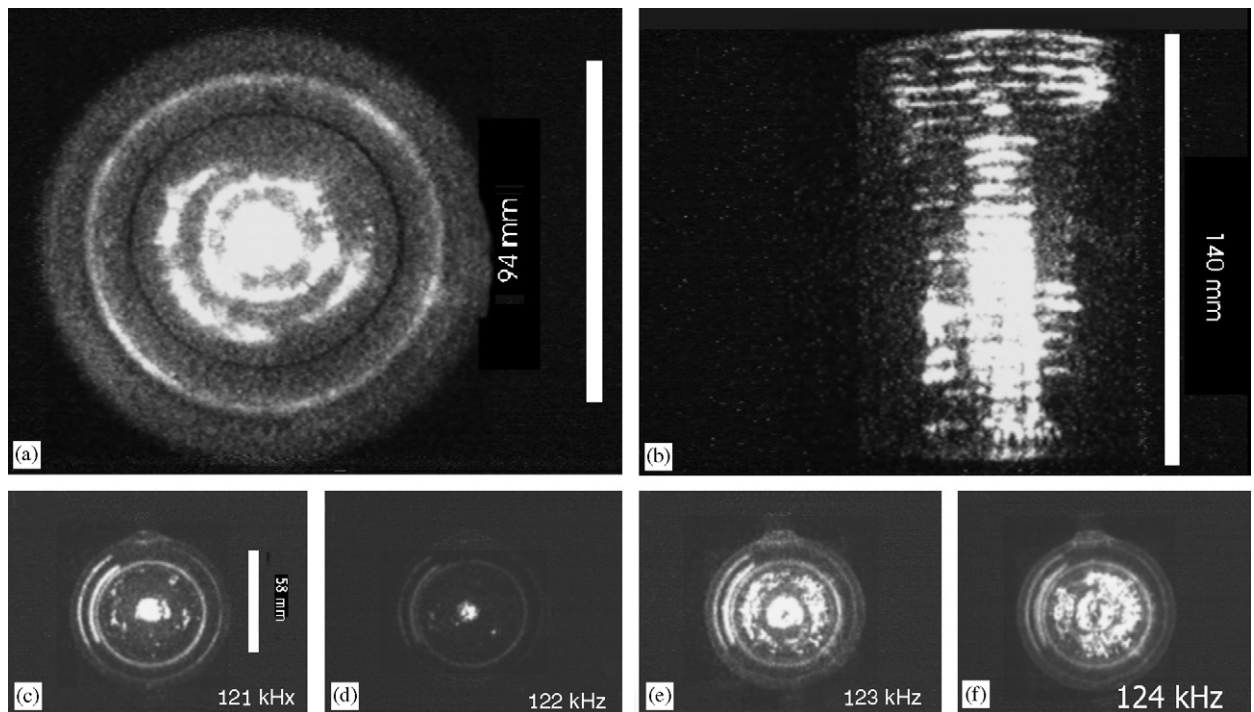
Fig. 19. The acoustic pressure antinodes within reverberant water-filled cylinders (with vertical axis of symmetry, and the sound source at the cylinder base) are made visible through the chemiluminescence which occurs there. (a) Plan and (b) side views of luminescence (which occurs at pressure antinodes) in a water-filled cell which had a polymethylmethacrylate wall (9.4 cm internal diameter, 10 cm external diameter; height of aqueous solution = 14 cm) for insonification at 132.44 kHz where the spatial peak temporal fluctuation in pressure in the liquid was 75 kPa (all quoted zero-to-peak). Frames (c)–(f) (to which the scale bar of length 5.8 cm in frame (c) refers) were taken in a double-walled, water-jacketed cell (5.8 cm internal diameter, 8.5 cm external diameter, and liquid height 8 cm) which was maintained at a constant liquid temperature of 25 °C. For a constant applied drive voltage, as the insonifying frequency changed, so too did the spatial peak acoustic pressure, providing the following combinations: (c) 121 kHz; 139 kPa; (d) 122 kHz; 150 kPa; (e) 123 kHz; 180 kPa; (f) 124 kHz; 200 kPa. The effect of tuning into particular acoustic modes is evident: a 1 kHz change in frequency can dramatically alter the amount and distribution of the luminescence. Hence the not uncommon practice of incrementing frequencies by O(100 kHz) when testing for the 'optimal processing frequency' in such arrangements is nonsensical. Similarly, if calorimetry were used to estimate the ultrasonic field, the change of sound speed resulting from the rise in liquid temperature could detune the mode. By noting the modal resonance frequencies in these and similar cylinders, the sound speed in this bubbly water was found to be in the range 868–1063 m/s, implying void fractions of 2.9–4.2 × 10^{-3}%. Frames selected from several figures in Birkin et al. (2003a). (Figure courtesy P.R. Birkin, J.F. Power, T.G. Leighton and A.M.L. Vincotte).

both the growth and collapse phases. Submariners wish to suppress any cavitation noise generated by their propellers since it can give away their location. They know that submerging their vessel will tend to reduce cavitation noise by suppressing the propeller cavitation. However when the cavitation is strong and the vessel is at high speed, increasing the depth of the vessel will first cause an increase in the cavitation noise, before suppression occurs. This so-called ''anomalous depth effect'' is due to the fact that, an increase in static pressure increases the violence of each individual bubble collapse, before (at greater depths) it suppresses the growth phase. 'Pitting' can also be caused by an aspherical form of collapse which can occur when the bubble is close to an inhomogeneity such as a solid boundary: The bubble can invert on collapse such a that a high-speed liquid jet can pass through the bubble and, on impacting a nearby boundary, can create damage (Leighton, 1994, Section 5.4.1; Leighton, 2004). Inertial cavitation produces shear in the liquid, and generates free radicals through the compression of gas during the collapse stage.

Inertial cavitation is a threshold phenomenon. The threshold is defined in terms of the amplitude of the driving sound field (usually the peak negative pressure), its frequency, and the size of the bubble which is pre-existing and available to nucleate the inertial cavitation event. The prevalence of such 'cavitation nuclei' is evident from the fact that, even with the most extensive measures in place to remove such nuclei from the

liquid, tensile strength tests on liquids hardly ever measure the actual tensile strength of the pure liquid. Rather, the liquid 'fails' through the growth of these pre-existing microscopic bubbles, which are stabilised against dissolution by hydrophobic contaminants in the liquid, or in cracks in the container walls or suspended solids; or even freshly-created by cosmic rays (Leighton 1994, Section 2.1.2). Because of this dependence of the threshold on the size of the nuclei available (as well, to a lesser extent, on the amplitude of the sound field, which may be inhomogeneous (see Fig. 19)), unless special measures are taken (Gaitan and Crum, 1990), then for most sound fields in which inertial cavitation is occurring, some non-inertial cavitation is also occurring (see Figs. 20 and 21).

When bubbles within a certain size range (that tends to be smaller than resonance) are driven strongly, they undergo a dramatic change in behaviour (Flynn, 1975a, b; Apfel, 1981; Apfel and Holland, 1991; Church, 1993; Leighton, 1994, Sections 4.2 and 4.3; Church, 2002). This transition from non-inertial to inertial cavitation (where the bubble undergoes rapid explosive growth, followed by a violent collapse, generating high gas temperatures, gas shocks, and liquid shocks) is characterised by the onset of effects such as erosion, sonoluminescence, chemiluminescence etc. Both the high gas temperatures and the gas shocks may generate free radicals (e.g. in aqueous solution, H atoms, OH radicals, and products such as H_2O_2, hydrogen peroxide). These are highly reactive and may represent a hazard (they are sources of sonochemical reaction). As regards the hot-spot itself, although its temperature is high, it does not contain significant energy or last for a long time. The rebound pressure pulse emitted into the liquid as the bubble rebounds from minimum size may cause mechanical damage to structures close to it. However in a cloud of bubbles the shocks may act to greater distances through a co-operation effect between many bubbles (cloud concentration).

The threshold is such that there is a critical size range, which increases with increasing acoustic pressure amplitude and decreasing frequency, over which bubbles will undergo inertial cavitation if insonified by an appropriate sound field. This is illustrated in Fig. 20, which contains three curves. Each curve represents the threshold condition if a bubble of radius given on the abscissa is insonified by a sinusoidal wave of peak negative pressure as shown on the mantissa. It is usually (but not always) the case that the sound frequency and amplitude are known or, if necessary (e.g. in vivo) can be estimated, but the radii of bubbles present is not. This is particularly so in the in vivo scenario. Suppose therefore that a continuum of bubble sizes is present. For a given frequency, the parameter space above the curve indicates that inertial cavitation will occur, within the limits of the model and for the specific definition of inertial cavitation chosen (Neppiras, 1980; Flynn and Church, 1988; Leighton 1994, Section 4.3; Holland and Apfel, 1989; Apfel and Holland, 1991; Allen et al.,
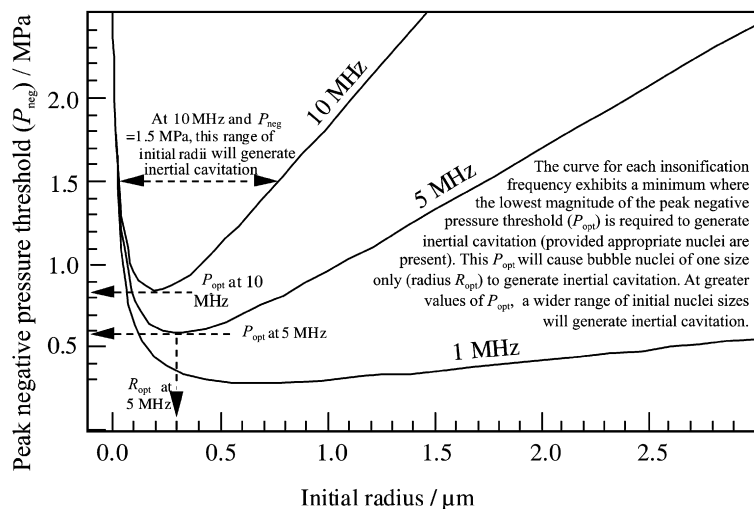

Fig. 20. Illustration of the threshold for inertial cavitation, after the calculation of Apfel and Holland (1991), in terms of the variation in the peak negative pressure required to generate inertial cavitation from a free-floating spherical gas bubble nucleus, as a function of the initial radius of that bubble. Above the curve, inertial cavitation will occur. As the acoustic frequency increases, the threshold tends to increase for all initial bubble sizes, and the radius range which will nucleate inertial cavitation decreases. Redrawn by permission from Ultrasound in Medicine and Biology, vol., 17, pp. 179–185; Copyright © 1991 Pergamon Press Ltd.

1997). Therefore, for a given frequency and sound pressure amplitude, bubbles within a certain radius range will undergo inertial cavitation, and those outside of it will not. This range is illustrated in Fig. 20 for 10 MHz insonification with a peak negative pressure of 1.5 MPa.

Why should bubbles outside this radius range not undergo inertial cavitation? The simple answer is that inertial cavitation comprises both explosive bubble growth, followed by a sufficiently rapid collapse. If the bubble is too small, then surface tension forces prevent the initial sudden growth, and inertial cavitation does not occur (Leighton, 1998). This is because the Laplace pressure (the $2\sigma/R$ term in Eq. (50)) varies inversely with bubble size, and therefore increases rapidly with decreasing radius (Leighton, 1994, Section 2.1.1).

Conversely, if the equilibrium size R_0 of the bubble nucleus is initially too large, then it may grow, but insufficiently to then concentrate the energy sufficiently on collapse to generate free radicals etc. There are several ways of understanding this. For example, the timescales on which such large bubbles respond to pressure (i.e. grow during a rarefaction) are relatively slow compared to smaller bubbles (as evidenced by the approximately inverse relationship between bubble radius and natural frequency in Eq. (54). Approximate analytical expressions for this time were given by Holland and Apfel (1989), who considered the delay times in bubble response to be the summation of three components, corresponding to contributions caused by surface tension (Δt_σ), inertia (Δt_I) and viscosity (Δt_η), their sum being:

$$\Delta t_\sigma + \Delta t_I + \Delta t_\eta \approx \frac{2\sigma}{P_A - P_B}\sqrt{\frac{3\rho_0}{2(P_A - P_B)}} + \frac{2R_0}{3}\sqrt{\frac{\rho_0}{\Delta P_{wall}}} + \frac{4\eta}{\Delta P_{wall}}, \tag{65}$$

where P_A is the acoustic pressure amplitude of the insonifying field (assumed to be sinusoidal), and where P_B is the Blake threshold pressure, the difference between the hydrostatic pressure which exists in the liquid at equilibrium, and the critical tension in the liquid which must be generated in order to produce explosive growth in bubbles which are initially very small (Leighton, 1994, Section 2.1.3.(b))

$$P_B \approx p_0 + \frac{8\sigma}{9}\sqrt{\frac{3\sigma}{2R_0^3(p_0 + 2\sigma/R_0)}} \tag{66}$$

and where ΔP_{wall} is the time-averaged pressure difference across the bubble wall:

$$\Delta P_{wall} \approx (P_A + P_B - 2p_0 + \sqrt{(P_A - p_0)(P_A - P_B)})/3. \tag{67}$$

Since we are considering the large-bubble limit of the range of bubble radii which can nucleate inertial cavitation, the issue is not with P_B, and hence the dependence in (65) of the time for growth on initial bubble radius is primarily through the inertial term $\Delta t_I \approx (2R_0/3)\sqrt{\rho/\Delta P_{wall}}$, which is in this regime approximately proportional to R_0. Therefore the larger the bubble, the more slowly it grows, and so during a given rarefaction cycle, the less the degree of growth it achieves. To put this another way, the maximum radius R_{max} achieved by a bubble during the growth phase of inertial cavitation is:

$$R_{max} \approx \frac{4}{3\omega}(P - p_0)\sqrt{\frac{2}{\rho_0 P_A}}\left[1 + \frac{2(P_A - p_0)}{3p_0}\right]^{1/3} \tag{68}$$

(Apfel, 1981; Leighton, 1994, Section 4.3.1(b)(ii)) which is independent of the initial bubble radius R_0 (a point in agreement with high speed photography—Fig. 21). Again, it is because large bubbles do not grow to such a great extent as small bubbles (assuming the small bubbles are sufficiently large to grow at all—Eq. (66)), that bubbles larger than the threshold size in Fig. 20 do not have subsequent collapses which attain conditions sufficiently extreme to be termed 'inertial cavitation'. This is because, if one considers a bubble which has expanded to a maximum radius R_{max}, then during the subsequent collapse the wall accelerates inwards under the external pressure in the liquid p_∞. The kinetic energy acquired by the liquid when the wall speed has reached $\dot{R}$ is $\phi_{KE} = \frac{1}{2}\rho_0\int_{r=R}^{r=\infty} 4\pi r^2 \dot{r}^2\, dr = 2\pi\rho_0 R^3\dot{R}^2$. This must equal the work done by the difference in pressure between that found far from the bubble (p_∞) and the pressure in the liquid at the bubble wall (p_L),
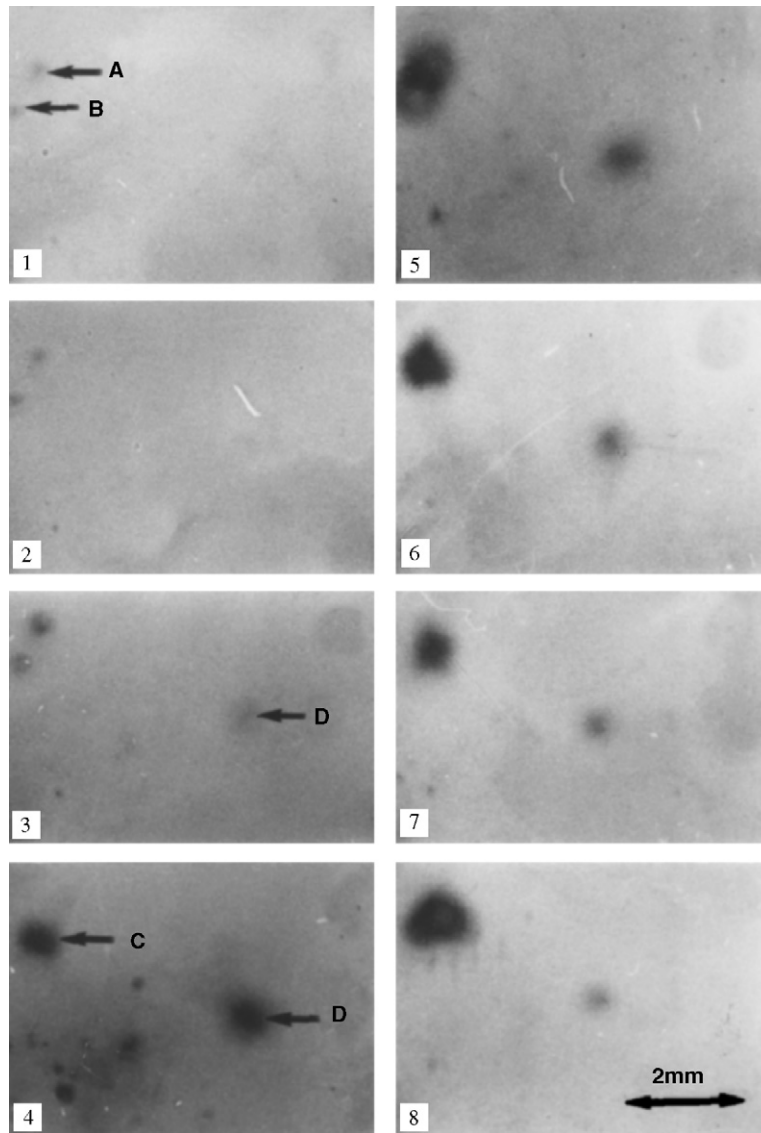
Fig. 21. Eight consecutive frames from a high-speed sequence filmed at 8000 frames per second. The onset of insonification (10 kHz, 0.2 MPa acoustic pressure amplitude in tap water) occurs between frames 1 and 2. The bubbles labelled A, B and D have initial sizes which make them too large to undergo inertia cavitation (Fig. 20). They undergo non-inertial pulsations (bubble D entering the depth of field in frame 3). Bjerknes forces cause A and B to coalesce in frame 4 to form bubble C, although its subsequent oscillation appears to be asymmetrical (it is difficult to be certain because timescales of the pulsations frequency are not resolved). A cloud of many bubbles which had initial sizes that were too small to be visible (in frames 1 and 2) undergo very rapid and extensive growth, all attaining a similar maximum size in frame 4 (roughly 250–400 μs after the onset of insonification, which concurs with modeling–Leighton 1994, Section 4.2.3). Unlike the non-inertial bubbles (A, B and D) they rapidly collapse. This phenomenon was very repeatable (Leighton et al., 1989).

which is $\int_{R_{\max}}^{R} (p_L - p_\infty) 4\pi R^2 \, \mathrm{d}R = 2\pi\rho_0 R^3 \dot{R}^2$. In the limit that the cavity contains no gas at all, the liquid pressure p_L just outside the cavity is zero (if surface tension is assumed to be negligible): this is the Rayleigh collapse, and bubbles which were initially very small would tend to this in the early stages, since their gas pressure when $R = R_{\max}$ is very low. However bubbles which are initially much larger than this will contain a significant gas pressure when $R = R_{\max}$ since they have not undergone such an extreme expansion. As a result, p_L will take a finite value in the above energy balance (Leighton, 1994, Section 4.2.1(a)), and the kinetic energy achieved by the liquid on collapse will be less.

There is therefore a critical size range[22] in which, for a given sound field, the initial size of the bubble must fall if it is to nucleate inertial cavitation (Apfel, 1981; Flynn and Church, 1984; Holland and Apfel, 1989; Leighton, 1994, Section 4.3.1). The lower the frequency, the wider this range. This is one reason why ultrasonic cleaning baths exploit relatively low ultrasonic frequencies (20–30 kHz), in order to generate as much cavitation is possible. To take an example from the opposite end of the frequency scale, the original plot on which Fig. 20 is based played a part in defining the mechanical index (MI) (Holland and Apfel, 1989; Apfel and Holland 1991). The MI is defined as the ratio of the peak rarefactional pressure (expressed in MPa) to the square root of the centre frequency of the pulse (in MHz). The MI can be used to provide a rough form of estimation of the likelihood of cavitation during MHz insonification (Barnett et al., 1993; Meltzer, 1996; Carstensen et al., 1999; Duck, 1999; Abbott, 1999). Since at MHz frequencies the U-shaped curves of Fig. 20 are narrow, the MI is defined with the assumption that a bubble nucleus having a radius corresponding to the minimum of the curve will be present. However it is important to appreciate the additional assumptions which have been made now that the MI is now part of the AIUM/NEMA Real Time Output Display Standard for the on-screen labelling of acoustic output on diagnostic ultrasound systems (thermal effects are characterised by the Thermal Index; AIUM/NEMA, 1992, 1998). These assumptions arise primarily because in clinical use there is no direct measurement of the peak rarefactional pressure (and indeed, since this pressure varies throughout the field, the cited MI refers to one point in the field, usually near the transmit focus of the transducer and near the centre of the scanned plane). The value of MI which is displayed on-screen is automatically estimated by the circuitry in the scanner using the output to the transducer, and as such it assumes that the medium is simple and uniform and has an attenuation of 0.3 dB/cm MHz. The circuitry does this, of course, without having any direct knowledge of the medium which is being scanned (i.e. whether it is in vivo or in vitro, or whether it contains contrast agent or not), such that it is possible to set up conditions (e.g. in vitro) where the ability of the on-screen MI to estimate the likelihood of cavitation is compromised.

5. Scales in space and time

5.1. Frequency ranges

Fig. 22 shows several identifiable features on a scale of the frequencies. It is based on a demonstration of such scales, where five markers (indicating, respectively, 20, 40, 60, 80, and 100 kHz) were placed in a lecture hall at 1 m intervals from a datum (representing 0 Hz). The low frequency limit of human hearing, which is taken to be at 20 Hz, would occur 1 mm from the datum on this scale. The upper frequency limit of human hearing, taken to be 20 kHz, occurs 1 m from the datum, and represents the lower frequency limit for the ultrasonic range.

It is in this low kHz regime that some key technologies operate, for physical reasons which are different depending on whether the modality is being used for diagnosis or material processing (termed 'therapy' for biomedical applications).

Consider diagnostic modalities. Sub-bottom profiling of the seabed, for example, uses audio and ultrasonic frequencies up to a few tens of kHz for geophysical surveying for industries involved in harbour construction, petrochemical prospecting etc. (Fig. 23). The frequency chosen illustrates a compromise found in much of diagnostic ultrasonics. The first component of this compromise arises because an increase in ultrasonic frequency promises better spatial resolution (for example in imaging). This is based not only on the Rayleigh criterion for

---

[22]An imperfect analogy of this can be found by imagining shooting a stone from a catapult. As discussed in the text, it is a feature of inertial cavitation that those bubbles which undergo it in a given sound field tend to grow to a maximum size (prior to collapse) which is similar for all such bubbles (Leighton, 1994, Section 4.3.1(b)(iii)). In the analogy, this is similar to the stretching of the catapult elastic to a length of approximately 1 m: the *Y*-shaped stick is held out in front, in one hand, whilst the stone is held in the other hand, which is drawn back behind the shoulder. The tension in the elastic is an imperfect analogue of the gas within the bubble which, because of the expansion, is at low pressure. If one were to be considering a very small bubble, this might be represented by very short elastic: the forces causing expansion are insufficient to produce growth to the degree required (one cannot draw the elastic to 1 m length, just as the surface tension forces in the bubble hinder growth). The draw in the catapult is small, and the stone does not project far. If one were to consider a large bubble, this might be like having elastic which initially (i.e. when relaxed) is too long (say, 80 cm). Though it can readily expand to the full 1 m, when it does so the elastic energy stored is insufficient to project the stone very far. There is a critical range of relaxed lengths for the elastic which will cause the stone to be projected to far distance.
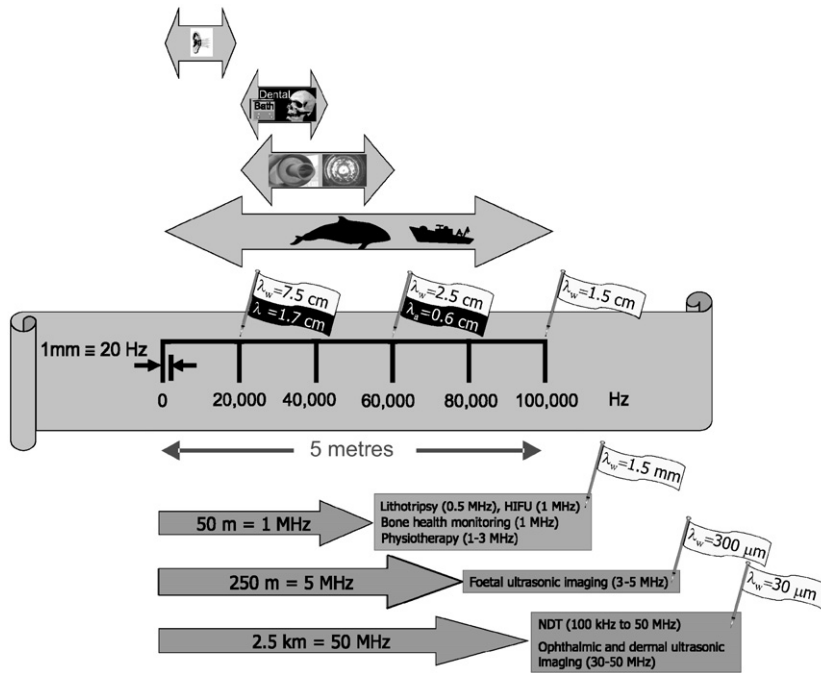
Fig. 22. The figure shows several identifiable features on a scale of the frequencies. It is based on a demonstration of such scales, where five markers (indicating, respectively, 20, 40, 60, 80 and 100 kHz) were placed at 1 m intervals from a datum (representing 0 Hz). The figure illustrates this schematically through an unfurled banner, onto a 5 m section of which are placed the six markers for 0–100 kHz. The position on this scale of 20 Hz, which is generally taken to be the lowest frequency audible to humans, is shown as being 1 mm from the datum. Above the banner, double-ended arrows indicate important frequency ranges. At the top of the figure, the range of human hearing is shown. The two arrows below that show the ranges typically adopted by several power ultrasound technologies: first, ultrasonic cleaning baths and dental ultrasonics; second, (illustrated by transducers fitted to pipelines and rings of luminescence similar to those shown in Fig. 19), power ultrasonic devices for processing materials, for example in pipelines. This frequency range tends to be popular: it is restricted to <20 kHz to avoid hearing hazard, but does not go too high in the ultrasonic range for a number of reasons. These include lower attenuation and the ease at which cavitation can be generated compared to O(100 kHz). Of course, some applications wish to avoid cavitation, and may chose higher frequencies for that reason. The lowest arrow above the banner indicates the fact that this whole range of frequencies is used in the oceans, both by cetaceans and humans. Humans use these ranges for purposes which vary from geophysical surveying at low frequency (as in Fig. 23) to zooplankton monitoring at >100 kHz (Griffiths et al., 2001) and even using pulses containing energy up to 300 kHz (Holliday, 2001). There are also military uses.
Arrows below the banner show that the markers for 1, 5 and 50 MHz would occur at distances from the datum of 50, 250, and 2500 m, respectively, on this scale. The associated applications (mainly biomedical) are indicated.
Six flags are 'pinned' into the figure, indicating the wavelength in water λ_w at the frequency where the pin is attached. The wavelength in air λ_a is also shown, but only for the pins at 20 and 60 kHz, artificially to emphasise the fact that, compared to ultrasound in water or metals, applications in air are far more rare at higher frequencies because of the higher absorption there (Table 2).

the separation of objects laterally (which in its most basic terms requires that, for good imaging, the wavelength be significantly smaller than the object to be resolved,) but also for resolution in terms of the range from the sensor. This is determined by the duration of the ultrasonic pulse, which in general can be more brief (increasing range resolution) the greater the ultrasonic frequency. However with increasing frequency comes, in general, an increase in absorption, and hence a decrease in the depth from which echoes can be received with an acceptable SNR. A compromise must be found between this loss of 'penetration depth' and the ability to resolve the size of object of interest. For geophysical work, this compromise is illustrated in Fig. 23 and its caption: the highest resolution profilers currently available, with resolutions of the order of 1 cm (i.e. O(1 cm)) require a frequency of 150 kHz, which gives a penetration depth of about 3 m (Mindell and Bingham, 2001). In contrast standard geophysical surveying (where resolutions of O(10 cm) or less are adequate) uses frequencies of <10 kHz, and commensurately has greater penetration depths (up to ~20 m depending on the seabed type). The wavelengths in pure air (λ_a) and pure water (λ_w) under STP at key frequencies are shown in Fig. 22.
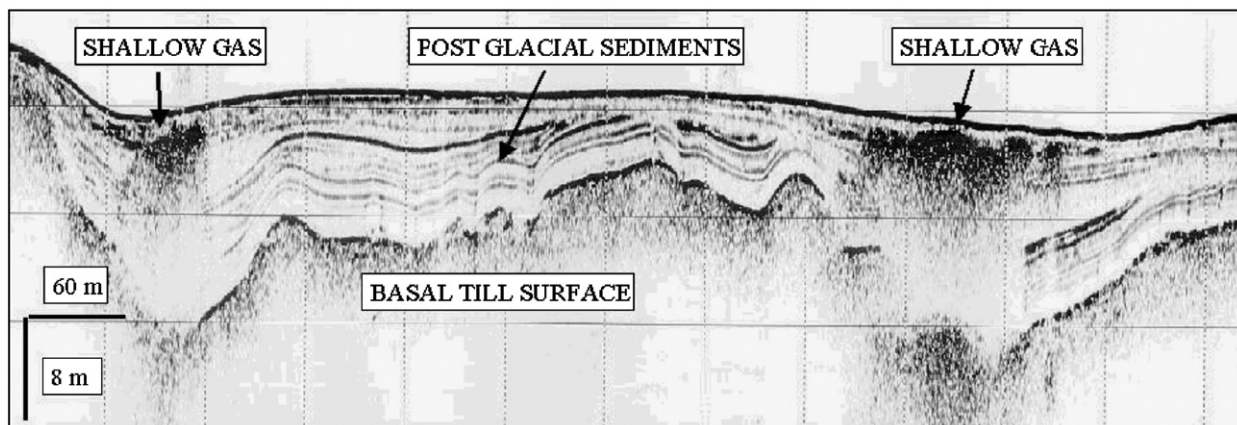
Fig. 23. A chirp sonar image, showing a cross-section of the seabed (maximum penetration approximately 20 m) in Strangford Lough, Northern Ireland. The dark line, which is usually 8–10 m from the top of the frame, indicates the sea floor. Hence the labelled features are beneath the seabed. These include shallow gas deposits in the underwater sediment. The sonar cannot penetrate these, as the majority of the sound is scattered from the gas bubbles. As a result, very little information is obtained from beneath the gas layers. Reproduced by permission of Southampton Oceanography Centre (J.S. Lenham, J.K. Dix and J. Bull). These data were taken at audio frequencies (covering 2–8 kHz in a Chirp sweep, with a Blackman-Harris envelope). However frequencies up to 150 kHz have been used for sub-bottom profiling (Mindell D.A. and Bingham B., 2001).

For material processing, the compromise is based on other criteria, some of which overlap with the above. Penetration depth is also an issue here, particularly as the material to be processed is often contained in pipework. If this is the case, the insonifying field must propagate with sufficient amplitude to the point of interest, often crossing numerous interfaces. For example, if the transducers are mounted on the outside of a pipe, then the sound needs not only to propagate through the material of the pipe and its contents without severe attenuation: it must in addition not suffer too great attenuation at the material interfaces between transducer faceplate and the outer wall of the pipe, and between the inner wall of the pipe and its contents (note the values of $\left|1 - R^2\right|$ shown in Table 1). Whilst to first order these reflection losses are frequency independent, there are numerous complexities, such as the generation of other modes (e.g. shear waves) when a compressional wave is incident on an interface. If the choice of frequency is done carefully, other features might come into account: the pipe example illustrates this well, when the choice of frequency may be made to coincide with, or avoid, modes of the pipe (Leighton et al., 2002; Birkin et al., 2003a, b). Alternatively, if the ultrasound field is to be used for processing the material in the pipe, for example to cause crystallisation, it may be very important to avoid leakage of the sound from the region where processing is intended to occur, to other regions of the pipe (where premature crystallisation might cause blocking): this can be prevented by careful engineering, which includes consideration of the choice of frequencies.

If the objective is to process the material, then the mechanism by which that processing occurs may influence the choice of frequency. If heating (hyperthermia) is required for the processing, a high frequency may be chosen to generate this. Increasing the frequency tends to reduce the likelihood of cavitation (Section 4.3). Therefore for ultrasonic cleaning baths, ultrasonic frequencies of 20–30 kHz are chosen. Alternatively, some processes (e.g. in food production) may require that the ultrasonic processing (e.g. crystallisation) be undertaken while eliminating the risk of cavitation, as it can oxidise the product and generate 'off-flavours'. For such a field the frequency should be high (Section 4.3), the I_{TP} should be low, but the I_{TA} should be sufficiently high to generate the processing. Conversely lithotripsy requires cavitation without hyperthermia. As a result the I_{TP} for lithotripsy is high, but the I_{TA} is made low by having a duty cycle of $1:10^5$ (i.e. 1 s off-time for every 10 μs on-time), with an oscillatory frequency centred on several hundred kHz (Fig. 24). Note that, although cavitation is required, the chosen frequency is rather higher than the 30 kHz used in the cleaning bath example above, where cavitation was also required. The reason why lithotripsy uses higher frequencies is the need to focus the sound field onto the kidney stone in order to fragment it, without damaging the surrounding tissue. Therefore the ability to focus, and to resolve (in both space and time/range), are also factors in the choice of frequency.
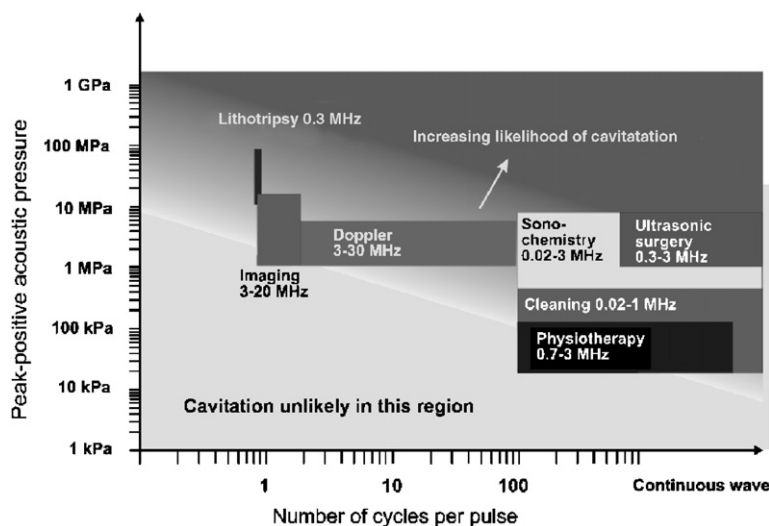
Fig. 24. A rough schematic of the acoustic pressures and pulse lengths employed in some of the applications of ultrasound. Parameters are meant as a rough guide only. If an application lies outside the zone where 'cavitation is unlikely' this does not necessarily imply that inertial cavitation will certainly occur: this would depend on a number of factors, not least the likelihood of nucleation in the liquid sample in question (from Leighton et al., 2005a).

In recent years there have been many papers investigating which is the 'best' frequency for a given ultrasonic processing application, by 'spot-checking' the sonochemical effect at a half-a-dozen frequencies covering the range 20 kHz to over 1 MHz (Mark et al., 1998; Hung and Hoffmann, 1999; Sato et al., 2000; Kojima et al., 2001; Becket and Hua, 2001). Such approaches do not convey the message that, because net frequency response of the system is dependent on the frequency responses of several particular pieces of apparatus, the results could be highly laboratory-specific. As a specific example, the results of Fig. 19 show that a change of 1 kHz (<1% of the driving frequency) can dramatically change the chemiluminescence produced by cavitation: in such a system, spot-checking the chemical activity at half-a-dozen frequencies spaced 10s or even 100s of kHz apart would provide a experiment-specific result for the 'best' frequency. This is because in most applications, the amount of processing generated is strongly dependent on the amplitude of the sound field in the material which is to be processed,[23] a point upon which the remainder of this subsection will expand.

Having said that the amplitude is important, how this manifests itself depends on the mechanisms in question (pressure or intensity, spatial and temporal averaging, etc.). In many cases, that acoustic pressure which corresponds both to the spatial peak and to the temporal peak is a useful indicator of the processing conditions. However the value of this depends on many factors. In the words of Apfel (1984): "Know thy liquid; know thy sound field; know when something happens." As shown in Fig. 25, the chemical, physical and biological effects of cavitation depend on both the type of cavitation (e.g. inertial, non-inertial, jetting, fragmentary) and its location (Leighton, 1995; Leighton et al., 2005a). Both of these factors depend strongly on the local sound field at the bubble and on the sizes of bubble present in the population. These two together, for example, characterise the inertial cavitation threshold, and also the locations to where bubbles might migrate and accumulate under radiation forces (depending on the other relevant forces present, e.g. flow, turbulence, streaming, etc.). Such accumulations will in turn affect the local sound field, through the processes of channelling, dispersion, absorption, diffraction, scattering and shielding (Fig. 13). They will in turn affect the bubble size distribution through their influence on the processes of coalescence, fragmentation, rectified

---

[23]That is not to say that the amplitude is the only factor: Section 5 illustrates in addition how the frequency can contribute to the spatial and temporal characteristics of the ultrasound field. As shown in Section 2, the frequency is important for considering hyperthermia and, with cavitation, the initial distribution of bubble nuclei is also key (Section 4.2). The nuclei distribution is often ignored, partly because it is often (but not always—Shortencarier et al., 2004) outside of the control of the user, and also because if many pulses are to be projected into the liquid, each causing cavitation, the initial distribution might not be as important as the hysteretic effect generated by the nuclei which survive from one pulse to the next—Leighton et al., 1994, Section 5.3).
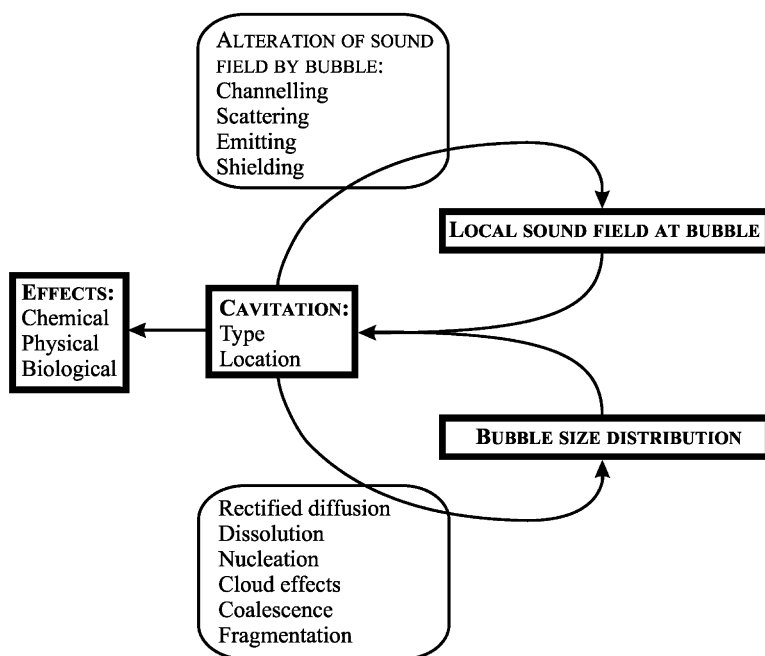
Fig. 25. The behaviour of a given bubble depends on the initial bubble size, and the sound field at the location of that bubble. In turn the sound field at the bubble depends on the properties of the bubble population as a whole. The interaction of these two, in turn, influences the initial bubble size. These interactions are illustrated schematically in the figure (After Leighton, 1995).

diffusion and shape stability. As a result, the observed effect depends on the characteristics of the cavitation, which are determined by the local sound field and the bubble size distribution. However there is feedback from the cavitation, which influences these two key parameters.

It should be noted that the words of Apfel, quoted above, specify the *minimum* criteria that must be met if a reference for cavitation is to be produced. This is because they refer to the *threshold* for cavitation, and not to the degree of cavitational 'activity'. The latter is quantified through measurement of some effect produced by cavitation, be it luminescent, chemical, acoustic, erosive, biological, etc. (Leighton et al., 2005a). Hence to measure cavitational 'activity', it is necessary to understand what is being measured, and its place amongst the other effects. It is for example no use basing a sensor to monitor the efficacy of cleaning baths on acoustic emission if that emission bears no relation to the amount of cleaning which occurs. Birkin et al. (2003b) attempted to identify the existence, or otherwise, of such correlations. A cylindrical sonochemical reactor was driven at frequencies from 20 to 160 kHz, with frequency increments as small as 1 kHz. Over the same frequency band, a hydrophone was used to monitor the acoustic pressure at three locations within the cell. A number of experimental parameters which reflect cavitation were monitored: multibubble sonoluminescence (MBSL), multibubble sonochemiluminescence, degradation of an organic species (medola blue), the Fricke reaction, the Weissler reaction, hydrogen radical trapping using the formation of $CuCl_2^-$, and the emission of in-air broadband acoustic signals across the audio frequency range as the drive frequency varied from 20 kHz to 160 kHz. Strong correlations were observed between both luminescences and the sonochemical reaction rates. The peaks in activity followed the frequencies at which strong modal structures occurred within the reactor, rather than reflecting the resonances of the drive transducer (Birkin et al., 2003b). The in-air acoustic emission did not correlate so well with the luminescences and sonochemical indicators. Measurements of the drive acoustic pressure amplitude, which was measured at only three locations in the cell, could be used to predict at which frequencies cavitation (and hence sonochemical activity) would be initiated: when a peak in one occurred, a peak in the other was seen. However the relative magnitudes of the peaks in drive pressure amplitudes did not reflect the relative magnitudes of the peaks in sonochemical activity. These results were interpreted in terms of the frequency dependencies of the various components of the system (Fig. 26).

Signal generator: frequency dependence usually negligible.

↓

Power amplifier: frequency dependence usually slowly varying.

↓

Ultrasonic transducer: often highly resonant frequency dependence.

↓

Reaction vessel: the net sound field contains contributions from the direct and reverberant fields. Where the latter dominates, the frequency dependence is modal below the Schroeder frequency, where at any given frequency the activity will vary with location within the cell.

↓

Detector: usually exhibits negligible dependence on the drive frequency, but spatial and temporal averaging of reading (e.g. footprint) can be important.
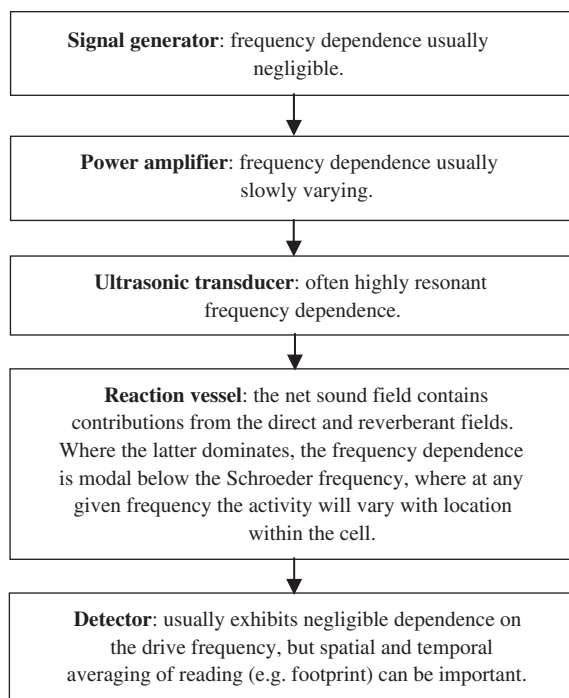
Fig. 26. Diagram showing the components and their various frequency dependencies commonly employed in sonochemical experiments (after Birkin et al., 2003b).

This section outlined the range of frequencies used for ultrasonic applications, and the reasons for choosing a particular frequency. Having made this choice because of a given priority (such as generating a resonance, cavitation, hyperthermia, or a particular resolution), there are implications of this choice with respect to how it affects the process in question. Perhaps the most important of these is through the spatial interactions of the sound field with its surroundings, as characterised by the value of ka. This is the topic of next section.

5.2. Implications of the choice of ka

If a is the characteristic linear dimension of a physical inhomogeneity in a medium, its interaction with the sound field depends, amongst other quantities, on the value of ka, where k is the acoustic wavenumber.

The degree to which consideration of this parameter is very common in acoustics may surprise readers who are more familiar with consideration of electromagnetic radiation. This is because the speed of sound is so much less than the speed of light. If $ka = \omega a/c = 2\pi \Upsilon a/c$ is much less than unity, the body is considered to be too small to disturb the wave field: if such a body is placed in the sound field, barely any diffraction occurs,[24]

---

[24]Although the issue may not be simple. Birkin et al. (2005) examined an ultrasonic horn, operating at 23 kHz and with a transducer faceplate of radius $a = 1.5$ mm. A simple calculation for such a horn would show that $ka = 0.14$ for the horn. In the free field it would be an approximately omnidirectional transmitter, although since it is normally dipped into water from above, its emissions would resemble a dipole depending on how close the tip was to the surface. Into the sound field was placed an erosion sensor for which the characteristic dimension a was ~ 1 mm: hence for this sensor $ka \sim 0.1$. Therefore the sound field from the horn should not have been directional (although the presence of the pressure-release air/water interface through which the horn tip was dipped would in practice lend a dipole character to the field), and the sensor should have been too small to perturb the field significantly. However these calculated values of ka are made assuming that the wavenumber of interest is that associated with the 23 kHz sound field from the horn. In fact, the ultrasonic cavitational effect detected by the sensor was strongly affected by the shock waves produced by the cavitation immediately preceding the measurement. For these shock waves, the sensor has sensor $ka > 0.5$. Reflection of these shock waves by the sensor greatly influenced the subsequent cavitation. This demonstrated showed how a sensor of radius a, where $ka \ll 1$ as regards the wavenumber of the insonifying field from an ultrasonic horn, nevertheless strongly influences the ultrasonic processing of the medium because ka can be much larger for those shock waves generated by the cavitation collapse which is produced by the field from the ultrasonic horn.

and if such a body is a sound source or receiver, its shape has no effect on the sound field, and it projects and receives omnidirectionally (Wells, 1977; Kinsler et al., 1982; Leighton, 1994, Section 3.3.2(b)). A 1 MHz radio wave has a wavelength of 300 m: most bodies smaller than buildings would present this wave with a $ka \ll 1$, and hence reflection and diffraction of this wave by them would be small. In contrast, a 5.3 MHz ultrasonic wave in water has a wavelength of ~280 μm. Even a 400 μm radius needle hydrophone is seen as large by the sound field ($ka \sim 9$) (Fig. 27). Such sensors can therefore be invasive with respect to perturbing the ultrasonic field they are in place to measure. Even if they were not invasive, the large ka values means that if the directionality of the sensor is not measured (Fig. 28), and its orientation precisely known, it would be impossible to be apply a calibration to measured data. That some researchers have obtained data using hydrophones in inaccessible places (such as the vagina) where its orientation is difficult to monitor and control, is a testament to the care with which the experimentation was undertaken (Daft et al., 1990).

The ka issue is further complicated for the propagating wave, since not only will it often encounter physical objects for which $ka > 1$, but the acoustic impedance mismatches between the object and the host medium will often be large (Table 1). Consider a 30 kHz bench-top cleaning bath field in which the wavelength[25] is 5 cm, such that each side of the bath will be approximately several half-wavelengths long. This will make the field inhomogeneous (Fig. 29), complicating its measurement (even if the users are aware of the inhomogeneity) and making its performance very dependent on the exact position within it of the item to be cleaned. When the investigations are extended to the studies which describe the 'best' frequency for an ultrasonic process (Section 5.1), it is clear that not only are the transfer functions of Fig. 26 a consideration, but also the frequency response(s) of the particular vessel(s) used for the test can dominate the measurement.

The final example of the implications of having sound speeds such that ka will commonly exceed unity, is found in the transducers used to generate sound fields. Consider first the opposing case, that of a transducer for which $ka \ll 1$ with respect to the driving oscillatory field in the free field. A simple calculation (i.e. one which disregards the cautionary tale of footnote 24) would suggest that such a transducer would act as a monopole source, and exhibit no near field. However for transducers with larger values of ka, there will be a measurable near field (Fig. 30). This is characterised by a regions where, for constant driving conditions, even in the free field the sound field amplitude can change dramatically for very small changes in the relative position of the sensor with respect to the transducer. Similarly, any perturbations to the field (such as the passage through the beam of inhomogeneities in the medium which change the sound speed or scatter the field), can give rise to very large fluctuations in amplitude in the detected signal. As one moves away from the transducer faceplate along the axis of the transducer, the near field region is characterised by a series of closely-spaced maxima and minima. The near-field extends out from the transducer to a distance of around:

$$L_{near} \approx \frac{a^2}{\lambda} = \frac{ka^2}{2\pi}. \tag{69}$$

This corresponds to the distance from the faceplate to the axial acoustic pressure maximum which is furthest from the faceplate (Wells, 1977; Fig. 30). At further ranges, in the free field the beam amplitude should fall off steadily with increasing on-axis range from the source.

Because the propagation speed of sound is much less than that of light, these near field complications can be very much more commonly a problem in ultrasonics than they are in electromagnetic studies. Even in ostensibly unfocused beams, apparently negative attenuations can readily be detected, since the amplitude further from the source can be greater than that close to the source. If the attenuation of the beam is being attributed to absorption by the medium, and then inverted to determine physical properties of that medium (as is done for bubble detection, osteoporosis monitoring, the quality of pharmaceuticals, foodstuffs, domestics, paint and pottery, etc. (Leighton, 2004)) then lack of appreciation of near field effects would lead to nonsensical answers. A typical scenario, unfortunately very common in both experimentation and commercial ultrasonic technology, outlines several of these problems (all the issues here are not merely fictitious examples, but rather, have been identified by the author in sensors he has been asked to validate). Consider a thin-walled pipe of internal diameter 30 mm. A source and a receiver transducer (each of 10 mm faceplate radius) are to be

---

[25]Whilst it is acceptable for the purposes of the thought-experiment described here (such that at 30 kHz the wavelength is 5 cm), it is not safe to assume that the sound speed in a cavitating field is that of bubbly water (see (Fig. 19)).
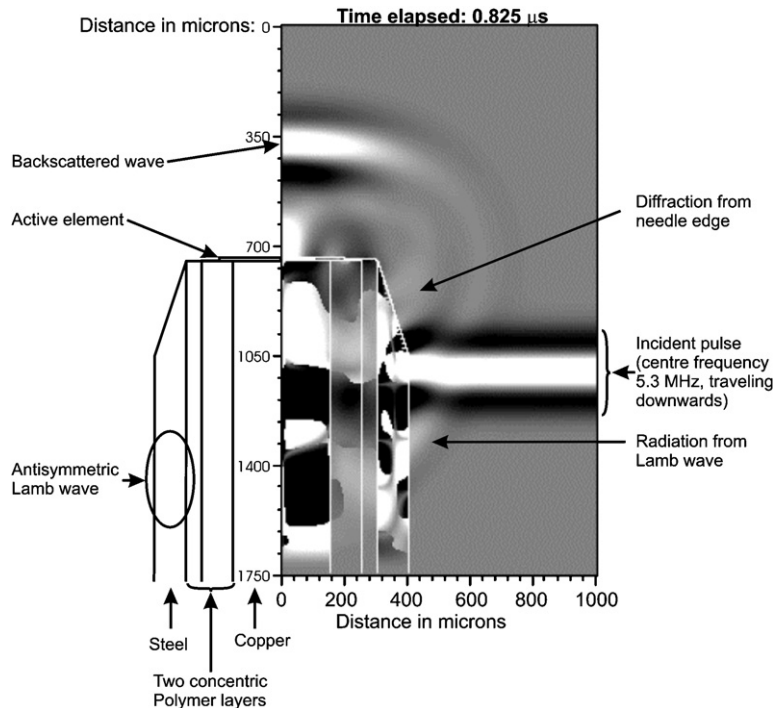
Fig. 27. Simulation using acoustoelastic finite difference solver (AfiDS—Hurrell, 2002) showing the effect on the acoustic field of a needle hydrophone. The left side of the graph is an axis of rotational symmetry. A plane pulse waveform (having centre frequency 5.3 MHz) has travelled through water, downwards from the top of the figure. It is shown at the moment when it has passed the base of the tapering in the stainless steel tubular tip of the needle hydrophone. Contained within this steel are (working from the outside towards the centre) a thin layer of polymer, a thicker layer of polymer, and finally, in the centre, a rod of copper. At the very tip of the needle is the active sensing element of the hydrophone, a disc of radius 200 μm. The pressure perturbations of the pulse are broader in the copper, and have travelled further downwards, than in the water, because the sound speed there is greater than in the water. Amongst the pressure field in the steel can be seen the antisymmetric Lamb wave, and its radiation into the liquid can be seen ahead of (i.e. below) the original pulse in the water. With a radius of 400 μm, the *ka* of the hydrophone to this waveform in water is about 9. Reflected waves, travelling back upwards from the hydrophone tip, are clearly visible and, even with tapering, diffraction from the tip perimeter is evident. The waves is shown at a time 0.825 μs after the incident pulse first appears at the top of the figure (simulation by A Hurrell). A schematic to the left of the graph clarifies the geometry and features.

mounted opposite each other, ostensibly to interrogate the cross-section of the pipe (Fig. 31). A coupler is added to each faceplate to mould the shape of the flat transducer faceplates to the curved wall of the pipe, and to match their impedances and ensure no air gap between transducer and pipe (which would introduce large impedance mismatch (Table 2)). A practical example of the use of such a coupler is shown in Fig. 32. In the hypothetical situation of Fig. 31, the source emits a signal (continuous wave, tone-burst or chirp) and this waveform is seen in the output from the receiver. The amplitude of this signal is inverted using a model (let us say of acoustic absorption by bubbles, the inversion being used to estimate the bubble population in the pipe, by projecting a series of tones extending from 30 to 300 kHz). All seems to go well, and the experimenters progress to emitting as series of pulses, like the ones shown in Fig. 4, so that the inversion can be based on both attenuation and sound speed. Again, all goes well, until the discovery that the signals are also detected when the receiver is not in contact with the pipe. Being acoustically uncoupled from the pipe, it should detect nothing, but in fact its output is the result of electromagnetic pick-up from the amplifier/transmitter ((i) in Fig. 31). Unless a decoupling test is undertaken, this can be overlooked as the EM pick-up closely resembles the transmitted waveform and so is as the experimenter expects. However the problem should have been spotted from the lack of an appropriate delay introduced by the transit time of the pulses (of roughly 0.03 m/ 1500 m s^{-1} ~20 μs). Suitable electromagnetic shielding is added, and the detector now receives far less 'clean' waveforms, as expected for such a reverberant environment. Again, no problems are found in either
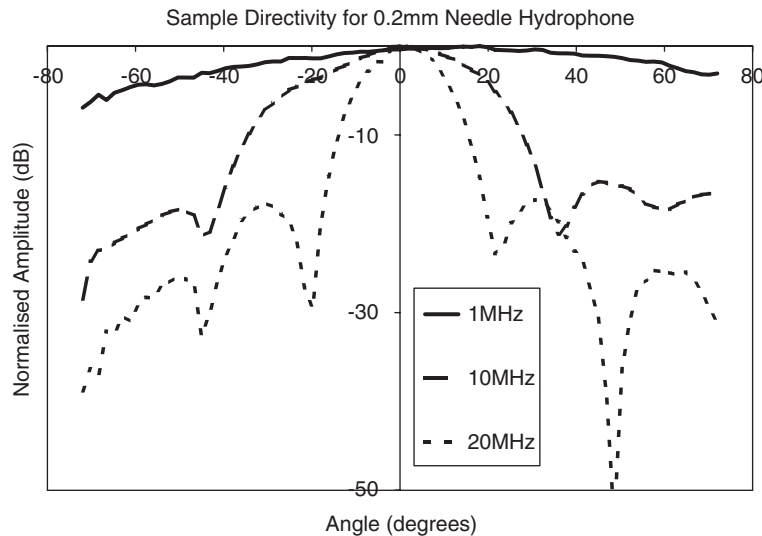
Fig. 28. Directionality plots for a needle hydrophone of radius 200 μm (data courtesy of A. Hurrell, Precision Acoustics Ltd.).

continuous-wave or pulsed operations, but after a while of apparently satisfactory operation, the pipe is one day emptied and the waveforms are still detected (and the inversion still uses them to invert for a now obviously fictitious bubble population). The problem is identified as being the result of waves (for which there can be several types—see Fig. 1) propagating through the pipe walls between transmitter and receiver, which dominate the signal ((ii) in Fig. 31). As a result the transducers are designed to be embedded in the pipe wall, and insulated from it acoustically. This new set-up appears to work and the detected waveform is inverted to generate a bubble population, but the now cautious users ask for ground truthing, a separate measurement of the bubble population, which disagrees with that of the original device. This exposes a number of problems in the arrangement. There is reverberation in the pipe ((iii) in Fig. 31), so that the measured attenuation contains contributions from much longer path lengths than that provided by the aligned axes of the transducer, making conversion of such an attenuation into a dB/m estimation difficult. Attempts to remove reverberation by time-gating the received signals prove to be unsuccessful: the path difference between the direct path (30 mm) and the first echo from the pipe wall ($2 \times \sqrt{15^2 + 15^2} \approx 42.4$ mm) corresponds to an interval in pure water of $(42.4 - 30) \times 10^{-3}/1500 \approx 8$ μs, i.e. less than three cycles at 300 kHz, and only one quarter of a cycle at 30 kHz. This difficulty is compounded if the system has a time-response (such as a ring-up in the response of the bubbles, noting that the inversion assumes they are at steady state). Even without reverberation, the beam pattern that would occur in free field would be problematic: As a simple application of equation (Eq. (69)) would have shown, the near-field for this transducer can extend well into the measurement volume (at 300 kHz, $a^2/\lambda = 20$ mm, Fig. 30). As a result, the introduction of small inhomogeneities like bubbles into the measurement volume can give changes which are difficult to interpret. For example, since the path difference (between the path along the transducer axis and the path from the edge of the transmitter to the centre of the receiver in Fig. 31) is $\sqrt{30^2 + 10^2} - 30 \approx 1.6$ mm, equivalent to $> 30\%$ of a wavelength at 300 kHz, then a small change in sound speed along one of those paths could dramatically change the received signal, such that a sound speed change will be interpreted as a change in absorption.[26,27] Indeed, those changes can be of either sign: the problem of apparent negative absorption in the near field was introduced earlier, and it is insufficient for the operator to reject such nonsensical results but retain those which, whilst similarly compromised, are

---

[26]This is because of phase changes induced along some propagation paths, which affect the signal on summation at the receiver. Indeed even in the far field, changes in sound speed can affect beam patterns sufficiently to appear as additional attenuations, although here it is far simpler to correct for the effect (Robb et al., 2006).

[27]The assumption is made here that receivers are 'phase sensitive' rather than 'phase insensitive' (Busse and Miller, 1981).
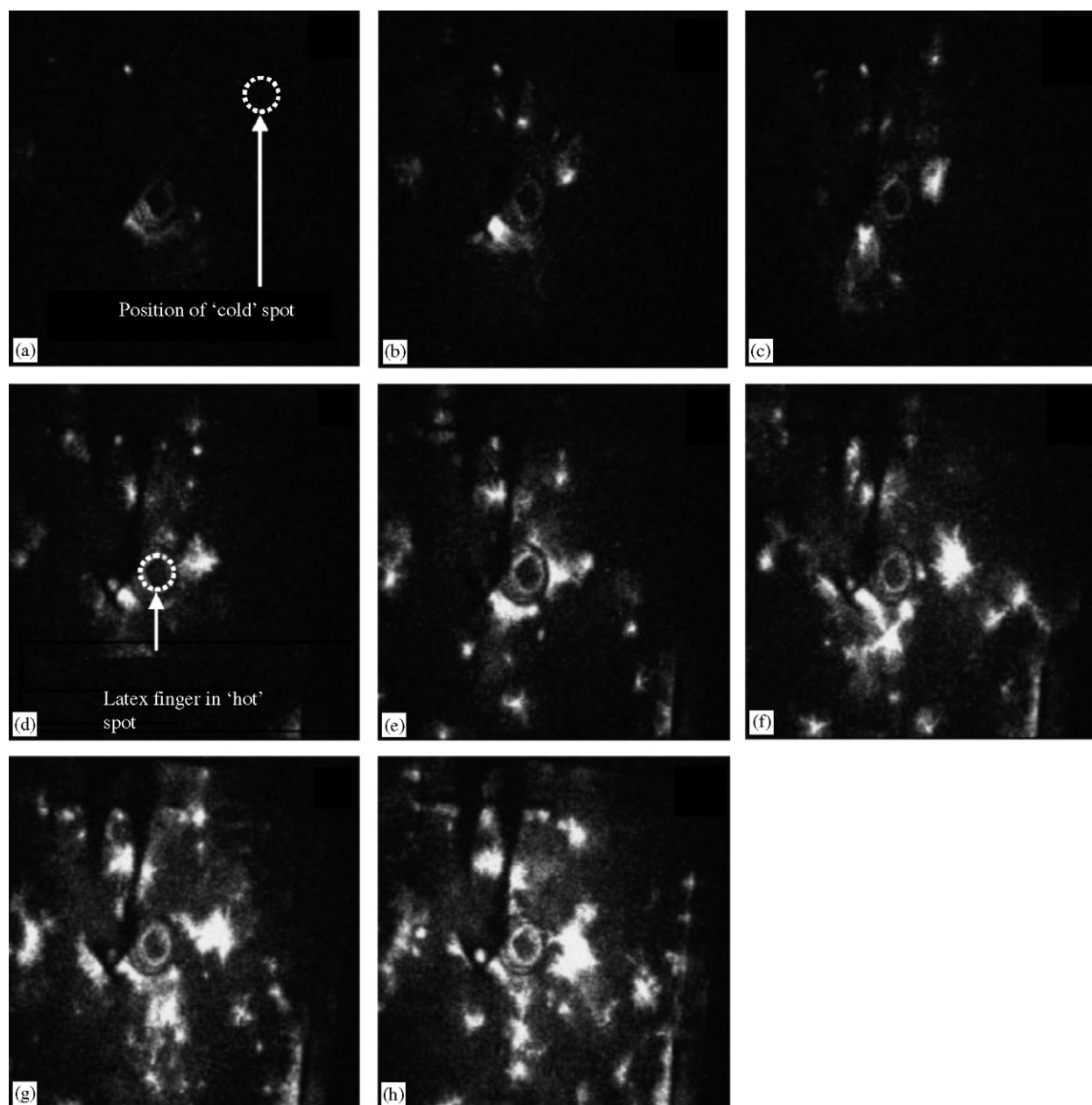
Fig. 29. Sonochemiluminescent pictures recorded in an ultrasonic bath as a function of the volumetric power density. The volumetric power density increases, respectively, from picture (a) to (h). The power settings were 2.5, 5, 7.5, 10, 20, 32.5, 42.5 and 47.5 W dm^{-3}, respectively. The temperature of the bath was 21 °C. The height of the camera above the surface of the 18 l luminol solution was 45.5 cm $\pm$ 1 cm. Regions of high cavitational activity ('hot' spot) and low cavitational activity ('cold' spot) are labeled. Also labelled is the cross-section of the finger of a latex glove which was used to contain sonochemical reactions (from Leighton et al., 2005b).

not so obviously erroneous. Indeed, it is apparent that measurement of attenuation and pulse propagation speed using a single source-receiver pair is difficult, even in the far field, as both quantities are realised through the propagation of a signal past two measurement points. If only one hydrophone is used, assumptions must be made about the signal amplitude and timing at the source, which can be simple to make but very difficult to verify.
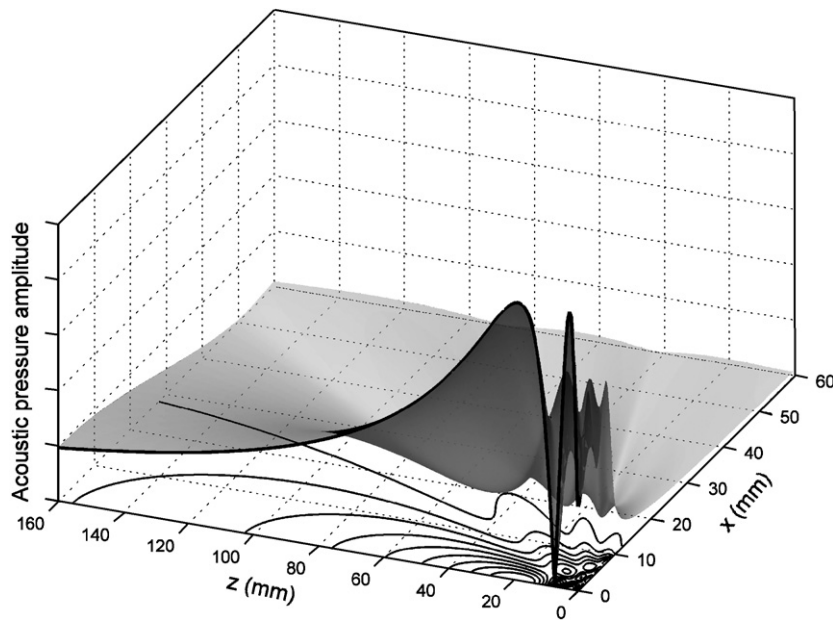
Fig. 30. The normalised acoustic pressure amplitude of the radiated field in the xz plane from a disc-like faceplate of radius 10 mm undertaking sinusoidal piston-like oscillation at 300 kHz, mounted in a rigid baffle (see Leighton et al., 2004, Section 1.2.1). Conditions in front of the transducer are assumed to be free field. The centre of the faceplate is at the origin, and it lies in the xy plane, so that the z-axis ($x = 0$, $y = 0$) describes the axis of rotational symmetry of both the transducer and the sound field. The locus of the points where the plot intersects this axis are shown by a thick black line, which therefore plots the acoustic pressure amplitude on the axis of rotational symmetry, from a point close to the origin to $z = 160$ mm, $x = 0$. From the origin out to $z = 20$ mm on this axis describes the near-field region, characterised by a series of maxima and minima in the acoustic pressure amplitude. After the last maximum ($z = 20$ mm), the acoustic pressure amplitude falls at further distances on-axis from the transducer. Off-axis, the amplitude of the field can be seen both in the 3D plot, and in the contours projected onto the xz plane. The maxima and minima which characterise the near field can also been seen off-axis, and in the far field it is just possible to see weak sidelobes radiating away from the main on-axis beam (G.T. Yim and T.G. Leighton).

As a result of these problems, the device is drastically redesigned to use two hydrophones, and to place them in the far-field zone of the transducer. Even here, there are problems. The measurement is of group velocity, which enters the inversion theory as phase velocity. In this hypothetical scenario, the theory assumes that free-field conditions exist (Commander and Prosperetti, 1989; Commander and McDonald 1991), whereas in the pipe they do not (Leighton et al., 2002). The theory assumes steady state, but there is considerable ring-up and ring-down (Leighton et al., 2004). Experimentally, when the attenuation is high (at the highest frequencies, say) the source amplitude is increased to obtain a good SNR, but no corresponding increase is seen in the detected signals. The problem is that the propagation is becoming nonlinear, such that energy is being pumped out of the fundamental frequencies to higher harmonics (in the manner discussed in Section 3). These are at higher frequencies than the upper limit of the receiver bandwidth (300 kHz), and so this energy is becoming 'invisible' to the detector. Increasing the source amplitude increases the nonlinearity and augments the effect.

6. Ultrasound in air

6.1. Categories of exposure of humans to ultrasound in air

The circumstances under which humans and animals can be subjected to ultrasound in air fall into three categories. First there is the unintended exposure because some process (such as an engine, ultrasonic dental tool, or ultrasonic cleaning bath) generates ultrasound as a by-product of its operation. This might be termed 'ultrasonic noise exposure'. Second, there is the unintended exposure because some process (such as an
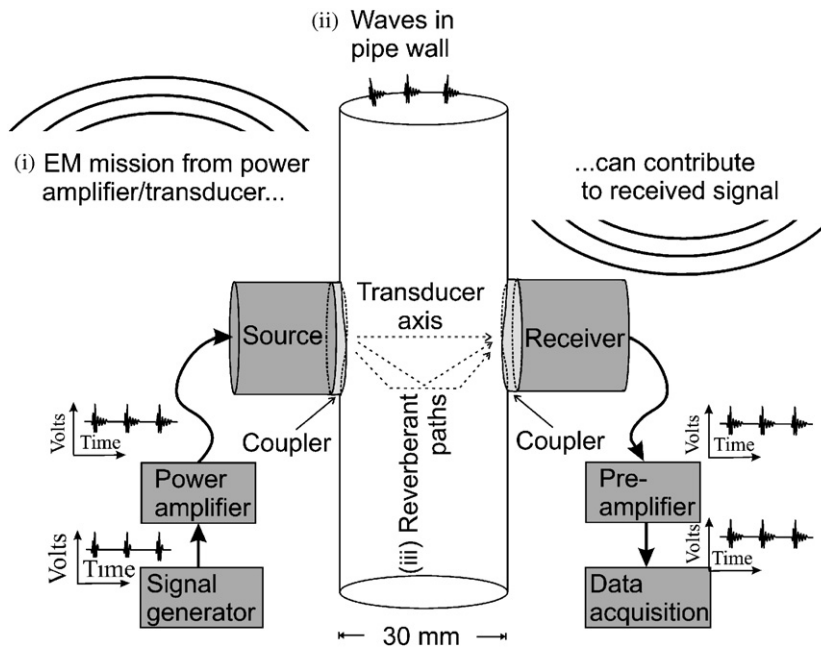
Fig. 31. Consider a thin-walled pipe of internal diameter 3 cm. A source and a receiver transducer (each of 1 cm faceplate radius) are to be mounted opposite each other, ostensibly to interrogate the cross-section of the pipe (the beam pattern of one such transducer, in a rigid baffle and radiating into the free field, is shown in Fig. 30). However the received signal can also receive contribution from path other than along the transducer axis, including (i) EM pickup of the driving signal, (ii) waves within the pipe wall, and (iii) reverberation in the pipe. In addition, the beam pattern for one of these transducers, operating at 300 kHz, is modelled in Fig. 30, indicating that much of the interior of the pipe would be in the near field at this frequency.

ultrasonic range finder) requires the generation of a specific ultrasonic signal as key to completing its task, but in addition to insonifying its inanimate target, it also exposes a human or animal to ultrasound. This would correspond to the in-air equivalent of the unintentional exposure of cetaceans to sonar discussed in Section 2.3. Third, there are devices which are designed to expose humans and/or animals to ultrasound in air in order to elicit some subjective response.

As regards the first category, whilst numerous examples exist, as well as anecdotal evidence of varying quality, to the author's knowledge there has been no census of such 'ultrasonic noise exposure'. Where the generation of ultrasonic noise also generates audiofrequency noise, the level of audible noise might stimulate the use of hearing protection which could act fortuitously to protect against ultrasonic hazard. The third category has shown a rapid increase in products, many with the intention of generating discomfort and with little ability to undertake measurements to comply with what few safety guidelines there are. These will be given special consideration in Section 6.4. With respect to the second category, as has been stated earlier the applications of ultrasound in air are not as numerous as those in liquids and solids. This is in part because of the plethora of alternatives available for use in air, most notably optical and other EM methods. Where they do occur, they are restricted to the low ultrasonic frequency range, because of the high absorption in air and its increase with frequency (Table 2).

In the vast majority of circumstances, the hazard issues associated with ultrasound in air relate to their interaction with the hearing and balance organs, because otherwise the acoustic impedance mismatch between air and tissue hinders penetration (Section 2). The issues associated with ultrasound in liquids and tissue (hyperthermia, cavitation, microstreaming, etc.) would not normally be an issue unless direct contact is made between the user and the source. Whilst this may at first sight appear to be a remote possibility, the presence of ultrasound in air might not just be the result of a 'category two' application with exploits the ultrasound as a signal (such as in range finding, intruder detection, or pest deterrence). It might also be the result of a 'category one' noise leakage from apparatus designed to generate ultrasound in solids, liquids or even other organs in the body (such ultrasonic apparatus include cleaning baths, welding, drills, NDT equipment and

Fig. 32. An ultrasonic device for the detection of bubbles in the opaque liquid 'casting slip' which is used by the pottery industry. The detector consists of ultrasonic source (*S*) and receiver (*R*) transducers mounted across from each other on the pipe (*P*). The body of each transducer is labelled 'T', and the faceplate of each is coupled to the pipe by an insert (*M*) which can be used to overcome mismatches both in shape and acoustic impedance. The system held in place by a clamp (*C*) which is easily portable, and can be mounted at any position along the pipe, so allowing the operator to track down the source of the bubbles (Leighton, 2004; Yim and Leighton, 2006).

lithotripters—Dawson et al., 1994). In such circumstances the contact hazard is more obvious, and the user may be unaware of the presence of ultrasound in the air. In other circumstances, whilst ultrasound can be generated, it is accompanied by significantly high levels of audiofrequency noise, which would deter users from hazardous locations (or, as discussed above for 'category one' noise, it might force the use of hearing protection). The jet engine, which was (probably erroneously) cited in the popular press as a source of "ultrasonic sickness", falls into this category (Parrack, 1966; Lawton, 2001). Whilst the earliest studies arose from concerns about occupational exposure to industrial ultrasound, there has been a growth in domestic, and even recreational, devices which could generate ultrasound. These could generate category two or category three exposures. Section 3.3 introduced devices to generate a localised sound field by utilising nonlinearity in the propagation. Other commercial devices include humidifiers, positioning devices, echo rangers, garden pest repellents and ultrasonic weapons to be used by joggers against dogs. "Ultrasonic weapons" are now advertised. Note that with a wavelength of more than 1.5 cm in air, a 22 kHz handheld device would be unlikely to be large enough to generate a tight beam of ultrasound, without leakage into directions other than

that in which is it 'fired'. The author could find no census of devices which quantified their ultrasonic output. In addition, surveys of the effectiveness of ultrasonic devices have found evidence of claims in advertising which are not warranted by the proven effectiveness.[28]

6.2. Contact and non-contact exposure—the example of dental ultrasonics

For several decades guidelines have been proposed for the maximum recommended exposures for humans to low frequency ultrasound (i.e. having frequencies of between about 20 and 60 kHz, although the upper limit is not fixed). These are discussed in Section 6.3. However these discussions have two major assumptions which are seldom explicitly stated. First, they refer to in-air, non-contact exposure. Second, barring subjective effects for which a mechanisms of generation is unknown, the assumption is made that the hazard is best monitored by the effect of the ultrasound on the ear (usually quantified through the ability of ultrasound to produce a temporary threshold shift for hearing at some low-kHz audiofrequency).

Before the review in Section 6.3, it is enlightening to recall the discussions regarding the differences between contact and non-contact ultrasonic exposure, as introduced in Section 2.2. That section stressed the importance, of including in the assessment of hazard, (i) the various transmission paths to the organ in question and (ii) the possibility that more than one organ should be considered. Examples have been given throughout this paper of where it is obvious that contact ultrasound should be considered (e.g. with MHz biomedical ultrasonics). In many applications, it is clear that only non-contact exposure will occur in normal practice (such as in the 'museum' example of Section 3.3), although the possibility of contact exposure should be considered with respect to accidental touching of the transducer. Whilst this might seem remote in normal operation for some devices, for others (such as hand-held devices to deter dogs from joggers) it is not.

This point is well illustrated by discussion of the considerations which should be undertaken to assess the hazard caused by dental ultrasonic apparatus (which includes drills, files, and scalers). There is the obvious question of what acoustic levels occur at the ear as a result of through-air transmission (Wilson et al., 2002). This might be thought of as an issue primarily for the dental practitioners who, unlike the patients, are routinely close to such apparatus and so receive day-to-day exposure. However the patients themselves are in physical contact with the instruments, so that conduction pathways other than airborne should be considered: the acoustic impedance mismatch between the tool and the tooth, the tooth and the jawbone, the jaw and the skull, and the skull to cochlea, are all very likely to be less severe than the tool-air-to-skin pathway, and without detailed consideration it would be difficult to assess the relative importance of the various conduction routes (Walmsley et al., 1987a). Other potential sources of hazard from ultrasonic scalers have been raised, including heating of the tooth during scaling, vibrational hazards causing cell disruption, possible platelet damage by cavitation, associated electromagnetic fields that can interrupt pacemakers, auditory damage to patient and clinician and the release of aerosols containing dangerous bacteria (Trenter and Walmsley, 2003). The possibility of such hazards is not unexpected given that this ultrasonic device is designed to produce beneficial effects through aggressive action at the interface of solid, liquid and gas (Walmsley et al., 1987b Ahmad et al., 1987; Roy et al., 1994; O'Leary et al., 1997).

Given the complexities which should be considered, the simplistic approach taken in the literature is surprising. As discussed in Section 2.3, it is extremely difficult and potentially very misleading to assign a single dB 'sound level' to a signal which contains ultrasonic or infrasonic components. It is possible to obtain a false sense of security from such statements as "Kilpatrick (1981) has listed the decibel ratings for various office instruments and equipment, which amount to 70–92 dB for high-speed turbine handpieces, 91 dB for ultrasonic cleaners, 86 dB for ultrasonic scalers, 84 dB for stone mixers and 74 dB for low-speed handpieces" (to quote from Szymańska, 2000). This was written (without reference levels for the dB scale) in an article assessing the hearing hazard associated with dental surgeries, and goes on to state "The dentist should maintain a proper distance from the operating field. Kilpatrick (1981) recommends the distance from the dentist's eye to the patient's mouth to be 14 in, i.e. about 35 cm. When the operator is closer, decibel rating increases." The attention is wholly on the through-air transmission path to the dentist's pinna. There is no

---

[28]See for example the warning issued in 2001 by the Federal Trade Commission's Division of Enforcement on the effectiveness of ultrasonic rodent and insect repellents at http://www.ftc.gov/opa/2001/05/fyi0128.htm.

reference made to the route by which sound may affect the patient's cochlea through, for example, bone conduction from the jaw, a route for which the transmission losses from the working tip may be much less (Table 1). Furthermore, not only is that transmission path uncharacterised, but the source level is unknown. To explain, an ultrasonic dental drill operating in air would most likely be an inefficient source of radiated acoustic energy. It becomes a more powerful source once the drill is in contact with the tooth, but whilst we may well measure the acoustic energy in the air which results from that contact, it is very difficult to measure the levels in the tooth, jaw, skull and hearing apparatus. The levels at audio-frequencies might be subjectively estimated using loudness matching (although the bandwidth of the signal might make this difficult), by measuring the thresholds by which the noise masks of a series of tones of different frequencies, but these would not be possible for the ultrasonic components. This might require measuring the acoustic signal radiated into the ear canal through the canal walls and drum during drilling, and then placing a bone vibrator on the teeth and measuring the transfer function between the bone vibrator and the ear canal pressure. The analogy of a masonry drill is illuminating: it generates more sound when in contact with a brick to drill a hole than when running in air, but whilst we can measure the noise in air resulting from such drilling, it is no simple matter non-invasively to measure the levels in the brick.

6.3. Guidelines for non-contact in-air exposure to ultrasound

The mechanisms by which ultrasound interacts with the various sensing organs of the ear is not as well understood as the various physical interactions with less receptive matter (involving cavitation, hyperthermia, microstreaming, etc.). Unlike the latter case, in-air ultrasonic hazard has tended to be assessed more by audiologists than biophysicists.

Grigor'eva (1966) found no shift in hearing threshold in the range 250–10,000 Hz, when an unreported number of subjects were exposed to 20 kHz at 110 dB re 20 μPa for an hour (for comparison, a 90 dB insonification for 1 h at 5 kHz did produce a substantial shift). Notable amongst other studies in the 1960s (Smith, 1967; Parrack, 1966) is the work of Acton (1968) who, like Grigor'eva, was also concerned about hearing damage as a result of occupational exposure to industrial ultrasonic equipment. He concluded that 8 h exposures to 110 dB re 20 μPa in the one-third octave bands centred on 20, 25 and 31.5 kHz should not cause hearing loss at audio frequencies. Lawton (2001) points out that, stated in this way, a broadband signal could exhibit levels which satisfy the criteria for each of the one-third-octave bands, but when these levels are added to give the octave level it could exceed the limit. Later, Acton (1975) revised the limit to 75 dB re 20 μPa for the lowest of these frequency bands, as its frequency range extended from 22.5 kHz down to 17.6 kHz, i.e. to within the audio frequency range (and certainly audible to many young females). It was already known that exposure to high frequencies in the audible range could produce subjective effects, including nausea, fatigue, tinnitus, persistent headaches, and "fullness in the ears" (Knight, 1968, Acton, 1973,1974; International Non-Ionizing Radiation Committee, 1984; Damongeot and André, 1988; von Gierke and Nixon, 1992; Lawton, 2001; National Occupational Health and Safety Commission, 2002). In addition, criteria for narrowband emissions were introduced (Acton, 1975; Acton and Hill, 1977).

From such studies in the 1960s, tentative Damage Risk Criteria, and Maximum Permissible Levels, were therefore first proposed, although without thorough investigations into dose–response relationships (which are still far from complete, given that there is only partial data on occupational—and other—sources of ultrasound). The limits for ultrasound were set to avoid hearing damage at audio frequencies, with the need to avoid any subjective effects also being introduced. This led to further guidelines of exposure to ultrasonic (≥20 kHz) and 'very high frequency' audible sound (10–20 kHz) (International Labour Office, 1977; International Non-Ionizing Radiation Committee, 1984; Damongeot and André, 1985; Health Canada, 1991). Amongst these works Lawton (2001) also discusses one which stands out as being more lenient in its limits (American Conference of Governmental Industrial Hygienists, 1988), of which he states "This reviewer believes that the ACGIH has pushed its acceptable exposure limits to the very edge of potentially injurious exposure".

No temporary hearing loss was produced by ultrasound limited to one-third-octave band levels of 105–115 dB re 20 μPa, levels which were then taken to be non-hazardous with respect to generating permanent hearing damage (Lawton, 2001). A temporary threshold shift was found in subjects exposed to 150 dB re

20 µPa at 18 kHz for about 5 min (Acton and Carson, 1967). According to Lawton (2001) "since the introduction of these recommended limits, there have been no reports showing systematic hearing loss associated with occupational exposure to very high frequency noise". It is important, of course, to understand fully the implications of treatment of ultrasonic exposure as 'noise'. This term implies that the emission is a by-product of some other process, and considered to be an 'occupational exposure'. Such emission might be broadband, or narrow band (Skillern, 1965; Roscin et al., 1967; Dobroserdov, 1967; Acton and Carson, 1967; Herman and Powell, 1981; Holmberg et al., 1995). In the author's opinion, these historical studies focused on category one and category two exposures, and even here the temporal and frequency characteristic of the emissions may vary greatly, from broadband noise to tonal. The growth in category three exposures in recent years (such as the museum example given in Section 3.3) has probably escaped these historical studies.

As noted in Section 2.3, the dB(A) scale is wholly inadequate for providing guidelines of hazard from in-air ultrasound. Korpert and Vanek (1987) proposed a scheme to introduce a single-number quantification of the levels of airborne ultrasound, both for convenience and to attempt to overcome drawbacks with the Acton guidelines. Their approach has however been criticised by Lawton (2001).

Howard et al. (2005) reviewed the current recommended acceptable exposure limits from standards organisations around the world. They note the general consensus amongst standards bodies on limits for the exposure of ultrasound. However one feature of particular concern to them was the revision by the United States of America's Occupational Health and Safety Administration to increase the exposure limit by an additional 30 dB under some conditions (equivalent to a factor of 1000 in intensity).

6.4. Category three exposures: deliberate exposure of humans and animals to ultrasound to elicit some subjective response

Of the three categories of exposure defined in Section 6.1, category three exposures are unique in that the exposure is intentional, and indeed is driven by a commercial imperative. The revision by the United States of America's Occupational Health and Safety Administration, discussed at the end of the preceding section, is of particular concern given the proliferation of commercial 'category three' devices which could expose humans (intentionally or through misuse of, say, a dog deterrent) to high levels of ultrasound. The in-air equivalent of parametric sonar, for which the 'museum' example was given in Section 3.3, is one manifestation. Because the generation of the difference frequency is a second-order process (Eq. (16)), the power of the primary frequencies (here, the ultrasonic ones) needs to be very great in order to generate a loud signal at audio frequencies. Whilst the analysis of Section 3.3 describes the role played by propagation in generating nonlinearity, it is not clear to what extent the ear, when driven at high levels, is capable of its own nonlinear response, such that the level of difference frequency generated in the ear may be different from that monitored by a microphone. Whilst power series expansions of the type discussed in of Section 3.3 will never of course describe a subharmonic, a nonlinearity in the ear which is capable of doing so could of course generate an audible response as a result of exposure to a single ultrasonic frequency.

Similarly, there has recently been a proliferation of devices whose mechanism of operation is not clear (even to the extent of whether they generate ultrasound or very high frequency sound). However many are described as 'ultrasonic', and advertised for their ability to generate unpleasant subjective effects and engender discomfort, for example for homeland or personal defence. The advertised ability to be able to generate "140 + dB" (for a "Pain Field Generator", for "potential crowd control applications") at an unspecified ultrasonic frequency is alarming, even given the comment in Section 2.3 that it would currently be impossible to substantiate the '140 + dB' measurements above 20 kHz in a traceable way using methods which have been internationally validated. Other devices include a "Blast wave pistol", advertised as producing "130 dB" (again, with no reference pressure or indication of the location of the measurement) for "animal control, predators for bird feeders, control of unruly dogs, cats even people". Whilst it is of course difficult to verify the output of such devices, or even to assess the operating frequency, the intention of using high outputs to generate discomfort is clear.

Indeed, the fact that the sensitivity of the ear to high frequencies is personal, and often age-related, is now being exploited to target specific demographic groups, for example by using high frequencies below 20 kHz to prevent teenagers loitering around shops: "Police have given their backing to a gadget that sends out an ultra

high-pitched noise that can be heard only by those under 20 and is so distressing it forces them to clutch their ears in discomfort'' (Alleyne, 2006). However a mother with babe-in-arms would not be sensitive to the radiation which distresses her child, and therefore would require extra protection to avoid holding it in close proximity to the 'silent' (to her) transducer. Whilst the definition of ultrasound cites a 20 kHz boundary, based on the statistics of populations, for the practical purpose of protecting individuals the distinction between ultrasonic and sonic is not so sharp.

7. Conclusions

In answer to the question 'what is ultrasound?' there are some simple answers. There is a range of ultrasonic waves which can propagate (Fig. 1). They are commonly described as waves which transport mechanical energy through the local vibration of particles, with no net transport of the particles themselves. The term "ultrasonic" is generally taken to mean that the "frequency" of the wave is greater than the upper limit of human hearing (usually taken to be 20 kHz).

In practice these simple ideas do not translate readily into our experience of ultrasonics. This is in part a result of the extreme sensitivity of the ear. Because of this, audio frequency sounds are restricted to "intensities" (noting from Section 2.3 that it is important to define the intensity with care) which, for most physical interactions of sound with matter other than the ear, would be thought of as being extremely low (Fig. 33). Since the vast majority of our experience with acoustics occurs at such audio frequencies, acousticians have been as culpable as any in propagating, as general truths, those characteristics of acoustics which relate to linear propagation only (Section 2). In practice, the high amplitudes used for much of ultrasonic work means that even the two apparently self-evident statements made in preceding paragraph are questionable: there may indeed be a net transport of particles (see Figs. 9 and 10), and the frequency content of the tonal wave may change in such a way that it becomes misleading to assign to it a single frequency (Section 3) and, further, to compare it to 20 kHz when protecting individuals (see end of Section 6).

This acute sensitivity of the ear leads to the conclusion that there is no single satisfactory way to discuss "exposure". Consider the range of acoustic pressure amplitudes which are shown in Fig. 33. As for Fig. 22, the schematic is based on a lecture demonstration that was undertaken. It is based on a linear scale, such that the marks corresponding to 20, 40, 60, 80 and 100 kPa occur at respective distances of 1, 2, 3, 4 and 5 metres from the datum.

As discussed earlier (Sections 1 and 6), the particular sensitivity of the ear ensures that the acoustic pressures associated with hearing all occur close to the datum. The commonly accepted threshold for human hearing at 1 kHz, 28.9 μPa (zero-to-peak—see footnote 7) occurs at about 1 nm from the datum on this scale. An amplitude of 20 Pa (which occurs at 1 mm from the datum) would cause pain, and hearing damage would occur at 200 Pa (1 cm from the wall). The range of human hearing is therefore typified by the first cm on this scale.

In contrast, even applications considered by physicists and chemists to be 'low-amplitude' (such that, for example, they are used only for material diagnosis and not processing) occur much further from the datum on this scale. Although the signal amplitudes are not often recorded, it is likely than many ultrasonic systems used in ocean monitoring employ amplitudes at the sensor[29] of not more than 10 kPa (50 cm from the datum on this scale). As one increases in frequency (Fig. 22) the source amplitudes tend to increase to ensure an adequate SNR at reception.

Under sea surface conditions, an amplitude of just over 100 kPa (5 m from the datum) corresponds to the cavitation threshold for low frequencies (tens of kHz—see Section 4.3). Ultrasonic cleaning baths, sonochemical reactors, dental tools, humidifiers and other devices designed to operate with continuous-wave and pulsed ultrasound at a few tens of kHz, operate in this range of 100–300 kPa (i.e. 5–15 m from the datum on this scale). We will assign to these the inexact label 'power ultrasound devices'. However the fact that they operate in a frequency range designed to promote cavitation has an interesting consequence. Specifically, the source amplitudes used by such devices does not increase without limit because, whilst cavitation is required for effective operation, increasing the source amplitude for such devices will not deliver

---

[29]Of course the amplitudes at the source can be much greater (Leighton et al., 2001; Leighton 2004)—see Sections 2.2 and 2.3.
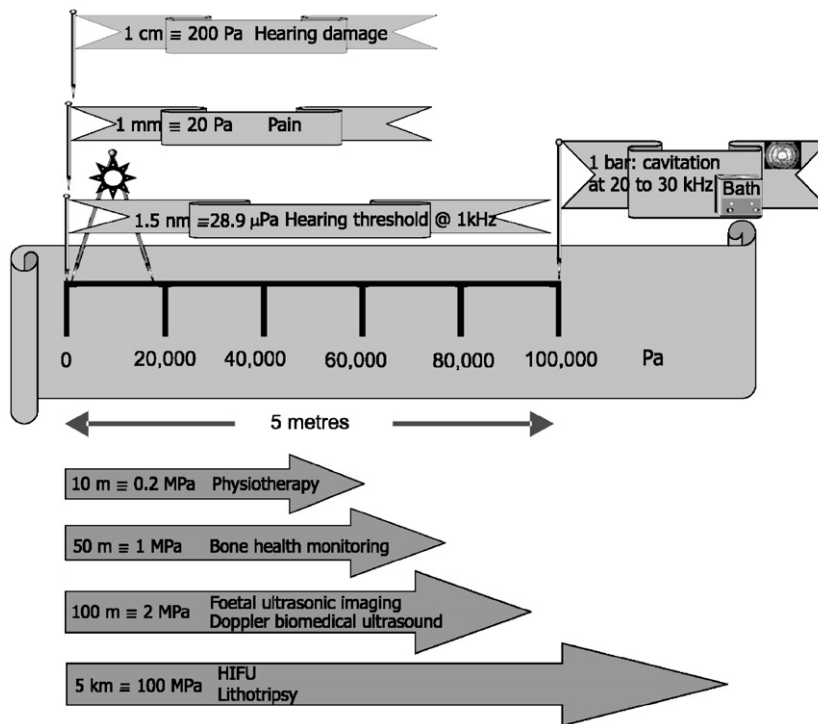
Fig. 33. The figure shows several identifiable features on a scale of the acoustic pressure amplitude. It is based on a demonstration of such scales, where five markers (indicating, respectively, 20, 40, 60, 80 and 100 kPa) were placed at 1 m intervals from a datum (representing 0 Pa). The figure illustrates this schematically through an unfurled banner, onto a 5 m section of which are placed the six markers for 0–100 kPa.

Human hearing occupies a small part of this range, as indicated by three flags which have been stacked at the top left of the figure because there is not enough space to pin them in their proper places. At 1.5 nm from the datum is placed the pin indicating an acoustic pressure amplitude of 28.9 μPa, taken to be the threshold for hearing at 1 kHz. At 1 mm is placed the pin for an acoustic pressure of 20 Pa, which would cause pain in humans; and at 1 cm is placed the pin for 200 Pa, which would cause hearing damage in normal human ears.

A pair of dividers, topped with a sun, is drawn with its points at 300 and 17 kPa. This is done to illustrate the point that, although even the lower point of the divider (300 Pa) exceeds the threshold for hearing damage, nevertheless the intensities are what physically we might regard as 'low'. This is because the two point of the dividers correspond to the acoustic pressure amplitudes (in air and water) which would provide in a plane wave the same intensity as daylight. Bright sunshine is considered to be occurring when the solar radiation level exceeds 100 W m^{-2} (although in actual fact this level would be perceived to correspond to a dull day). Equivalent plane wave intensity occurs in water for zero-peak acoustic pressure amplitudes of 17 kPa in water and 300 Pa in air. The final flag is pinned at the 5 m mark, corresponding to 1 atmosphere of pressure, the threshold for cavitation at low ultrasonic frequencies.

Below the scale are arrows indicating tentative values for the acoustic pressure amplitudes which can be measured from a range of biomedical ultrasonic devices operating *in degassed water* (measurement in vivo in tissue is difficult—see Section 5.2—but would produce lower values than those that could be generated in degassed water). Additional reasons why these values can only be tentative include the difficulty in assigning pressure amplitudes (to systems shown below the banner) because of the range of waveforms and pulse durations used, the question of whether one refers to the peak positive or peak negative pressure, etc., and because of the acceptable error limits in many ultrasonic measurements (see footnote 2).

Biomedical applications which are considered to be 'low intensity' (physiotherapy, bone health monitoring etc.) occur at respective distances of 10 and 50 m on this scale (equivalent to acoustic pressure amplitudes of 0.5–1 MPa). Foetal ultrasonic imaging and Doppler biomedical ultrasound are tentatively located at 100 m from the datum on this scale, corresponding to acoustic pressure amplitudes of about 2 MPa. The therapeutic applications of HIFU and lithotripsy are placed at a range of 5 km on this scale (corresponding to acoustic pressures of 100 MPa).

enhanced cavitation in such devices. This is because the high amplitudes which occur at the faceplate can cause such active cavitation there that the ultrasound is prevented from propagating in to the body of the liquid, and the device ceases to function (Fig. 14).

Most biomedical applications, both diagnosis and therapy, require better localisation/focusing of the ultrasound than is required for the 'power ultrasound devices' discussed above. As a result, they tend to use

higher frequencies (Fig. 22). Because of this, although the acoustic pressure amplitudes they use tend to be greater than those employed by the 'power ultrasound devices' (100–300 kPa at 10s of kHz), the risk of cavitation has not increased proportionally[30] (Fig. 20). The range 10–100 m from the datum on this scale covers those devices operating with peak acoustic pressure amplitudes of 0.2–2 MPa. These include diagnostic devices, both for imaging (like foetal scanners) and measurement through attenuation and sound speed (as used for bone health monitoring). The only therapeutic devices operating in this range are considered to be 'low power', such as physiotherapy devices. Note that the values assigned to acoustic pressures on this scale are tentative (see caption), and that they reflect measurements in water as opposed to tissue (Duck, 1987; Harris, 1999; Duck and Martin, 1991).

A distance of 5 km from the datum corresponds to 100 MPa, typical of the acoustic pressure amplitudes used in High Intensity Focused Ultrasound (HIFU) and lithotripsy. Given the range from 1 nm to 5 km on this scale, it is difficult to find general ideas which span the entire 12 decades in acoustic pressure (or 24 decades in intensity) covered by common interactions of man with acoustic fields. This is particularly the case given that such phenomenon as cavitation can occur, and can generate sound speed fluctuations of a factor of 2 or more on rapid timescales. Furthermore, cavitation can focus the energy both in terms of space and time to create extreme conditions of shear, temperature and pressure. In particular, it would be imprudent to extrapolate from the bulk of our experience with acoustics (i.e. linear acoustics at audiofrequencies) to provide a baseline understanding of what occurs in the ultrasonic regime.

To close the article, some salient points for addressing the question 'what is ultrasound' (with respect to the safety topic of this journal issue) are now listed:

(i) Ultrasound affects tissue through a variety of mechanisms. Whilst there are commonly recognised regimes in which certain mechanisms produce noticeable effects (in approximate order of ascending acoustic pressure amplitude: microstreaming, streaming, radiation forces (with and without bubbles and particles), hyperthermia, cavitation), there is a special regime at very low intensities (Fig. 33) for consideration of the effect of ultrasound on the hearing and balance organs of the ear. The degree to which these ear-related effects are understood is generally much less than the degree to which the higher-amplitude effects are understood. The conduction of ultrasound to the ear could be very different if the body is submerged (see (v), below).

(ii) We do not measure 'ultrasound' itself, but rather monitor the effects it produces (see (i)). The closest we get to monitoring 'ultrasound' is perhaps optically measuring the vibration of a fixed pellicle in a field (Bickley et al., 2004), which is not dissimilar to the processes involved in hearing. Even here, however, what we actually measure is some *effect* of ultrasound. The nature of this effect often reflects the interests of the user: to give three examples, photographers use Schlieren photography to monitor ultrasonically induced changes in refractive index (Kudo et al., 2004); chemists commonly use calorimetry; electrical engineers estimate the acoustical energy input through knowledge of the electrical measurements and estimations of transfer efficiencies. The latter two illustrate the problems of this approach well, and indeed compared poorly in a controlled comparison of the two when measuring the same field (Leighton et al., 2005a). Both have features in common. First, they use indirect measurements (temperature rise and electrical power, respectively) and make certain assumptions regarding the efficiencies with which that power is converted from/to (respectively) acoustical power. Second, both give only a spatial average (and for calorimetry, a temporal average) measure. Third, both have been accepted as satisfactory, indeed the best, methods of estimating the acoustical power for many years by different groups of users. For any system of ultrasonic measurement to be precise, the mechanism by which the measured effect occurs, and how it relates to the acoustic parameters, must be understood. However a disturbing feature of ultrasonics is that this mechanism is not always even identified. For example, the heating measured in calorimetry could come about through ultrasonic absorption in the liquid, or in the container walls, or through direct conduction of heat from the transducer, whose temperature can rise significantly during operation. Hence the occurrence and use of the term "ultrasonic exposure" should be subjected to

---

[30]Although it is possible to use such devices to generate cavitation in water, the ability of them to generate cavitation in tissue is generally less (Leighton et al., 1990).

rigorous scientific examination of the underlying measurement method, and the use of the term "ultrasonic dose" should be treated with scientific scepticism (see Section 2.3). There is no clear understanding of the dosimetric unit in ultrasound. Quite apart from the difficulties in measuring ultrasonic fields, cited above, and the problems with the in vivo environment, this is in part because there is a wide range of mechanisms by which ultrasound can affect tissue. Because of this, there is no simple measure which can be used, for example in bioeffect studies. In particular this has implications for the ease with which epidemiological studies of foetal scanning can be interpreted (Ziskin and Pittiti, 1988): there is no quantitative 'dose' against which effects can be correlated. This difficulty is further compounded if no record is kept of even the duration, or of nominal (manufacturer's) power setting, for the scan. Currently the duration and 'output intensity' for each foetal scan are not recorded.

(iii) Currently the two most useful effects exploited to measure 'ultrasound' are the piezoelectric development of charge in a hydrophone, and the measurement of radiation force on a target (ranging from precise local measurements of pressure (Bickley et al., 2004) to spatial average measures for checking the output of physiotherapeutic devices (Zeqiri et al., 2004)). Calibrated systems based on one or other should certainly be used to monitor current sound fields in most cases (the only viable exceptions being where the probes are too invasive). From marine zoologists to cell biologists, from chemists to food scientists, in the vast majority of cases the measurement and understanding of the acoustic field comes second to characterisation of the biological and chemical conditions of the experiment. Hence we find many papers where there are paragraphs devoted to listing the provenance and purity of the purchased chemicals or cells, but where these items are then exposed to a sound field about which nothing is quoted other than the frequency. This makes it impossible to repeat the experiment and very difficult to interpret the meticulously recorded biological or chemical effects. The tendency to quote only the on-screen MI (or a peak negative pressure which is derived solely from the on-screen MI) with in vitro fields is nonsensical at best, and in many cases misleading. The MI is popularly used to characterise fields involving contrast agents, even though their presence reduces the validity of the MI in representing the conditions. However such poor reporting is prevalent because an MI value is available on-screen when clinical instruments are, for example, used as sources in in vitro experiments.

(iv) Even if hydrophones are used to monitor the field, it is important fully to appreciate the ability of the environment to change the sound field through, for example, nonlinear propagation, or through reflection and diffraction. The importance of considering the interaction between the hydrophone, the ultrasonic field, and liquid environment is in part a reflection of the small wavelengths involved, such that mm-sized hydrophones and cm-sized vessels can represent large scattering or diffracting targets to an ultrasound field, and the measurement can be complicated by directionality, spatial averaging etc. As a result, a single hydrophone measurement in a reverberant environment (where the sound field might be highly inhomogeneous—see Figs. 19 and 29) can be misleading. Similarly, the ability of the sound field to affect the environment can lead to a cycle where the environment and the sound field continually change each other. For example, in Fig. 19 a $<1\%$ change in the frequency produces a dramatic change in the sound field and its subsequent luminescent effect, because of the tuning of the modes of the vessel. This same effect could be produced if the vessel were used at a fixed frequency, but the liquid temperature changed by $2.5\,^{\circ}\mathrm{C}$ (as might occur during the course of an experiment, or even be used as the source for a calorimetry measurement) (Fig. 12). The generation of a bubble population can change the sound speed by much more (Fig. 19), and that population can in turn be affected by the sound field, which it then changes (e.g. by scattering, introducing impedance mismatches, or refraction—Figs. 11 and 25).

(v) The acoustic reflections which are important to the generation of reverberant fields in (iv) are a specific example of the importance of the acoustic impedance matches and mismatches that can occur (Table 1). The sensitivity of the ear mentioned in (i) is in part an exercise in overcoming the impedance mismatch between the air and the cochlear. As an example, consideration of the submerged body introduced in (i) must determine whether the ear canal is air- or fluid-filled, and whether other conduction routes become important (such as from surrounding liquid to cochlea via skull, jawbone, etc.—see Section 6.2). The degree of protection afforded by the acoustic impedance mismatch introduced by partial covering by a wet-suit or a dry-suit should be considered (Fig. 34). In particular, the level of ultrasound at the tissue in question will dramatically increase as the impedance conditions change, as indeed may the tissue of
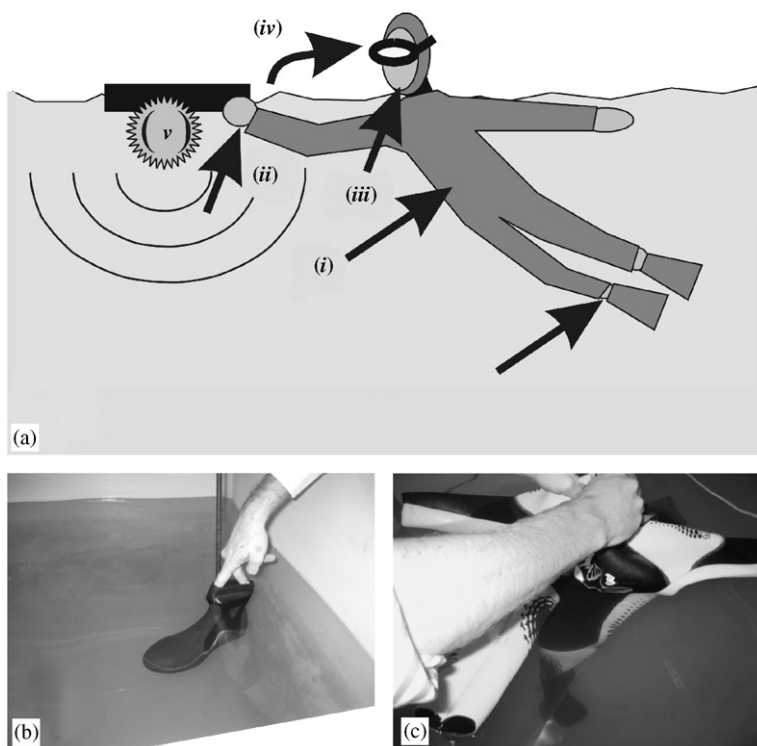
Fig. 34. (a) Schematic of diver in water pushing raft containing an acoustic source, introduced to stimulate debate and not to imply an established hazard. Speculative route by which ultrasound might enter the body are shown: (i) directly through the suit, (ii) through the hand (or, if gloved, through a possible skin exposure at the wrist), (iii) through parts of the face not in covered by mask but in contact with the water, (iv) through transmission from water to air, and thence to the ear, and (v) from direct contact (i.e. without a water path) if the diver were to touch the source. The figure is introduced for discussion purposes. Issues of importance include: whether the diver is wearing a wetsuit or a drysuit; the acoustic wavelength, and implications for sound transmission through the body (e.g. along jawbone or limbs) once it has entered the body; whether we can model the acoustics sufficiently well, and whether we can work with, say, a $\pm 3\,dB$ uncertainty; what routes could sound and ultrasound take into body, and what protection is available for conductive routes. It may also be important to consider the mechanisms for hazard: Whilst at MHz frequencies we are used to assessing possible manifestations of hyperthermia, cavitation, streaming, the issue becomes more difficult in the scenario shown in the figure. If the insonification frequency were 21 kHz, it is not sufficient just to discuss the usual 'ultrasonic' hazards listed above. In addition, the effect on the ear should be considered, because even though the air-path (iv) introduces a considerable transmission loss at the air-water interface (see Table 1), the sensitivity of the ear suggests that its response, even at 21 kHz, should be assessed given that, at audiofrequencies, pain occurs at acoustic pressure amplitudes (e.g. 20 Pa) which are 5000 times less than the threshold for cavitation at 21 kHz (corresponding to a factor of 25 million in the respective intensities). Conversely, if the insonification frequency were 19 kHz, would there be an assumption that the safety of the diver is assured if the levels in-air at the ear present no hazard to hearing? Such an assumption might not be safe, given the significant transmission loss at the pressure release interface for route (iv), compared to route (v) which might generate effects normally considered to be 'ultrasonic' (e.g. cavitation). Given such considerations, it may be unwise draw an artificial distinction at 20 kHz when it comes to assessing hazard. (b) Acoustic testing of a boot and (c) a wetsuit. A hydrophone is placed at a specific location, and the signal level measured with and without the garment in place. The results indicated that, for insonification at 22 kHz, the boot introduced a transmission loss of 26 dB, and the glove introduced 28 dB. Measurements made in the thigh region of a child's suit (3 mm thick Polychloroprene (i.e. Neoprene) rubber bonded nylon laminate) indicated that, with the boot on the leg, the suit introduced a transmission loss of 20 dB, which reduced to 19 dB when the boot was taken off. (Data G. T. Yim. D. C. Finfer and T. G. Leighton).

interest. Consider the differences that occur when an ultrasonic dental scaler is in contact with the patient's tooth, compared to the conditions when it operates in air. The issue to consider when a human is close to (but not touching) a 30 kHz ultrasonic cleaning bath will almost wholly be a question of the effect of the in-air conduction path to, and effect on, the ear. However if he/she touches the transducer or liquid, the issue may change to one of cavitation in the tissue of the finger.

(vi) When ultrasound is passed through liquid or liquid-like media, bubbles represent the most potent natural sources for interfering with the sound field: if you use ultrasound in liquids and do not think you

have a problem with bubbles, you probably do not completely understand the problem. The tensile strength of water has never been experimentally measured, because even with filtering, degassing and shielding in place to remove bubble nucleation by cosmic rays, a small number of microbubbles have been present which fail at lower tensions than would the water–water molecular bond. Even a low amplitude sound field can be refracted, absorbed and scattered by sparse populations of bubbles. High amplitude fields can generate cavitation. Bubbles concentrate the energy of the acoustic wave, and focus the timescales and lengthscales over which effects are observed (see the introduction to Section 4). If acoustic fields are difficult to measure directly (see Section 5), cavitation is very much more difficult. Recall that we do not measure cavitation itself, but the *effects* of cavitation: Biologists might measure haemolysis; Chemists chose a wide range of reactions (Leighton et al., 2005a); Industry favours erosion tests which are very difficult to standardise; Physicists sometimes prefer luminescence. Whilst each of these measurement technologies has its supporters who claim that one technique or another is ideal, only one cross-comparison has been performed to identify the strengths and weaknesses of each method (Leighton et al., 2005a).

(vii) The perception that acoustics in general, and ultrasound in particular, are uncomplicated disciplines with established technologies, has produced numerous errors both in practice and in the literature. This paper provided example scenarios of how such misconceptions arise. These included casual and misleading use of the dB scale (Sections 2.3 and 6.2); the ambiguities inherent in a simple source-to-receiver transmission sensor (Fig. 31); the way in which the frequency of interest might not be the frequency at which the source is driven (Section 3; footnote 24), such that energy may become 'invisible' to the detector and saturation might occur (Section 3.2); the complexities inherent in the frequency transfer function of the ultrasonic system as a whole (caption to Fig. 19 and (iv), above; Figs. 25 and 26); the prevalence of self-interaction effects (Fig. 11); the importance of identifying the transmission paths and all tissues of interest (Section 6; Fig. 34; (v), above); the directionality of sensors and the effect of the environment on the sound field (Section 5.2). As a result, ultrasonic sensors can rarely be used off-the-shelf with the confidence one would apply to sensors of many other radiations; a power ultrasound transducer is not an uncomplicated combination heater-stirrer for a chemical reaction; and the parameters by which we describe the waves (intensity, pressure, frequency and the decibel) are not a simple and foolproof.

(viii) As regards the use of ultrasound in liquid and tissue, there are many established applications, and much work has been done on providing international guidelines for safe use. Whilst the mechanisms by which ultrasound can interact with tissue are very many, there is a considerable body of research on these to aid our understanding of them. In contrast, the use of ultrasound in air has had relatively few applications which do not involve a subjective human or animal response (in part because of the attenuation issues discussed in Section 2). Historically the assessment of safety guidelines for ultrasound in air is a much smaller enterprise than that undertaken for the assessment of the safety of foetal ultrasonic scanning. There has recently been an increase in available products, primarily based upon the evocation of a subjective human or animal response. Those which exploit the nonlinearity to generate audiofrequency signals from an in-air equivalent of parametric sonar should be critically assessed, given that the inefficiency of the conversion requires high signal levels in the primary beams. Another category exploits the discomforting effects of in-air ultrasound (to pests for whom it is within their audible frequency range, or to humans for whom it is not, but who can experience unpleasant subjective effects and, potentially, shifts in the hearing threshold). Commercial products are advertised with cited levels which cannot be critically accepted, given that there is a lack of traceability (Sections 2.3 and 6.4) for measurements of ultrasound in air, and little understanding of the mechanism by which they may represent a hazard.

Acknowledgements

contributions are acknowledged, and to Martyn Hill, Bajram Zeqiri, Alan McAlpine and Ben Lineton for useful discussions.

References

Abbott, J.G., 1999. Rationale and derivation of MI and TI—a review. Ultrasound Med. Biol. 25 (3), 431–441.

Acton, W.I., 1968. A criterion for the prediction of auditory and subjective effects due to air-borne noise from ultrasonic sources. Ann. Occup. Hyg. 11, 227–234.

Acton, W.I., 1973. The effects of airborne ultrasound and near-ultrasound. In: Ward, WD. (Ed.), Proceedings International Congress on Noise as a Public Health Problem, Dubrovnik, Document 550/9-73-008. US Environmental Protection Agency, Washington, DC, pp. 349–359.

Acton, W.I., 1974. The effects of industrial airborne ultrasound on humans. Ultrasonics 12, 124–128.

Acton, W.I., 1975. Exposure criteria for industrial ultrasound. Ann. Occup. Hyg. 18, 267–268.

Acton, W.I., 1983. Exposure to industrial ultrasound: Hazards, appraisal and control. J. Soc. Occup. Med. 33, 107–113.

Acton, W.I., Carson, M.B., 1967. Auditory and subjective effects of airborne noise from industrial ultrasonic sources. Br. J. Ind. Med. 24, 297–304.

Acton, W.I., Hill, C.R., 1977. Hazards of industrial ultrasound. Protection 12, 15–16.

Ahmad, M., Pitt Ford, T.R., Crum, L.A., 1987. Ultrasonic debridement of root canals: acoustic streaming and its possible role. J. Endod. 13 (10), 490–499.

Allen, J.S., Roy, R.A., Church, C.C., 1997. On the role of shear viscosity in mediating inertial cavitation from short-pulse, megahertz-frequency ultrasound. IEEE Trans. Ultrasonics Ferroelectr. Freq. Control 44, 743–751.

Alleyne, R., 2006. Plagued by teenagers? You'll like the sound of this. Daily Telepgraph online, ⟨http://www.telegraph.co.uk/news/main.jhtml?xml = /news/2006/02/16/noise16.xml⟩.

American Conference of Governmental Industrial Hygeienists, 1988. TLVs and BEIs. Threshold Limit Values for chemical substances and physical agents, Biological Exposure Indices. In: American Conference of Governmental Industrial Hygeienists, Cincinnati, OH, 1988.

American Institute of Ultrasound in Medicine, 1993. Bioeffects and Safety of Diagnostic Ultrasound. AIUM Publications, Rockville, MD.

American Institute of Ultrasound in Medicine/National Electrical Manufacturers Association, 1992. Standard for real-time display of thermal and mechanical acoustic output indices on diagnostic ultrasound equipment. AIUM/NEMA. AIUM Publications, Rockville, MD.

American Institute of Ultrasound in Medicine/National Electrical Manufacturers Association, 1998. Standard for Real-time Display of Thermal and Mechanical Acoustic Indices on Diagnostic Ultrasound Equipment. AIUM/NEMA. AIUM Publications, Laurel, MD.

Apfel, R.E., 1981. Acoustic cavitation prediction. J. Acoust. Soc. Am 69, 1624–1633.

Apfel, R.E., 1984. Acoustic cavitation inception. Ultrasonics 22, 167–173.

Apfel, R.E., Holland, C.K., 1991. Gauging the likelihood of cavitation from short-pulse, low-duty cycle diagnostic ultrasound. Ultrasound Med. Biol. 17, 179–185.

Au, W.W., Banks, K., 1998. The acoustics of the snapping shrimp *Synalpheus parneomeris* in Kaneohe Bay. J. Acoust. Soc. Am. 103 (1), 41–47.

Auf der Maur, A.N., 1985. Limits for exposure to airborne ultrasound. Ann. Am. Conf. Ind. Hyg. 12, 177–181.

Bailey, M.R., Couret, L.N., Sapozhnikov, O.A., Khokhlova, V.A., Ter Haar, G.R., Vaezy, S., Shi, X., Roy, M.R., Crum, L.A., 2001. Use of overpressure to assess the role of bubbles in focused ultrasound lesion shape in vitro. Ultrasound Med. Biol. 27 (5), 695–708.

Bailey, M.R., Khokhlova, V.A., Sapzhnikov, O.A., Kargl, S.G., Crum, L.A., 2003. Physical mechanisms of the therapeutic effect of ultrasound. Acoust. Phys. 49 (4), 437–464.

Barnett, S.B., 1980a. The effect of ultrasonic irradiation on the structural integrity of the inner ear labyrinth. Acta Otolaryngol. 89, 424–432.

Barnett, S.B., 1980b. The influence of ultrasound and temperature on the cochlear microphonic response following a round window irradiation. Acta Otolaryngol. 90, 32–39.

Barnett, S.B., Kossoff, G., Edwards, M.J., 1993. International perspectives on safety and standardization of diagnostic pulse ultrasound in medicine. Ultrasound Obstetr. Gynecol. 3 (4), 287–294.

Barnett, S., et al., 1998. World federation for ultrasound in medicine and biology, task group report for safety committee of the WFUMB: conclusions and recommendations on thermal and non-thermal mechanisms for biological effects of ultrasound. Ultrasound Med. Biol. 24, S11–S21.

Barnett, S.B., Ter Haar, G.R., Ziskin, M.C., Rott, H.-D., Duck, F.A., Maeda, K., 2000. International recommendations and guidelines for the safe use of diagnostic ultrasound in medicine. Ultrasound Med. Biol. 26 (3), 355–366.

Basauri, L., Lele, P.P., 1962. Simple method for the production of trackless focal lesions with focused ultrasound—statistical evaluation of effects of irradiation on central nervous system of a cat. J. Physiol. 160, 513–534.

Bennett, M.B., Blackstock, D.T., 1975. Parametric array in air. J. Acoust. Soc. Am. 57 (3), 562–568.

Becket, M.A., Hua, I., 2001. Impact of ultrasonic frequency on aqueous sonoluminescence and sonochemistry. Phys. Chem. A 105, 3796–3802.

Beyer, R.T., 1998. The parameter B/A. In: Hamilton, M.F., Blackstock, D.T. (Eds.), Nonlinear Acoustics. Academic Press, San Diego, pp. 25–29 (Chapter 2).

Bickley, C.J., Zeqiri, B., Robinson, S.P., 2004. Providing primary standard calibrations beyond 20 MHz. Proceedings of the First Conference in Advanced Metrology for Ultrasound in Medicine. J. Phys.: Conf. Ser. 1, 20–25.

Bies, D.A., Hansen, C.H., 1996. Engineering noise control: theory and practice, second ed. E & FN Spon, London, New York.

Billard, B.E., Hynynen, K., Roemer, R.B., 1990. Effects of physical parameters on high temperature ultrasound hyperthermia. Ultrasound Med. Biol. 16, 409–420.

Birkin, P.R., Watson, Y.E., Leighton, T.G., Smith, K.L., 2002. Electrochemical detection of Faraday waves on the surface of a gas bubble. Langmuir Surf. Coll. 18, 2135–2140.

Birkin, P.R., Leighton, T.G., Power, J.F., Simpson, M.D., Vincotte, A.M.L., Joseph, P.F., 2003a. Experimental and theoretical characterisation of sonochemical cells. Part 1: cylindrical reactors and their use to calculate speed of sound. J. Phys. Chem .A 107, 306–320.

Birkin, P.R., Power, J.F., Vincotte, A.M.L., Leighton, T.G., 2003b. A 1 kHz resolution frequency study of a variety of sonochemical processes. Phys. Chem. Chem. Phys. 5, 4170–4174.

Birkin, P.R., Offin, D.G., Joseph, P.F., Leighton, T.G., 2005. Cavitation, shock waves and the invasive nature of sonoelectrochemistry. J. Phys. Chem. B 109, 16997–17005.

Bithell, J.F., Stewart, A.M., 1975. Prenatal irradiation and childhood malignancy: a review of British data from the Oxford Survey. Br. J. Cancer 31, 271–287.

Broecker, H.C., Siems, W., 1984. The role of bubbles in gas transfer from water to air at higher windspeeds. Gas Transfer at Water Surfaces, Reidel.

Busse, L.J., Miller, J.G., 1981. Detection of spatially nonuniform ultrasonic radiation with phase sensitive (piezoelectric) and phase insensitive (acoustoelectric) receivers. J. Acoust. Soc. Am. 70 (5), 1377–1386.

Carstensen, EL., 1987. Acoustic cavitation and the safety of diagnostic ultrasound. Ultrasound Med. Biol. 13 (10), 597–606.

Carstensen, E.L., Dalecki, D., Gracewski, S.M., Christopher, T., 1999. Nonlinear propagation and the output indices. J. Ultrasound Med. 18 (1), 69–80.

Chalmers, I., 1984. Hazards of ultrasound. Br. Med. J 289, 184–185.

Chapman, D.M.F., Ellis, D.E., 1998. The elusive decibel: thoughts on sonars and marine mammals. Can. Acoust./Acoust. Can. 26 (2), 29–31.

Chaussy, C., Schmiedt, E., Jocham, D., Brendel, W., Forssmann, B., Walther, V., 2002. First clinical experience with extracorporeally induced destruction of kidney stones by shock waves. 1981. J. Urol. 167 (2), 844–847.

Church, C.C., 1993. An alternative to the mechanical index as a means of assessing the safety of exposures to diagnostic ultrasound. J. Acoust. Soc. Am. 93 (4), 2348.

Church, C.C., 2002. Spontaneous homogeneous nucleation, inertial cavitation and the safety of diagnostic ultrasound. Ultrasound Med. Biol. 28 (10), 1349–1364.

Clarke, P.R., Hill, C.R., 1970. Physical and chemical aspects of ultrasonic disruption of cells. J. Acoust. Soc. Am. 50, 649–653.

Coleman, D.J., Lizzi, F.L., Silverman, R.H., Dennis, P.H., Driller, J., Rosada, A., Iwamoto, T., 1986. Therapeutic ultrasound. Ultrasound Med. Biol. 12, 633–638.

Commander, K.W., Prosperetti, A., 1989. Linear pressure waves in bubbly liquids: comparison between theory and experiments. J. Acoust. Soc. Am. 85, 732–746.

Commander, K.W., McDonald, R.J., 1991. Finite-element solution of the inverse problem in bubble swarm acoustics. J. Acoust. Soc. Am. 89 (2), 592–597.

Cosgrove, D., 1996. Why do we need contrast agents for ultrasound? Clin. Radiol. 51 (Suppl 1), 1–4.

Cosgrove, D., 1997. Echo enhancers and ultrasound imaging. Eur. J. Radiol. 26 (1), 64–76.

Daft, C.M.W., Siddiqi, T.A., Fitting, D.W., Meyer, R.A., O'Brien, W.D., 1990. In-vivo fetal ultrasound exposimetry. IEEE Trans. Ultrasonics Ferroelectrics Frequency control 37, 501–505.

Damongeot, A., André, G., 1985. Low frequency ultrasound: effects and limits. Proceedings Inter-Noise 85 (Munich) 2, 1049–1052.

Damongeot, A., André, G., 1988. Noise from ultrasonic welding machines: risks and prevention. Appl. Acoust. 25, 49–66.

Davies, P., 1984. Hazards of ultrasound. Br. Med. J 288, 2001–2002.

Dawson, C., Chilcott-Jones, A., Corry, D.A., Cohen, N.P., Williams, H.O., Nockler, I.B., Whitfield, H.N., 1994. Does lithotripsy cause hearing loss? Br. J. Urol. 73, 129–135.

Dayton, P.A., Pearson, D., Clark, J., Simon, S., Schumann, P.A., Zutshi, R., Matsunaga, T.O., Ferrara., K.W., 2004. Ultrasonic analysis of peptide and antibody targeted microbubble contrast agents for molecular imaging of $\alpha_v\beta_3$-expressing cells. Mol. Imaging 3 (2), 125–134.

De Sarabia, E.R.F., Gallego-Juarez, J.A., Rodriguez-Corral, G., Elvira-Segura, L., Gonzalez-Gomez, I., 2000. Application of high-power ultrasound to enhance fluid/solid particle separation processes. Ultrasonics 38, 642–646.

Deane, G.B., Stokes, M.D., 1999. Air entrainment processes and bubble size distributions in the surf Zone. J. Phys. Oceanogr. 29, 1393–1403.

Dix, J.K., Arnott, S., Best, A.I., Gregory, D., 2001. The acoustic characteristics of marine archaeological wood. In: Leighton, T.G., Heald, G.J., Griffiths, H., Griffiths, G. (Eds.), 'Acoustical Oceanography', Proceedings of the Institute of Acoustics, Vol. 23, Part 2. Institute of Acoustics, pp. 299–305.

Dobroserdov, V.K., 1967. The effect of low frequency ultrasound and high frequency sound on exposed workers. Occup. Safety Health Abstr. 5, 658 (abstract).

Doust, P.E., Dix, J.F., 2001. The impact of improved transducer matching and equalisation techniques on the accuracy and validity of underwater acoustic measurements. In: Leighton, T.G., Heald, G.J., Griffiths, H., Griffiths, G. (Eds.), 'Acoustical Oceanography', Proceedings of the Institute of Acoustics, Vol. 23, Part 2. Bath University Press, pp. 100–109.

Duck, F.A., 1987. The measurement of exposure to ultrasound and its application to estimates of ultrasound 'dose'. Phys. Med. Biol. 32, 303–325.

Duck, F.A., 1999. Acoustic saturation and output regulation. Ultrasound Med. Biol. 25 (6), 1009–1018.

Duck, F.A., 2002. Nonlinear acoustics in diagnostic ultrasound. Ultrasound Med. Biol. 28 (1), 1–18.

Duck, F.A., Martin, K., 1991. Trends in diagnostic ultrasound exposure. Phys. Med. Biol. 36, 423–1432.

Duck, F.A., Baker, A.C., Starritt, H.C., 1998. Ultrasound in medicine. Institute of Physics Publishing, Bristol, Philadelphia, PA.

Everest, F.A., Young, R.W., Johnson, M.W., 1948. Acoustical characteristics of noise produced by snapping shrimp. J. Acoust. Soc. Am. 20 (2), 137–142.

Faraday, M., 1831. On the forms and states assumed by fluids in contact with vibrating elastic surfaces. Phil. Trans. Roy. Soc. Lond. 121, 319–340.

Farmer, D.M., McNeill, C.L., Johnson, B.D., 1993. Evidence for the importance of bubbles in increasing air–sea gas flux. Nature 361, 620–623.

Fedele, F., Coleman, A.J., Leighton, T.G., White, P.R., Hurrell, A.M., 2004. A new sensor for detecting and characterising acoustic cavitation *in vivo* during ESWL. Acoust. Bull. 29, 34–39.

Ferguson, B.G., Cleary, J.L., 2001. In situ source level and source position estimates of biological transient signals produced by snapping shrimp in an underwater environment. J. Acoust. Soc. Am. 109 (6), 3031–3037.

Flynn, H.G., 1975a. Cavitation dynamics I. A mathematical formulation. J. Acoust. Soc. Am. 57, 1379–1396.

Flynn, H.G., 1975b. Cavitation dynamics II, Free pulsations and models for cavitation bubbles. J. Acoust. Soc. Am. 58, 1160–1170.

Flynn, H.G., Church, C.C., 1984. A mechanism for the generation of cavitation maxima by pulsed ultrasound. J. Acoust. Soc. Am. 76, 505–512.

Flynn, H.G., Church, C.C., 1988. Transient pulsations of small gas bubbles in water. J. Acoust. Soc. Am. 84, 985–998.

Foldy, L.L., 1945. The multiple scattering of waves. Phys. Rev. 67, 107–119.

Frantzis, R., 1998. Does acoustic testing strand whales? Nature 392, 29.

Frizzell, L.A., Lee, C.S., Aschenbach, P.D., Borrelli, M.J., Morimoto, R.S., Dunn, F., 1983. Involvement of ultrasonically induced cavitation in the production of hind limb paralysis of the mouse neonate. J. Acoust. Soc. Am. 74, 1062–1065.

Fry, W.J., Dunn, F., 1956. Ultrasonic irradiation of the central nervous system at high sound levels. J. Acoust. Soc. Am. 28, 129–131.

Fry, F.J., Johnson, L.K., 1978. Tumour irradiation with intense ultrasound. Ultrasound Med. Biol. 4, 337–341.

Fry, W.J., Mosberg, W.H., Barnard, J.W., Fry, F.J., 1954. Production of focal destructive lesions in the central nervous system with ultrasound. J. Neurosurg. 11, 471–478.

Fry, F.J., Kossoff, G., Eggleton, R.C., Dunn, F., 1970. Threshold ultrasonic dosages for structural changes in the mammalian brain. J. Acoust. Soc. Am. 48, 1413–1417.

Gaitan, D.F., Crum, L.A., 1990. Observation of sonoluminescence from a single cavitation bubble in a water/glycerine mixture. In: Hamilton, M.F., Blackstock, D.T. (Eds.), Frontiers of Nonlinear Acoustics, 12th ISNA. Elsevier, New York, pp. 459–463.

Gaitan, D.F., Crum, L.A., Church, C.C., Roy, R.A., 1992. Sonoluminescence and bubble dynamics for a single, stable, cavitation bubble. J. Acoust. Soc. Am. 91, 3166–3183.

Geng, X., Yuan, H., Prosperetti, A., 1999. The oscillations of gas bubbles in tubes: Experimental results. J. Acoust. Soc. Am. 106, 674–681.

Goddard, G., Kaduchak, G., 2005. Ultrasonic particle concentration in a line-driven cylindrical tube. J. Acoust. Soc. Am. 117, 3440–3447.

Gol'dberg, Z.A., 1956. Second approximation acoustic equations and the propagation of plane waves of finite amplitude. Sov. Phys. Acoust. 2, 346–350.

Griffiths, G., Fielding, S., Roe, H.S., 2001. Some observations of biophysical interaction in the ocean using high frequency acoustics. In: Leighton, T.G., Heald, G.J., Griffiths, H., Griffiths, G. (Eds.), 'Acoustical Oceanography', Proceedings of the Institute of Acoustics, Vol. 23 Part 2. Institute of Acoustics, pp. 189–195.

Grigor'eva, V.M., 1966. Effect of ultrasonic vibrations on personnel working with ultrasonic equipment. Soviet Phys. Acoust. 11, 426–427.

Haake, A., Neild, A., Radziwill, G., Dual, J., 2005. Positioning, displacement, and localization of cells using ultrasonic forces. Biotechnol. Bioeng. 92, 8–14.

Hamilton, M.F., Blackstock, D.T. (Eds.), 1998. Nonlinear Acoustics. Academic Press, San Diego.

Hand, J.W., Vernon, C.C., Prior, M.V., 1992. Early experience of a commercial scanned focused ultrasound hyperthermia system. Int. J. Hyperthermia 8 (5), 587–607.

Harris, G.R., 1999. Medical ultrasound exposure measurements: update on devices, methods, and problems. IEEE Ultrasonics Symp. 2, 1341–1352.

Harris, N.R., Hill, M., Beeby, S.P., Shen, Y., White, N.M., Hawkes, J.J., Coakley, W.T., 2003. A silicon microfluidic ultrasonic separator. Sens. Actuat. B 95, 425–434.

Haugan, P.M., Drange, H., 1992. Sequestration of CO_2 in the deep ocean by shallow injection. Nature 357, 318–320.

Hawkes, J.J., Coakley, W.T., 2001. Force field particle filter, combining ultrasound standing waves and laminar flow. Sens. Actuat. B: Chem. 75 (3), 213–222.

Health Canada, 1991. Guidelines for the safe use of ultrasound: part II industrial and commercial applications Safety Code 24. Document EHD-TR-158, 1991, Health Protection Branch, Environmental Health Directorate, National Health and Welfare, Canada

Herbst, A.L., Scully, R.E., 1970. Adenocarcinoma of the vagina in adolescence. Cancer 25, 745–757.

Herman, B.A., Powell, D., 1981. Airborne ultrasound: measurement and possible adverse effects. HHS Publication (FDA) 81-8163, US Department of Health and Human Services, Food and Drug Administration. Rockville, MD.

Herrick, J.F., 1953. Temperatures produced in tissues by ultrasound: experimental study using various technics. J. Acoust. Soc. Am. 25, 12–16.

Hill, M., 2003. The selection of layer thicknesses to control acoustic radiation force profiles in layered resonators. J. Acoust. Soc. Am. 114, 2654–2661.

Holland, C.K., Apfel, R.E., 1989. An improved theory for the prediction of microcavitation thresholds. IEEE Trans. Ultrasonics Ferroelectrics Frequency Control 36, 204–208.

Holliday, D.V., 2001. Acoustical sensing of biology in the sea. In: Leighton, T.G., Heald, G.J., Griffiths, H., Griffiths, G. (Eds.), 'Acoustical Oceanography', Proceedings of the Institute of Acoustics, Vol. 23, Part 2. Institute of Acoustics, pp. 172–180.

Holmberg, K., Landstrom, U., Nordstrom, B., 1995. Annoyance and discomfort during exposure to high-frequency noise from an ultrasonic washer. Perceptual Motor Skills 81, 819–827.

Holt, R.G., Roy, R.A., 2001. Measurements of bubble-enhanced heating from focused, MHz-frequency ultrasound in a tissue-mimicking material. Ultrasound Med. Biol. 27 (10), 1399–1412.

Hosokawa, A., Otani, T., 1997. Ultrasonic wave propagation in bovine trabecular bone. J. Acoust. Soc. Am. 101, 558–562.

Howard, C.Q., Hansen, C.H., Zander, A.C., 2005. A review of current ultrasound exposure limits. J. Occup. Health Safety Austr. New Zealand 21 (3), 253–257.

Hughes, E.R., Leighton, T.G., Petley, G.W., White, P.R., 1999. Ultrasonic propagation in cancellous bone: a new stratified model. Ultrasound Med. Biol. 25 (5), 811–821.

Hughes, E.R., Leighton, T.G., Petley, G.W., White, P.R., 2001. Ultrasonic assessment of bone health. Acoust. Bull. 26 (5), 17–23.

Hughes, E.R., Leighton, T.G., Petley, G.W., White, P.R., Chivers, R.C., 2003. Estimation of critical and viscous frequencies for biot theory in cancellous bone. Ultrasonics 41, 365–368.

Hung, H., Hoffmann, M.R., 1999. Kinetics and mechanism of the sonolytic degradation of chlorinated hydrocarbons: frequency effects. J. Phys. Chem. A 103, 2734–2739.

Hurrell, A., 2002. Finite difference modelling of acoustic propagation and its applications in underwater acoustics. PhD Thesis, University of Bath, UK.

Hwang, J.J., Quistgaard, J., Souquet, J., Crum, L.A., 1998. Portable ultrasound device for battlefield trauma. IEEE Symp. Proc. 2, 1663–1666.

Hynynen, K., 1987. Demonstration of enhanced temperature elevation due to nonlinear propagation of focussed ultrasound in dog's thigh in vivo. Ultrasound Med. Biol. 13, 85–91.

Hynynen, K., 1991. The role of nonlinear ultrasound propagation during hyperthermia treatments. Med. Phys. 18 (6), 1156–1163.

International Electrotechnical Commission, 1991. IEC 61102, Measurement and characterisation of ultrasonic fields using hydrophones in the frequency range 0.5–15 MHz.

International Labour Office, 1977. Protection of workers against noise and vibration in the working environment. ILO Code of Practice, 1977; International Labour Office, Geneva.

International Non-Ionizing Radiation Committee, 1984. International radiation protection association. Interim guidelines on limits of human exposure to airborne ultrasound. Health Phys. 46, 969–974.

Kargl, S.G., 2002. Effective medium approach to linear acoustics in bubbly liquids. J. Acoust. Soc. Am. 111, 168–173.

Kennedy, J.E., 2005. High-intensity focused ultrasound in the treatment of solid tumours. Nat. Rev. Cancer 5, 321–327.

Kilpatrick, H.C., 1981. Decibel ratings of dental office sounds. J. Prosthet. Dent. 45, 175–178.

Kinsler, L.E., Frey, A.R., Coppens, A.B., Sanders, J.V., 1982. Fundamentals of Acoustics, third ed. Wiley, New York.

Knight, J.J., 1968. Effects of airborne ultrasound on man. Ultrasonics 6 (1), 39–41.

Kogan, S., Kaduchak, G., Sinha, D.N., 2004. Acoustic concentration of particles in piezoelectric tubes: Theoretical modeling of the effect of cavity shape and symmetry breaking. J. Acoust. Soc. Am. 116, 1967–1974.

Kojima, Y., Koda, S., Nomura, H., 2001. Effect of ultrasonic frequency on polymerization of styrene under sonication. Ultrasonics Sonochem. 8, 75–79.

Korpert, K., Vanek, R., 1987. Application of two exposure criteria to different types of industrial ultrasound. Proc. Ultrasonics Int. Lond. 87, 232–237.

Kossoff, G., Wadsworth, J.R., Dudley, P.F., 1967. The round window ultrasonic technique for the treatment of Meniere's disease. Arch. Otolaryngol. 86, 535–542.

Kotel'nikov, I.A., Stupakov, G.V., 1983. Nonlinear effects in the propagation of sound in a liquid with gas bubbles. Sov. Phys. JETP 57 (3), 555.

Kozyaev, E.A., Naugol'nykh, K.A., 1980. Parametric sound radiation in a two-phase medium. Sov. Phys. Acoust. 26, 48–51 (Akust. Zh. 1980; 26: 91).

Krautkramer, J., Krautkramer, H., 1977. Ultrasonic Testing of Materials. Springer, New York.

Kudo, N., Ouchi, H., Yamamoto, K., Sekimizu, H., 2004. A simple Schlieren system for visualizing a sound field of pulsed ultrasound. J. Phys.: Conf. Ser. 1, 146–149.

Kumar, M., Feke, D.L., Belovich, J.M., 2005. Fractionation of cell mixtures using acoustic and laminar flow fields. Biotechnol. Bioeng. 89, 129–137.

Kustov, L.M., Nazarov, V.E., Ostrovskii, L.A., Sutin, A.M., Zamolin, A.S., 1982. Parametric acoustic radiator with a bubble layer. Acoust. Lett. 6 (2), 15–17.

Kuznetsova, L.A., Coakley, W.T., 2004. Microparticle concentration in short path length ultrasonic resonators: roles of radiation pressure and acoustic streaming. J. Acoust. Soc. Am. 116, 1956–1966.

Langton, C.M., Palmer, S.B., Porter, R.W., 1984. The measurement of broadband ultrasonic attenuation in trabecular bone. Eng. Med. 13 (2), 89–91.

Lawton, B.E., 2001. Damage to human hearing by airborne sound of very high or ultrasonic frequency. Health and Safety Executive Research Report 343/2001.

Lee, C.S., Frizzell, L.A., 1988. Exposure levels for ultrasonic cavitation in the mouse neonate. Ultrasound Med. Biol. 14, 735–742.

Lee, K.I., Roh, H.S., Yoon, S.W., 2003. Acoustic wave propagation in bovine cancellous bone: application of the modified Biot–Attenborough model. J. Acoust. Soc. Am. 114, 2284–2293.

Leighton, T.G., 1994. The Acoustic Bubble. Academic Press, London.

Leighton, T.G., 1995. Bubble population phenomena in acoustic cavitation. Ultrasonics Sonochem. 2, S123–S136.

Leighton, T.G. (Ed.), 1997. Natural Physical Processes Associated With Sea Surface. University of Southampton.

Leighton, T.G., 1998. Fundamentals of underwater acoustics and ultrasound. In: Fahy, F.J., Walker, J.G. (Eds.), Noise and Vibration, Vol. 1. E & F Spon, Routledge, London, pp. 373–444 (Chapter 7).

Leighton, T.G., 2004. From seas to surgeries, from babbling brooks to baby scans: the acoustics of gas bubbles in liquids. Int. J. Mod. Phys. B Vol. 18, 3267–3314.

Leighton, T.G., Dumbrell, H.A., 2004. New approaches to contrast agent modelling. Proceedings of the first conference in advanced metrology for ultrasound in medicine. J. Phys.: Conf. Ser. 1, 91–96.

Leighton, T.G., Heald, G.J., 2005. Very high frequency coastal acoustics. In: Medwin, H. (Ed.), Acoust. Oceanogr.: Sound Sea. Cambridge University Press, Cambridge, pp. 518–547 (Chapter 21).

Leighton, T.G., Pickworth, M.J.W., Walton, A.J., Dendy, P.P., 1988. Studies of the cavitational effects of clinical ultrasound by sonoluminescence: 1. Correlation of sonoluminescence with the standing-wave pattern in an acoustic field produced by a therapeutic unit. Phys. Med. Biol. 33 (11), 1239–1248.

Leighton, T.G., Walton, A.J., Field, J.E., 1989. High-speed photography of transient excitation. Ultrasonics 27, 370–373.

Leighton, T.G., Pickworth, M.J.W., Tudor, J., Dendy, P.P., 1990. Studies of the cavitational effects of clinical ultrasound by sonoluminescence: 5, Search for sonoluminescence *in vivo* in the human cheek. Ultrasonics 28, 181–184.

Leighton, T.G., White, P.R., Marsden, M.A., 1995. Applications of one-dimensional bubbles to lithotripsy, and to diver response to low frequency sound. Acta Acustica 3, 517–529.

Leighton, T.G., Cox, B.T., Phelps, A.D., 2000. The Rayleigh-like collapse of a conical bubble. J. Acoust. Soc. Am. 107, 130–142.

Leighton, T.G., Heald, G.J., Griffiths, H., Griffiths, G. (Eds.), 2001. Acoustical Oceanography. Proceedings of the Institute of Acoustics, Vol. 23, Part 2. Bath University Press.

Leighton, T.G., White, P.R., Morfey, C.L., Clarke, J.W.L., Heald, G.J., Dumbrell, H.A., Holland, K.R., 2002. The effect of reverberation on the damping of bubbles. J. Acoust. Soc. Am. 112 (4), 1366–1376.

Leighton, T.G., Meers, S.D., White, P.R., 2004. Propagation through nonlinear time-dependent bubble clouds, and the estimation of bubble populations from measured acoustic characteristics. Proc. Roy. Soc. A 460 (2049), 2521–2550.

Leighton, T.G., Birkin, P.R., Hodnett, M., Zeqiri, B., Power, J.F., Price, G.J., Mason, T., Plattes, M., Dezhkunov, N., Coleman, A.J., 2005a. Characterisation of measures of reference acoustic cavitation (COMORAC): an experimental feasibility trial. In: Doinikov, A.A. (Ed.), Bubble and particle dynamics in Acoustic Fields: Modern Trends and Applications. Research Signpost, Kerala, pp. 37–94.

Leighton, T.G., White, P.R., Finfer, D.C., Richards, S.D., 2005b. Cetacean acoustics in bubbly water. In: Papadakis, J.S., Bjorno, L. (Eds.), Proceedings of the international conference on underwater acoustic measurements, technologies and results. Crete, pp. 891–898.

Lerner, A.M., Sutin, A.M., 1983. Influence of gas bubbles on the field of a parametric sound radiator. Sov. Phys. Acoust. 29, 388–392 (Akust. Zh. 1983; 29: 657).

Lighthill, J., 1978. Acoustic streaming. J. Sound Vibr. 61, 391–418.

Lilliehorn, T., Simu, U., Nilsson, M., Almqvist, M., Stepinski, T., Laurell, T., Nilsson, J., Johansson, S., 2005. Trapping of microparticles in the near field of an ultrasonic transducer. Ultrasonics 43, 293–303.

Lin, W., Qin, Y.X., Rubin, C., 2001. Ultrasonic wave propagation in trabecular bone predicted by the stratified model. Ann. Biomed. Eng. 29, 781–790.

Lizzi, F.L., Ostromogilsky, M., 1987. Analytical modelling of ultrasonically induced tissue heating. Ultrasound Med. Biol. 13, 607–618.

Lizzi, F.L., Coleman, D.J., Driller, J., Franzen, L.A., Jacobiec, F.A., 1978. Experimental, ultrasonically-induced lesions in retina, choroid and sclera. Invest. Ophthalmol. Vis. Sci. 17, 350–360.

Lizzi, F.L., Coleman, D.J., Driller, J., Ostromogilsky, M., Chang, S., Greenall, P., 1984. Ultrasonic hyperthermia for opthalmic therapy. IEEE Trans. Sonics Ultrason. SU 31, 473–481.

Lizzi, F.L., Driller, J., Lunzer, B., Kalisz, A., Coleman, D.J., 1992. Computer-model of ultrasonic hyperthermia and ablation for ocular tumors using B-mode data. Ultrasound Med. Biol. 18 (1), 59–73.

Mark, G., Tauber, A., Laupert, R., Schuchmann, H.P., Schulz, D., Mues, A., von Sonntag, C., 1998. OH-radical formation by ultrasound in aqueous solution. Ultrasonics Sonochem. 5, 41–52.

Martin, S.P., Townsend, R.J., Kuznetsova, L.A., Borthwick, K.A.J., Hill, M., McDonnell, M.B., Coakley, W.T., 2005. Spore and micro-particle capture on an immunosensor surface in an ultrasound standing wave system. Bio-Sens. Bioelectr. 21, 758–767.

Mason, T.J., Lorimer, J.P., Bates, D.M., 1992. Quantifying Sonochemistry: Casting some light on a "black art". Ultrasonics 30 (1), 40–42.

Medwin, H., (Ed.), 2005. Acoustical Oceanography: Sound in the Sea: From Ocean Acoustics to Acoustical Oceanography. Cambridge University Press, Cambridge.

Medwin, H., Clay, C.S., 1998. Fundamentals of Acoustical Oceanography. Academic Press, New York.

Meltzer, R.S., 1996. Food and drug administration ultrasound device regulation: the output display standard, the mechanical index, and ultrasound safety. J. Am. Soc. Echocardiogr. 9 (2), 216–220.

Merzkirch, W., 1987. Flow visualisation. Academic Press, New York.

Miller, D.L., 1985. On the oscillation mode of gas-filled micropores. J. Acoust. Soc. Am. 77, 946–953.

Miller, D.L., Quddus, J., 2000. Diagnostic ultrasound activation of contrast agent gas bodies induces capillary rupture in mice. Proc. Natl. Acad. Sci. USA 97 (18), 10179–10184.

Miller, D.L., Nyborg, W.L., Whitcomb, C.C., 1979. Platelet aggregation induced by ultrasound under specialized condition in vitro. Science 205, 505.

Miller, D.L., Williams, A.R., 1989. Bubble cycling as the explanation of the promotion of ultrasonic cxavitation in a rotating tube exposure system. Ultrasound med. Biol 15, 641–648.

Miller, M.W., Ziskin, M.C., 1989. Biological consequences of hyperthermia. Ultrasound Med. Biol. 15, 707–722.

Mindell, D.A., Bingham, B., 2001. A high-frequency, narrow-beam sub bottom profiler for archaeological applications. In: Proceedings of OCEANS 2001, MTS/IEEE Conference and Exhibition, vol. 4, pp. 2115–2123.

Minnaert, M., 1933. On musical air-bubbles and sounds of running water. Philos. Mag. 16, 235–248.

Morse, P.M., Ingard, K.U., 1986. Theoretical Acoustics, pp. 874–882.

National Occupational Health and Safety Commission, 2002. Noise—annual situation report 2002. Technical Report, Commonwealth of Australia.

Neppiras, E.A., 1980. Acoustic cavitation. Phys. Rep. 61, 159–251.

Nightingale, A., 1959. Physics and Electronics in Physical Medicine. Bell, London (p. 275).

Nightingale, K.R., Kornguth, P.J., Walker, W.F., McDermott, B.A., Trahey, G.E., 1995. A novel ultrasonic technique for differentiating cysts from solid lesions: preliminary results in the breast. Ultrasound Med. Biol. 21 (6), 745–751.

Njeh, C.F., Hans, D., Fuerst, T., Gluer, C-C., Genant, H.K., 1999. Quantitative ultrasound: assessment of osteoporosis and bone status. Martin Dunitz, London.

Nyborg, W.L., 1958. Acoustic streaming near a boundary. J. Acoust. Soc. Am. 30, 329–339.

O'Brien Jr., W.D., 1992. Ultrasound dosimetry and interaction mechanisms. In: Greene, M.W. (Ed.), Non-ionizing radiation: proceedings of the second international non-ionizing radiation workshop. Canadian Radiation Protection Association, Vancouver, BC, pp. 151–172.

O'Brien Jr., W.D., Frizzell, L.A., 2000. Ultrasound-induced lung hemorrhage is not caused by inertial cavitation. J. Acoust. Soc. Am. 108 (3), 1290–1297.

Oguz, H.N., Prosperetti, A., 1998. The natural frequency of oscillation of gas bubbles in tubes. J. Acoust. Soc. Am. 103, 3301–3308.

O'Leary, R., Sved, A.M., Davies, E.H., Leighton, T.G., Wilson, M., Kieser, J.B., 1997. The bactericidal effects of dental ultrasound on Actinobacillus actinomycetemcomitans and Porphyromonas gingivalis—an *in vitro* investigation. J. Clin. Periodonol. 24, 432–439.

Pangu, G.D., Feke, D.L., 2004. Acoustically aided separation of oil droplets from aqueous emulsions. Chem. Eng. Sci. 59, 3183–3193.

Parrack, H.O., 1966. Effect of air-borne ultrasound on humans. Int. Audiol. 5, 294–308.

Paunoff, P., 1939. La luminescence de leau sous laction des ultrasons. Comptes rendus hebdomdaires des seances de lAcademie des Sciences Paris 209, 33–36.

Petersson, F., Nilsson, A., Jonsson, H., Laurell, T., 2005a. Carrier medium exchange through ultrasonic particle switching in microfluidic channels. Anal. Chem. 77, 1216–1221.

Petersson, F., Nilsson, A., Holm, C., Jonsson, H., Laurell, T., 2005b. Continuous separation of lipid particles from erythrocytes by means of laminar flow and acoustic standing wave forces. Lab On A Chip 5, 20–22.

Pickworth, M.J.W., Dendy, P.P., Twentyman, P.R., Leighton, T.G., 1989. Studies of the cavitational effects of clinical ultrasound by sonoluminescence: 4. The effect of therapeutic ultrasound on cells in monolayer culture in a standing wave field. Phys. Med. Biol. 34 (11), 1553–1560.

Piercy, J.E., Embleton, T.F.W., Sutherland, L.C., 1977. Review of noise propagation in the atmosphere. J. Acoust. Soc. Am. 61 (6), 1403–1418.

Pitt, W.G., Husseini, G.A., Staples, B.J., 2004. Ultrasonic drug delivery–a general review. Expert Opin. Drug Delivery 1 (1), 37–56.

Polack, P.J., Iwamoto, T., Silverman, R.H., Driller, J., Lizzi, F.L., Coleman, D.J., 1991. Histologic effects of contact ultrasound for the treatment of glaucoma. Invest. Ophthalmol. Visual Sci. 32 (7), 2136–2142.

Postema, M., Van Wamel, A., Lancee, C.T., De Jong, N., 2004. Ultrasound-induced encapsulated microbubble phenomena. Ultrasound Med. Biol. 30 (6), 827–840.

Quain, R.M., Waag, R.C., Miller, M.W., 1991. The use of frequency mixing to distinguish size distributions of gas-filled micropores. Ultrasound Med. Biol. 17, 71–79.

Rabkin, B.A., Zderic, V., Vaezy, S., 2005. Hyperecho in Ultrasound Images of HIFU Therapy: Involvement of Cavitation. Ultrasound Med. Biol. 31 (7), 947–956.

Readhead, M.L., 1997. Snapping shrimp noise near Gladstone, Queensland. J. Acoust. Soc. Am. 101 (3), 1718–1722.

Richards, S.D., Leighton, T.G., Brown, N.R., 2003. Visco-inertial absorption in dilute suspensions of irregular particles. Proc. Roy. Soc. Ser. A 459 (2037), 2153–2167.

Riera, E., Gallego-Juarez, J.A., Mason, T.J., 2006. Airborne ultrasound for the precipitation of smokes and powders and the destruction of foams. Ultrasonics Sonochem. 13, 107–116.

Rife, J.C., Bell, M.I., Horwitz, J.S., Kabler, M.N., Auyeung, R.C.Y., Kim, W.J., 2000. Miniature valveless ultrasonic pumps and mixers. Sens. Actuat. A: Phys. 86 (1), 135–140.

Robb, G.B.N., Best, A.I., Dix, J.K., White, P.R., Leighton, T.G., Bull, J.M., Harris, A., 2006. The measurement of the in situ compressinal wave properties of marine sediments. IEEE J. Oceanic Eng., in press.

Rooney, J.A., 1972. Shear as a mechanism for sonically-induced biological effects. J. Acoust. Soc. Am. 52, 1718–1724.

Roscin, I.V., Mel'kumova, A.S., Lisickina, Z.S., Efimov, N.A., Luk'janov, V.S., Temkin, Ja.S., 1967. Occupational health hazards of technical applications of ultrasound. Occupat. Safety Health Abstr. 5, 657 (Abstract).

Roy, R.A., Ahmad, M., Crum, L.A., 1994. Physical mechanisms governing the hydrodynamic response of an oscillating ultrasonic file. Int. Endod. J. 27 (4), 197–207.

Saksena, T.K., Nyborg, W.L., 1970. Sonoluminescence from stable cavitation. J. Chem. Phys. 53, 1722–1734.

Sass, W., Braunlich, M., Dreyer, H.P., Matura, E., Folberth, W., Preismeyer, H.G., et al., 1991. The mechanisms of stone disintegration by shock waves. Ultrasound Med. Biol. 17 (3), 239–243.

Sato, M., Itoh, H., Fujii, T., 2000. Frequency dependence of H_2O_2 generation from distilled water. Ultrasonics 38, 312–315.

Shi, X., Martin, R.W., Vaezy, S., Crum, L.A., 2002. Quantitative investigation of acoustic streaming in blood. J. Acoust. Soc. Am. 111 (2), 1110–1121.

Shortencarier, M.J., Dayton, P.A., Bloch, S.H., Schumann, P.A., Matsunaga, T.O., Ferrara, K.W., 2004. A method for radiation-force localized drug delivery using gas-filled liposheres. IEEE Trans. Ultrasonics, Ferroelectrics Frequency Control 51 (7), 821–830.

Siddiqi, T.A., O'Brien Jr., W.D., Meyer, R.A., Sullivan, J.M., Miodovnik, M., 1995. In situ human obstetrical ultrasound exposimetry: estimates of derating factors for each of three different tissue models. Ultrasound Med. Biol. vol. 21 (3), 370–391.

Skillern, C.P., 1965. Human response to measured sound pressure levels from ultrasonic devices. Am. Ind. Hyg. Assoc. J. 26, 132–136.

Smith, P.E., 1967. Temporary threshold shift produced by exposure to high-frequency noise. Am. Ind. Hyg. Assoc. J. 28, 447–451.

Smith, O.W., Smith, G.V., Hurwitz, D., 1946. Increased excretion of pregnanediol in pregnancy from diethylstil-boestrol with special reference to prevention of late pregnancy accidents. Am. J. Obstet. Gynecol. 51, 411–415.

Starritt, H.C., Duck, F.A., Humphrey, V.F., 1989. An experimental investigation of streaming in pulsed diagnostic ultrasound beams. Ultrasound Med. Biol. 15, 363–373.

Starritt, H.C., Duck, F.A., Humphrey, V.F., 1991. Forces acting in the direction of propagation in pulsed ultrasound fields. Phys. Med. Biol. 36, 1465–1474.

Stephens, R.W.B., Bate, A.E., 1966. Acoustics and Vibrational Physics, Second ed. Edward Arnold Publishers, London.

Stewart, R.W., 1992. Understanding fluxes to and within the ocean: a key to understanding climate. J. Oceanogr. 48 (1), 5–12.

Stewart, A., Webb, J., Giles, D., Hewitt, D., 1956. Malignant disease in childhood and diagnostic irradiation in utero. Lancet, II: 447.

Strelitzki, R., Nicholson, P.H.F., Paech, V., 1998. A model for ultrasonic scattering in cancellous bone based on velocity fluctuations in a binary mixture. Physiol. Meas. 19, 189–196.

Symons, D.D., 2004. Inertial liquid loading on the nozzle of a needle-free injection system. Proc. Instrum. Mech. Eng. 218, 233–240.

Szabo, T.L., 2004. Diagnostic ultrasound imaging: inside out. Elsevier Science, Boston.

Szymańska, J., 2000. Work-related noise hazards in the dental surgery. Ann. Agric. Environ. Med. 7, 67–70.

Ter Haar, G.R., 1986. Therapeutic and surgical applications. In: Hill, C.R., (Ed.), Physical Principles of Medical Ultrasonics. Ellis Horwood Ltd., Chichester (for John Wiley and Sons, New York) (Chapter 13).

Ter Haar, G.R., 2001. High intensity focused ultrasound for the treatment of tumors. Echocardiography 18 (4), 317–322.

Ter Haar, G.R., Wyard, S.J., 1978. Blood cell banding in ultrasonic standing wave fields: a physical analysis. Ultrasound Med. Biol. 4, 111–123.

Ter Haar, G., Dyson, M., Oakley, E.M., 1987. The use of ultrasound by Physiotherapists in Britain, 1985. Ultrasound Med. Biol. 13 (10), 659–663.

Ter Haar, G., Rivens, I., Chen, L., Riddler, S., 1991. High intensity focused ultrasound for the treatment of rat tumours. Phys. Med. Biol. 36 (11), 1495–1501.

The Economist, 1998. Quiet please. Whales navigating, p. 85.

Thomas, C.R., Farny, C.H., Coussios, C.-C., Roy, R.A., Holt, R.G., 2005. Dynamics and control of cavitation during high-intensity focused ultrasound application. ARLO 6 (3), 182–187.

Thorne, P.D., Haynes, D.M., 2002. A review of acoustic measurement of small-scale sediment processes. Continent. Shelf Res. 22, 1–30.

Townsend, R.J., Hill, M., Harris, N.R., White, N.M., 2004. Modelling of particle paths passing through an ultrasonic standing wave. Ultrasonics 42, 319–324.

Trenter, S.C., Walmsley, A.D., 2003. Ultrasonic dental scaler: associated hazards. J. Clin. Periodontol. 30, 95–101.

Trinh, E.H., Robey, J.L., 1994. Experimental study of streaming flows associated with ultrasonic levitators. Phys. Fluids 6 (11), 3567–3579.

Urick, R.J., 1983. Principles of Underwater Sound, third ed. McGraw-Hill, New York.

Vaezy, S., Martin, R., Yaziji, H., Kaczkowski, P., Keilman, G., Carter, S., Caps, M., Chi, E.Y., Bailey, M., Crum, L., 1998. Hemostasis of punctured blood vessels using high-intensity focused ultrasound. Ultrasound Med. Biol. 24, 903–910.

Vaezy, S., Martin, R., Kaczkowski, P., Keilman, G., Goldman, B., Yaziji, H., Carter, S., Caps, M., Crum, L., 1999. Use of high-intensity focused ultrasound to control bleeding. J. Vasc. Surg. 29 (3), 533–542.

Vaezy, S., Martin, R., Crum, L., 2001. High intensity focused ultrasound: a method of hemostasis. Echocardiography 18 (4), 309–315.

Vivino, A.A., Boraker, D.K., Miller, D., Nyborg, W., 1985. Stable cavitation at low ultrasonic intensities induces cell death and inhibits 3H-TdR incorporation by con-a-stimulated murine lymphocytes *in vitro*. Ultrasound Med. Biol 11, 751–759.

Von Gierke, H.E., Nixon, C.W., 1976. Effects of intense intrasound on man. In: Tempest, W. (Ed.), Infrasound and Low Frequency Vibration. Academic Press, New York, pp. 115–150.

Von Gierke, H.E., Nixon, C.W., 1992. Noise and Vibration Control Engineering: Principles and applications. In: Leo, L.B., István, L.V. (Eds.), Damage Risk Criteria Got Hearing and Human Body Vibration. Wiley, New York, pp. 585–616 (Chapter 6).

Walmsley, A.D., Hickson, F.S., Laird, W.R., Williams, A.R., 1987a. Investigation into patients' hearing following ultrasonic scaling. Br. Dent. J. 162 (6), 221–224.

Walmsley, A.D., Laird, W.R., Williams, A.R., 1987b. Intra-vascular thrombosis associated with dental ultrasound. J. Oral. Pathol. 16 (5), 256–259.

Walton, A.J., Reynolds, G.T., 1984. Sonoluminescence. Adv. Phys. 33 (6), 595–660.

Warwick, R., Pond, J.B., 1968. Trackless lesions produced by high intensity focused ultrasound (high-frequency mechanical waves). J. Anat. 102, 387–405.

Watkins, R.D., Barrett, L.M., McKnight, J.A., 1988. Ultrasonic waveguide for use in the sodium coolant of fast reactors. Nucl. Energy 27, 85–89.

Wear, K.A., 2005. The dependencies of phase velocity and dispersion on trabecular thickness and spacing in trabecular bone-mimicking phantoms. J. Acoust. Soc. Am. 118, 1186–1192.

Wear, K.A., Armstrong, D.W., 2001. Relationships among calcaneal backscatter, attenuation, sound speed, hip bone mineral density, and age in normal adult women. J. Acoust. Soc. Am. 110, 573–578.

Wells, P.N.T., 1977. Biomedical Ultrasonics. Academic Press, London.

Wiklund, M., Toivonen, J., Tirri, M., Hanninen, P., Hertz, H.M., 2004. Ultrasonic enrichment of microspheres for ultrasensitive biomedical analysis in confocal laser-scanning fluorescence detection. J. Appl. Phys. 96, 1242–1248.

Williams, A.R., 1974. DNA degradation by acoustic microstreaming. J. Acoust. Soc. Am. 55, S17A.

Williams, A.R., 1977. Intravascular mural thrombi produced by acoustic microstreaming. Ultrasound Med. Biol. 3, 191–203.

Williams, A.R., Slade, J.S., 1971. Ultrasonic dispersal of aggregates of Sarcina lutea. Ultrasonics 9, 85–87.

Williams, A.R., Hugh, D.E., Nyborg, W.L., 1974. Hemolysis near a transversely oscillating wire. Science 169, 871–873.

Wilson, J.D., Darby, M.L., Tolle, S.L., Sever Jr., J.C., 2002. Effects of occupational ultrasonic noise exposure on hearing of dental hygienists: a pilot study. J. Dent. Hyg. 76 (4), 262–269.

Wu, F., Chen, W.Z., Bai, J., Zou, J.Z., Wang, Z.L., Zhu, H., Wang, Z.B., 2002. Tumor vessel destruction resulting from high-intensity focused ultrasound in patients with solid malignancies. Ultrasound Med. Biol. 28, 535–542.

Yang, X., Church, C.C., 2005. A model for the dynamics of gas bubbles in soft tissue. J. Acoust. Soc. Am. 118 (6), 3595–3606.

Yang, R., Sanghvi, N.T., Rescorla, F.J., Kopecky, K.K., Grosfeld, J.L., 1993. Liver cancer ablation with extracorporeal high-intensity focused ultrasound. Eur. Urol. 23 (1) (Suppl. 17–22).

Yeh, C.-K., Ferrara, K.W., Kruse, D.E., 2004. High-resolution functional vascular assessment with ultrasound. IEEE Trans. Med. Imaging 23 (10), 1263–1275.

Yim, G.T., Leighton, T.G., 2006. The use of acoustics for real-time on-line monitoring of ceramic slip in pottery pipe-lines. Proc. Inst. Acoust. 28 (1), 862–875.

Yoneyama, M., Fujimoto, J., Kawoamo, Y., Sasabe, S., 1983. The audio spotlight: an application of nonlinear interaction of sound waves to a new type of loudpseaker design. J. Acoust. Soc. Am. 73 (5), 1532–1536.

Zeqiri, B., 2005. Personal communication.

Zeqiri, B., Hodnett, M., Leighton, T.G., 1997. A strategy for the development and standardisation of measurement methods for high power/cavitating ultrasonic fields–Final project report. NPL Report CIRA(EXT)016 for National Measurement System Policy Unit, Department of Trade and Industry.

Zeqiri, B., Shaw, A., Gélat, P.N., Bell, D., Sutton, Y.C., 2004. A novel device for determining ultrasonic power. Proceedings of the first conference in advanced metrology for ultrasound in medicine. J. Phys.: Conf. Ser. 1, 105–110.

Zhao, S., Borden, M., Bloch, S., Kruse, D., Ferrara, K.W., Dayton, P.A., 2004. Radiation-force assisted targeting facilitates ultrasonic molecular imaging. Mol. Imaging 3 (3), 135–148.

Ziskin, M.C., 1987. The prudent use of diagnostic ultrasound. J. Ultrasound Med. 6, 415–416.

Ziskin, M.C., Pittiti, D.B., 1988. Epidemiology of human exposure to ultrasound: a critical review. Ultrasound Med. Biol. 14, 91–96.